THE UNIVERSITY OF TULSA

THE GRADUATE SCHOOL

BUILDING FROM THE GROUND UP: UNDERSTANDING AND PREDICTING THE STRENGTH OF COB, AN EARTHEN CONSTRUCTION MATERIAL

by
David J. Wright

A dissertation submitted in partial fulfillment of
the requirements for the degree of Doctor of Philosophy
in the Discipline of Mechanical Engineering

The Graduate School
The University of Tulsa

2019

THE UNIVERSITY OF TULSA

THE GRADUATE SCHOOL

BUILDING FROM THE GROUND UP:

UNDERSTANDING AND PREDICTING THE STRENGTH OF COB,

AN EARTHEN CONSTRUCTION MATERIAL

by
David J. Wright

A DISSERTATION

APPROVED FOR THE DISCIPLINE OF

MECHANICAL ENGINEERING

By Dissertation Committee

John M. Henshaw, Chair
Michael W. Keller
Todd P. Otanicar
Kenneth P. Roberts

COPYRIGHT STATEMENT

ABSTRACT

David J. Wright (Doctor of Philosophy in Mechanical Engineering)

Understanding and Predicting the Strength of Cob

Directed by John M. Henshaw

139 pp., Chapter 9: Conclusions and Future Work

(143 words)

This work examines the mechanical properties of cob, an ancient earth-based construction material composed of sand, clay, and straw. An estimated one-third of the global population currently lives in earthen structures, which can provide economical and durable alternatives to wood, concrete, brick, or steel structures. The purpose of this work is to experimentally test and analytically model the relationship between various parameters in the manufacture of cob, such as moisture, clay, and straw contents, and mechanical strength. Constituent materials in cob, sand, clay soil, and straw, were characterized using both traditional earthen construction evaluation techniques and appropriate ASTM standards. The strength of cob in both compression and three-point bending (flexure) was evaluated. Modeling functions were developed to predict compression strength with respect to clay and straw content. This work contributes to the quantitative understanding of cob performance and sensitivity to several process parameters.

ACKNOWLEDGEMENTS

I would like to thank Ianto Evans and Linda Smiley, who, along with Michael Smith, began the rediscovery of cob in Oregon and trained me in cob construction. Shawn King was also an excellent instructor and collaborator as I learned what questions to ask in this research. Thank you also to the members of the Cob Research Institute, especially Martin Hammer and Anthony Dente for their expertise in the intersection of building code and earth construction. My friends and co-cobbers from the Cob Cottage Company have also provided inspiration and motivation to keep advancing cob construction.

Thank you to Dr. Cornell for provided significant help in running x-ray diffraction analysis and modeling response results, as well as providing training in sand sieve analysis.

I also want to thank Hilario "Larry" Chavez of Taos, New Mexico for his donation of traditionally made adobe blocks and insights into the adobe construction process. His stories and generosity will always be remembered.

Finally, I would like to thank my wife, Carmen, who has worked hard to keep us fed and clothed while this research took place. Her support of the research, a balanced life, and deeper philosophical thinking through graduate school has been irreplaceable.

TABLE OF CONTENTS

LIST OF TABLES

LIST OF FIGURES

CHAPTER 1
INTRODUCTION

1.1 Shelter

If you grew up in the United States during the 20^{th} or early 21^{st} centuries, you probably were surrounded by wood framed walls, covered by drywall boards on the inside and brick, vinyl, aluminum or wood on the outside. Your home is probably very similar to the one in which your parents and even grandparents grew up. But as you move back in time, toward the trunk of your family tree, you begin to observe changes in housing styles and materials; the walls and roof begin to shift closer to materials available straight from nature without extensive modification. Medieval buildings were constructed of timber and stone, with roofs of thatch or slate. Before this, homes in Europe were built using stacked stone, earth, or sod. In what is now New Mexico, the people of the Mogollon culture constructed homes among clefts in cliffs and protected themselves from the southwest heat in deeply dug pit houses. Even beyond human behavior, the need for shelter is seen in many animals, from the dens and caves of bears to intricately woven bird nests. In all of these cases, the desire for safety and comfort drives the construction of shelters and dwellings.

Throughout human history, *home* has been nearly synonyms with safety and comfort. This is, in no small part, because of the security we feel in a well designed shelter. Each culture and region developed unique materials and designs for their homes to maximize comfort and safety using what was available. Thick-walled earthen buildings are found throughout the Middle East and arid regions of Northern Africa and North America. Light, breezy, shaded buildings of round-wood or bamboo are common throughout the tropical regions in Southeast Asia, and Central and South America. In tundra and sub-Arctic regions, heavy wood construction traps heat for a cozy winter. In each of these, the builders of shelter find safety and comfort within its walls.

However the world did not remain simple, with each family building their own house. As specializations developed and craftsmen were trained, houses began to be built by professionals rather than owners. Those living in the house were no longer intimately aware of how robustly it was constructed. A builder now could use inferior materials or omit some hidden internal reinforcements and not immediately be found out. In order to protect the public from underhanded or incompetent building practices, the first building codes were developed.

1.2 Building Codes and Standards

In 1666, a small fire broke out at King's bakery, Pudding Lane, London. The protruding upper stories of London's crowded homes let the flames leap easily across streets and alleys. The drought preceding this particular fire had perfectly prepared the densely packed wood and thatch structures for the most catastrophic fire London had ever seen. By the time the fire had been brought under control three days later, more than three quarters of the buildings in London had been destroyed. The narrow streets, inexpensive building materials, and close-packed upper stories of London buildings made the Great Fire of London spread quickly and hindered firefighting efforts [46]. In the aftermath of the fire, Charles II, through parliament, issued "Act for rebuilding the Citty [sic] of London." This proclamation issued requirements for building materials and wall dimensions for various sizes of building constructed within the city limits. This document also authorized building inspectors to examine and provide permission for each new construction. In addition to requiring conformity among buildings, the act also standardized lane and road widths, ensuring safe passage of fire-fighting equipment in case of emergency. These changes to the way urban buildings were constructed helped ensure that "great and outragious [sic] Fires . . . may be reasonably prevented or obviated for the time to come" [70]. To protect the public safety from future catastrophe, Charles II created the first set of modern building code.

Laws surrounding building practices have existed since nearly the beginning of written human history. The Code of Hammurabi, the first extant example of written law, devotes six articles to ensuring that craftsmen get paid for their work, build safe structures, and are held accountable for any structural failure of a building they construct [53]. Given the frequency of earth construction in ancient middle eastern regions, Hammurabi's requirement that builders were paid per unit of surface area of building correlated well to quantity of material needed and time required for earth construction appropriate to that region.

The book of Deuteronomy, the code of law given to the ancient Hebrew people, also records one regulation on the construction of common buildings, noting that "When you build a new house, make a parapet around your roof so that you may not bring the guilt of bloodshed on your house if someone falls from the roof" [53]. Again, this law is intended to defend the safety of those using man-made shelters.

Since this first attempts to regulate building safety, standards for building performance, especially durability against disaster, have been adopted ad hoc for the past several hundred years by individual cities, counties, or nations. The United States now uses "model code" to guide the development of individual county or state building code. Model code is a set of non-binding standards published as an example of the current state of the art, and is available for voluntary adoption by the appropriate authorities. The most widely adopted model code in the United States is the International Code Council's International Building Code (IBC)and associated standards. Regions may amend this model code to ensure safety against unique regional phenomena, such as earthquake resistance in Southern California. However, many counties adopt the IBC without significant modification.

This dissertation intends to provide an initial set of data for discussions between both natural builders and regulatory agencies. While cob and other earth materials can be built safely and reliably, building code to govern best practices would simplify permitting of such buildings for natural builders and reduce barriers to more widespread adoption of cob construction.

1.3 Varieties of Earth Construction

Talk all about the various kinds of earth construction and give region of origin, unique traits, and process of each. Adobe Cob Rammed Earth (Pise de terre)

1.4 Rammed Earth

1.4.1 France

The French countryside spawned many earth construction techniques. The most notable is pisé de terre, or rammed earth. This monolithic construction method differs from cob in two ways: the use of forms to create walls of the required shape and the lack of fiber reinforcement. More details on rammed earth are available in Chapter 1.

The Centre International De La Construction en Terre (CRAterre-EAG) (International Center for Earth Construction), a research organization within the National Superior Architecture School in Grenoble, France, published a thorough book dealing with the history and technical details of each major earth construction system [31]. This work provides some soil analysis as well as many successful historical building detail designs and construction techniques. Many of the sources drawn upon are from the French countryside, where the primary members of the center are located. The CRAterre research group remains active in research and in partnership with the Grenoble School of Architecture.

1.4.2 China

Earth construction was developed independently in both the eastern and western hemispheres. Much of the early portions of the Great Wall of China is made of rammed earth. After stonework was further developed, rammed earth construction was still used for the internal volume of the wall combined with stone facing. Additionally, earthen housing was used for protection of extended families and small villages. One of these clusters of buildings is now a UNESCO World Heritage Site. UNESCO describes the site as “Fujian Tulou (China), 46 multi-storey earthen houses built between the 12th and 20th centuries over 120 km in south-west of Fujian province” [82].

1.5 Adobe

1.5.1 New Mexico

New Mexico architecture adapted well to the hot dry desert climate by using earth block and mud slurry construction techniques. The native tribes living along cliffs used puddled adobe techniques to create iconic dome-shaped dwellings. Desert and mountain-dwelling natives as well as the subsequent Spanish inhabitants used discrete earth blocks and more rectilinear architecture to create dwellings that remained cool in hot desert conditions. Modern construction in traditional or modified adobe remains common to this day. New Mexico dedicates a portion of state building code to designate minimum safe, standard building methods in earth with or without cement modification. At the time of writing, New Mexico is the only state to adopt standards for earth construction of any sort.

1.5.2 Rome

An analysis of earthen materials used in Roman buildings tested constituent materials and resulting strength. Specimens showed a strength of 0.1-0.2 MPa in compression. An analysis of the constituent materials also showed that the sand grain size influenced compression modulus, that straw content influenced failure rate, and that the ideal clay content for peak strength was 12%-16% by weight [69].

1.5.3 India

Block-based earthen construction was also used in the dry regions of India and Tibet. One such structure are the Basgo Gompa (Maitreya Temples). These temples are located in the Himalayan foothills and built during the 16^{th} and 17^{th} centuries [89].

1.6 Sod

Sod construction is the removal of blocks of earth intact and drying and stacking these blocks into simple structures. Roots and other organic material can provide some reinforcement to the soil blocks. Sod construction provides a rapid method of constructing housing, but has typically been used as a temporary means of shelter while a more reliable home is constructed.

1.6.1 Wales

The welsh folk tradition of *ty unnos* (house in one night)held that if a person could build a house with four walls and a door in a single night and have smoke rising from the chimney at dawn, they had rightful claim to the site of waste land [58]. Due to the speed of construction, these houses often used sod walls in the initial construction [80]. These sod walls would soon be torn down and replaced with stone or other more permanent materials after the claim to land was recognized.

1.6.2 Oklahoma

Rapid construction using sod for the purposes of claiming land was also a common practice in the Oklahoma settlement in the late 1800s. Prairie grass provided fiber reinforcement to sod blocks, and blocks could be cut using a sod plow and shovel [64]. Sod houses were often semi-recessed into hillsides or below grade to reduce the height of walls constructed and maintain a comfortable interior temperature.

1.7 Properties of Earth Construction

1.7.1 Practicality

Availability: Earth construction is one of the oldest forms of artificial human shelter. One significant reason for this is the availability of soils with cohesive properties suitable for building simple dwellings. Almost every continent contains examples of earth construction using available local materials (no evidence is available of historical earth construction in Australia and Antarctica). While wood and stone in suitable quantity and kind for building houses may be hundreds of miles away, appropriate earth for building is available in some quantity across much of the United States. Figure 1.1 shows the distribution of clay content in surface soils as collected in State Soil Geographic Data and analized by Miller and White [58].

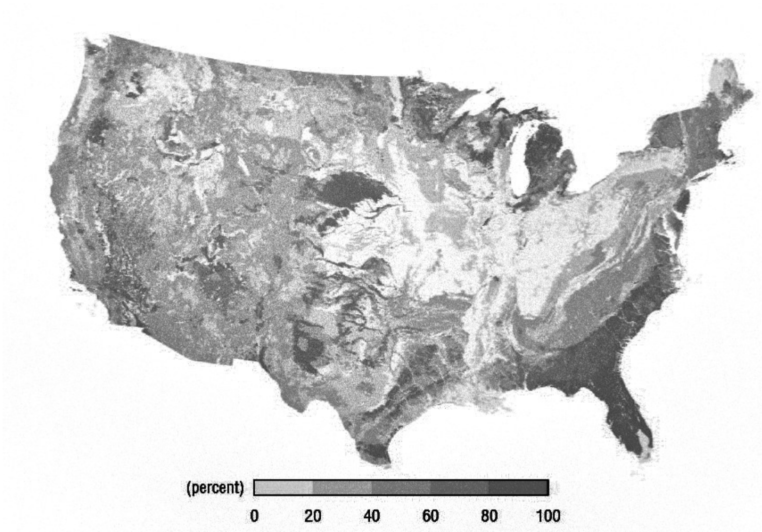

Figure 1.1: Clay contents of surface soil across the United States. Source: Miller and White [58]

Reduced material transportation and handling can also reduce cost, making inexpensive housing more broadly achievable. Using a material likely to be available closer to the build site reduces logistical requirements. Zami and Lee, in a literature review of economic factors of earth construction, found that the cost-effectiveness of cob is highly dependent on the quality of local materials and understanding of how to properly utilize local resources for durable building [93].

Ease of Construction: Earth construction is commonly simple to manufacture, allowing people with a wide array of abilities to contribute to the building progress. Cob, for example, can be mixed and added to the building in quantities scaled to the strength of the builder. The accessibility of earth construction is desirable for owner-builders of a wide variety of ages and physical conditions. Earthen construction can also scale with a variety of mechanization approaches. At the most basic, only a few buckets, a shovel, and a tarp are required to build cob walls. As speed and batch sizes scale, tractors can be used to mix large batches quickly, or automatic presses can produce large quantities of repeatable unfired compressed earth blocks without many operators.

Durability: Earth construction, when well built and maintained, is highly resistant to three of the four traditional elements: air, fire, and earth(qukes). While durability when exposed to water is poor, adhering to appropriate design guidelines for earthen material can mitigate risk for most regions.

Anecdotal and historical evidence suggests that earth walls withstand wind well. Earthen materials are typically dense, and earthen walls are commonly built between 18 and 24 inches thick. The significant compression forces generated by a single wall, when added to buttressing from intersecting walls, results in a structure highly resistant to wind loading. Roof beams may be anchored deep in the earthen wall to resist roof lift-off. The survival of earthen structures in high-wind regions such as those in Bam, Iran, where regular windspeeds of 8 m/s (18 mph) are recorded, indicates both dynamic load and erosion resistance [41].

Clay and sand do not burn, making earth walls resist to fire. According to most interpretations of English building code, cob walls do not quality as non-flamable, due to the inclusion of straw fibers [29]. However, when the wooden elements (loft floor joists, furniture, and roof) of a cottage in Oregon caught fire, the walls remained standing without evidence of damage, allowing wood floors and roof to be rebuilt. While further study is required to certify the fire safety of various earthen construction methods, experience shows that earthen structures are not highly susceptible to fire damage.

Historically, earth construction has shown varied resistance to seismic activity. Devastating earthquakes, such as in Ecuador in 2016, severely damaged many buildings even hundreds of kilometers away from the epicenter. Earthen construction is common in Ecuador, but many buildings failed during this disaster because national building codes, which include seismic considerations, were not followed for many buildings [67]. Various traditions of earth construction have shown good resistance to earthquakes. In New Zealand, earth construction has been performed for 150 years, and the oldest earthen house standing was built in 1841. Even earthen structures in the most severe earthquake zones that were built to siesmic building codes have survived well. [34]. The addition of fiber reinforcement in cob, such as these houses, provides residual tensile strength even when cracking in material forms, potentially delaying or preventing total structural failure. Well-built earthen materials that adhere to appropriate building codes can be built safely even in severe earthquake regions.

Comfort: Earth construction has remained common in may regions of the world because of the human comfort it can provide. In cold regions, Inuit people would partially recess their houses into the ground for shelter from wind and to maximize heat retention. In hot regions, traditional Middle Eastern houses maintain comfortable temperatures throughout the day capturing and releasing heat during the high daily temperature swings of much of these arid regions. Earthen materials have a significantly higher specific heat than a typical wood-frame wall, changing the thermal behavior of the whole structure. If well designed, this can lead to a reduction in heating and cooling requirements by capturing heat during peak temperature times and releasing it as temperatures fall.

Safety: The resistance of houses to forced entry was of critical importance for much of the time of development of earth housing. While still important today, the ability for a house's walls to resist attack is a secondary consideration to structural properties, environmental, and health factors of a material.

The use of fewer processed materials in favor of earthen materials may reduce exposure hazardous chemicals. In 2015, housing materials company Lumber Liquidators was found to have sold laminated flooring emitting up to twenty times the quantity of formaldehyde legally allowed. Volatile Organic Compounds (VOCs) like formaldehyde are present in many housing products, such as wood laminates and latex paint, and can cause a range of health problems, from eye irritation to organ damage and cancer [35]. The health concerns related to chemical exposure from modern housing materials has influenced some owner-builders to choose earthen materials for significant portions of the construction.

1.7.2 Environmental

Reduced embodied energy: Embodied energy is a common method of measuring the quantity of energy required to produce a material or product. A similar metric is embodied carbon, measuring the quantity of CO_2 produced or emitted. Both of these metrics typically include raw material extraction, refinement, and manipulation, transportation, use, and end-of-life processes [91]. Cement, for example, requires high temperatures to produce, and is energy-intensive to mine and transport. However, during curing, cement absorbs significant quantities of CO_2, somewhat reducing net emissions.

Earthen materials are commonly extracted from sites near the construction site. Sand often requires higher energy to extract and transport to the construction site. Straw requires minimal energy to harvest and include in earthen materials. A various comparisons of life-cycle energy required to produce a concrete block building and an earth block building have shown that earthen buildings require significantly less energy to create than concrete or wood structures [37, 52, 55, 74]. Heating and energy analysis shows that, despite having poorer insulation properties, earthen walls can effectively regulate interior temperatures through thermal mass [28].

High Reusability: Sand is a valuable global resource being rapidly consumed by modern construction practices. The typical recipe of concrete calls for roughly equal weights of sand and cement for peak strength [79]. The use of sand, primarily driven by concrete-based construction, has grown 23-fold between 1990 and 2010. This sand is being encased in concrete and can only be re-used with great difficulty, and the mining of sand is causing significant damage around the world [81].

While many forms of earthen construction require the addition of sand to local clay soil, sand used in earthen construction is not chemically bound to the material, unlike in concrete. As houses are torn down, sand used in the construction may be reclaimed or the earthen material may be completely reused in a new structure. Little research exists discussing properties of earthen materials after construction, demolition, and re-use, but experienced cob builders have found no tangible difference between recycled and virgin material.

1.8 Justification for Selection of Cob

With renewed interest in low-energy, environmentally friendly building materials, earthen construction has experienced in increase in recent research. Most of these research initiatives focus on the strength challenges of block-based earthen design, including strengthening mud morter joints [20], using novel additives to give earthen structures improved performance [92], and implementing re-bar-like structural reinforcement [32]. However, cob has seen only a small body of extant work when compared with rammed earth or adobe. Cob exhibits a combination of a fiber-reinforced material and monolithic construction technique that is unique in earth construction. Design using cob can be performed without consideration for the building unit scale, and load transmission and analysis is greatly simplified.

Cob is desirable for many owner-builders because the structure can be built without formwork, as is required for rammed earth, and does not require straight walls or dimensions equal to an integer number of blocks, as are common in adobe construction. Arches, curved walls, and round windows are common traits of cob houses. As noted above, cob requires minimal equipment to begin producing. The design freedom and minimal required equipment for cob construction entices owner-builders.

Cob was first developed, both historically and in the US-based renaissance, in conditions generally considered un-advisable for earth construction. Devon and Wales are exposed to driving rain and long, damp periods without a bright sun to bake the walls of houses dry. The Cob Cottage Company, located in Coquille Oregon, sees an average annual rainfall of over 55 inches, yet has not experienced a structural failure in any of the 10 or more cob buildings on the campus [83]. The use of cob is not limited to arid or hot regions typically associated with earth construction, and therefore offers a promising means of creating geographically broad interesting earth building.

In addition to industrial and owner-builder interest in further data, cob offers significant complexity in modeling the various mechanisms which contribute to mechanical behavior. As discussed in Chapter 2, prior academic work has tested various parameters, including straw content, clay content, and moisture content, of cob, but no work has proposed a model for predicting the strength of earthen materials. A model for strength would allow standards to be written ensuring safety of construction while minimizing cost of each new earthen building. Cob is being seriously considered for inclusion in the International Building Code, and a thorough understanding of critical factors influencing strength is necessary for efficient, reliable construction.

The goal of this work is to provide descriptive models of the strength of cob with respect to the critical parameters of water, clay, and straw content. Other factors, such as the significance of different regional clays and geometry of test specimens, are also examined. This work does not set out to test the significance of all possible variables influencing the behavior of cob, but simply establish initial models against which future data may be compared.

CHAPTER 2

HISTORY AND LITERATURE REVIEW

2.1 Overview

This chapter examines the traditional and scientific heritage of cob building. Available historic documents describe traditional and ancient methods of cob construction and regions in which cob building was most prevalent. Scientific results through the last century inform expectations for cob mechanical, thermal, environmental, and economic performance. Despite the long history of use and research, a quantitative understanding of cob's mechanical and structural performance still contains significant gaps. Construction with earth is regulated and accepted in some regions, though the United States currently has no nationally accepted building codes for cob construction. Finally, standards from various governments and regulatory bodies currently govern the testing of relevant earth construction materials.

2.2 Introduction

Earthen materials are some of the earliest known choices for creating human shelter. Sand and mud are still a rich creative medium for artists and the source of entertainment for children. However, this ancient construction material has largely been abandoned by the developed world for structural use.

In developing regions of the world, highly adapted traditional earthen construction techniques have are being paired with, or replaced by, modern manufactured materials [36]. In some cases these materials can improve quality of life for reasonable material costs. However, when the chosen building materials or construction are ill-suited to the environment, poor interior housing conditions can lead to increased rates of illness [22].

As discussed in Section 1.3, earth has been used to create shelters in a large variety of methods and combinations of materials. Cob has been used to create robust homes in harsh environmental conditions and shows promise for use in a wide variety of climates. The remainder of this chapter will largely focus on cob construction, including any monolithic and fiber-reinforced earth construction. However, experience applicable to cob from other earthen materials, such as rammed earth and adobe, will be referenced wherever possible.

2.3 Historical Cob

Cob was developed primarily in the United Kingdom, a region that would be typically considered unsuited for earthen building. The driving coastal rains, long periods of moist and cloudy weather, and often bitter cold would be expected to make a quagmire of any earthen building project by anyone from a more typical earth building tradition. Despite the environmental challenges, the earthen houses of Devon and Wales continue to provide safety and warmth to their occupants, sometimes hundreds of years after their construction.

England and Wales are home to the largest documented quantity of monolithic cob in the west. The material commonly called "monolithic cob" or simply "cob" is a mixture of sand, clay, and straw formed into a continuous solid wall without using discreet, joined blocks. The traditional cob of the U.K. was born from necessity and conveyed largely by oral tradition and experience [45]. A vignette of peasants searching for soil of sufficient quality for construction is depicted in the film Monty Python and the Holy Grail. One peasant comments to an approaching friend with a cart that "...there's some lovey filth down here." The rich and sticky soil surrounding this character indicates the gathering of clay-rich soil, possibly for cob construction [40]. The cob in these buildings was built to be sufficiently strong, but no systematic studies were recorded seeking to maximize the performance of the resulting buildings. Consequently, modern cob building efforts pay great respect to the traditional methods but do not limit themselves to these older ways.

2.3.1 Devon

The county of Devon, England, is particularly famous for a longstanding tradition of cob construction. Thirty to forty thousand cob houses are estimated to remain standing in Devon county alone [86], some dating back to the 14th century [60]. Cob construction is so common that both the Devon Historical Buildings Trust and Devon Earth Building Association (DEBA) have published on cob construction techniques, material properties, and maintenance.

The Devon Historical Buildings Trust compiled two publications detailing the history and maintenance of cob buildings [30, 50]. The first provides an introduction to the cob material and construction methods. The second addresses common structural concerns, regular desirable maintenance, and signs of compromised structural properties in cob walls. These contain much historical and descriptive information but are based on builder experience and do not provide quantified guidelines for damage evaluation or reconstruction.

The Devon Earth Building compiled a historical and technical overview of cob building regulation in England over the past 350 years [29]. In addition to historical context, the ability of cob to meet key points of regulatory language is addressed.

In partnership with the Devon Earth Building Association, the University of Plymouth performed experimental research on laboratory cob material samples and local Devon buildings. The work of Steven Goodhew [42] provided a thorough in-situ analysis of thermal performance of cob walls in buildings located in Devon. The active transient thermal probe technique used is able to evaluate test materials or in-situ structures. This work found that cob block with straw fiber reinforcement had a thermal conductivity of 0.5 W/mK and specific thermal capacity of 923 J/kgK at a typical test site. Modern fiberglass insulation, for comparison, has an average thermal conductivity of 0.008 W/mK [66]. Thermal diffusivity was also calculated for future thermal modeling of buildings.

2.3.2 Wales

Like Devon, Wales has a long history of earth construction. ‘Clom’ is the local name for structural earth similar to cob, except that rushes were sometimes substituted for straw. This material was used for hundreds of years to create farm cottages, some of which survive to this day. Earth building with hand-laid, straw-reinforced material was seen as a sign of poverty in much of the development of Wales, and stone supplanted clom construction where possible by 1900 [4].

Work is ongoing to maintain or restore historic earth buildings throughout Wales [26] and to study how earth construction interacted with social status, available materials, and technological development of European society at large [33, 39]. Like cob, clom was used for its low cost, accessible materials.

2.4 Scientific Investigation

In the wake of the destruction caused by World War I, and again after World War II, Sir Clough Williams-Ellis observed that the brick-manufacturing capabilities of the United Kingdom were insufficient to rebuild quickly. Remembering the more traditional houses made from cob and other earth construction techniques, he worked to systematically test these construction materials. He proposed that earth construction would provide a superior material to rebuild the U.K. housing than brick because it required almost no transportation to construction sites, was inexpensive, and could be utilized across the nation without overtaxing the brick production facilities [88].

In the early 1940s, the United States Department of Commerce, through the National Bureau of Standards (later NIST), conducted a comparative test of five earthen wall materials [87]. The purpose of the study was to provide engineers and architects with a more complete set of structural, thermal, and water-permeability data on various earth construction methods. A comparison of the strengths of wall sections of adobe block, bitudobe block, monolithic terracrete, terracrete block, and rammed earth showed moderate compressive strength and high impact and racking strength when compared with traditional wood or concrete block construction. Adobe block walls were found to have an average compressive strength of 200 PSI when tested in compression at a wall-section scale. Like today, the goal of this work was to provide designers and engineers with a quantitative understanding of earthen materials to allow greater use of earth for residential construction. The report refers to popular articles discussing using earth for low-cost housing at this time, but little technical work other than this was found.

2.4.1 Oregon Cob

The introduction of cob to the United States was begun by Ianto Evans, Linda Smiley, and Michael Smith in Oregon in 1993. Using a personal observation of traditional cob structures and stories of construction methods, these three reconstructed (and where necessary reinvented) structurally sound cob construction techniques. The resulting techniques differed from English methods and architectural taste in order to adapt to the materials and climate of the Oregon coast. Their methodology for design, materials, and construction is laid out in The Hand-Sculpted House [38] and The Cobber's Companion [75].

Oregon Cob techniques have become the de facto method of cob construction in the United States. Michael Smith continued to write on natural building using cob and other appropriate materials in The Art of Natural Building [51]. Oregon Cob techniques were adopted by Snell and Callahan in Building Green [76].

Work to produce code language for inclusion in model code such as the International Residential Code has been undertaken by The Cob Research Institute. This non-profit organization is made up of structural engineers, architects, and cob builders. A submission for a cob-construction appendix in the International Residential Code is being prepared for submission in Q1 2019.

Work by student teams from Santa Clara University have evaluated in-plane and out-of-plane shear strength of cob wall sections [24]. Average compressive strength of specimens tested was 0.786 MPa (114 psi). Specimens tested in four-point bending showed an average flexural strength of 0.375 MPa (54.4 psi). Cyclic shear testing was also performed, comparing methods of earthen wall reinforcement. Four point bending strength of cob beams was also evaluated by a student team at Santa Clara University, finding that beams of both 1% and

2% straw by weight achieved an average bending strength of approximately 0.214 MPa (31 psi) [54]. Comparison of bending behavior of cob made with 1% and 2% straw by weight showed an increase in strain to final failure with increasing straw content.

Wall sections were tested for seismic resistance using earthquake data from the magnitude 7.7 El Salvador earthquake of 2001 by students at the University of Technology Sydney [3]. Walls were tested scaled earthquake simulation data, ramping from 25% to 150% of the recorded earthquake intensity. For all four specimens, the shake table was unable to produce sufficiently high accelerations to cause failure in walls with and without bamboo reinforcement. An evaluation of earthquake resistant earthen design and case studies is presented by Minke [59].

Research conducted at the University of San Francisco found that prismatic specimens made with long straw fibers exhibited reduced peak compressive strength but improved ductility and energy absorption compared with traditional or chopped fiber specimens [71]. Long fiber specimens also exhibited reducing density. Table 2.1 shows the average results of specimens tested in compression and three point bending.

Table 2.1: Strength observed in prismatic adobe specimens by Rizza [71].

Straw Type	Compressive Strength [MPa (psi)]	Bending Strength [MPa (psi)]
Chopped Straw	0.522 (75.75)	0.977 (141.73)
Traditional	0.487 (70.71)	0.535 (77.56)
Long Straw	0.282 (40.86)	0.796 (115.39)

2.4.2 Modern English Cob

Much of the modern research from English universities has evaluated as-built cob structures or material. In England, new building in cob is scarce [56]. Kevin McCabe is the central figure in new cob construction, working with many respected natural builders and regulatory agencies to create highly efficient, beautiful natural dwellings in cob and straw bale using traditional, local designs and materials.

Research has been proposed by students at the University of Plymouth on the properties of cob with respect to constituent materials: sand, clay, straw, and moisture [86]. Characterization of a local soil and the resulting cob mixture was completed by Matthew Green two years later [43]. Time domain reflectometry probes were used to measure wall section moisture in-situ. His work also evaluated strength and modulus with respect to mix ratio and moisture content. His work found an increase in in failure stresses with reduced moisture content and demonstrated viability and repeatability of material testing practices on cob. This work evaluated three mixes of differing aggregate volume fractions, and observed increased strength at higher soil contents. However, no work to model strength with respect to constituent materials was performed, nor work to examine the influence of fiber reinforcement on strength.

Building With Earth: A Handbook provides detailed technical steps to construct several variations of earth building [63]. Examining all steps of construction, from soil analysis to wall finishes, Norton provides detailed and accessible techniques for constructing reliable structures using a variety of earth construction techniques. Field assessments of soil suitability and strength testing are also discussed.

2.5 Building Codes

In regions with many historical earthen structures, building codes have often been created to regulate safety of renovation and new construction using traditional methods. In the United States, these codes are implemented at a state level, and are implemented in only two states to date. Around the world, several countries have established national building codes to govern earth construction. Both United States state code and international code are being used as sources for writing a global model code, submitted to the International Code Council.

New Mexico Earthen Materials Building Code (New Mexico Adobe code) provides the de facto earthen building code for earth construction around the United States, despite being legally binding only in its own state [62]. The New Mexico code is the most complete set of standards for earthen construction currently accepted in the United States, and specifies minimum material properties, material reinforcement, and acceptable design practices. The code requires that adobe that does not contain any cement or lime (unstabilized adobe) may not be used within four inches of finished floor grade and must exhibit a minimum compressive strength of 300 PSI (2.07 MPa) and minimum modulus of rupture (strength in three point bending) of 50 PSI (0.345 MPa). Standards are also established for strength sampling rate from units used for construction and allowable specimen failure rate. When applying for special permitting for earthen construction, cob builders most commonly cite the New Mexico Adobe Code as a common basis for material strength.

California Historical Building Code briefly addresses the use of adobe for repair of historical buildings [25]. The California code establishes maximum height-to-thickness ratios for adobe walls (6 for first floors, 5 for second floors). Other than this, the brief discussion explicitly allows the use of adobe in historical structures, but does not provide means for using it in new construction.

Australian Earth Building Handbook provides siting guidelines, material specifications, acceptable design practices for earthen construction of residential single- and two-story structures [85]. The code states that these are for "lightly loaded" structures, as would be typical for residential construction outside of intense earthquake risk zones.

Indian Standard guidelines for improving earthquake resistance of earthen buildings outlines both material and design standards for earthen construction [47]. The standard discusses wood and metal wall reinforcement, material strength and typical load requirements, and recommended patterns for adobe block wall construction. The standard outlines a simple flexure strength field test: A 60-70 kg person standing on the center of a block supported on a span of 250mm should not cause failure in a block of adequate strength. Additionally, a compressive strength of 1-2 MPa is specified.

Peruvian earthen building standards provide design requirements for reinforcement of walls and design of structural elements to resist brittle failure during moderate and severe earthquakes [84]. Peru and Ecuador both experience intense seismic activity and have a tradition of adobe construction. This leaves many buildings vulnerable to damage or collapse, as occurred in the 2016 Ecuador earthquake killing at least 668 people.

ASTM D2392 references three additional national building standards which govern earthen construction: Chinese building standards, Ecuadorian Earthen Building Standards, and German Earthen building standards.

Finally, a unifying model code governing construction with cob was submitted to the International Code Council as an appendix to the International Residential Code in Spring, 2019. This model code is intended to unify standards from various regions. Adoption of this appendix would not be binding on any jurisdiction but could simplify the adoption of earth construction standards by areas that currently have no such regulation.

2.6 Material Testing Standards

For this work, American Society of Testing and Materials (ASTM) standards were chosen as the system of test standards for material characterization. ASTM standards govern a wide range of test processes, including the testing of common materials like concrete. Standards were examined which govern the characterization of soils, clays, and sands for descriptive and quantitative analysis. Where possible, standards were directly applied to strength tests conducted. When no standard directly addressed the testing of earthen materials, related standards from concrete and composite materials were referenced.

ASTM E2392, "Standard Guide for Design of Earthen Wall Building Systems," provides a standard for some design elements and simple construction using various earth building methods [16]. E2392 defines cob as:

> **cob** *noun* — a construction system utilizing moist earthen material stacked without formwork and lightly tamped into place to form monolithic walls.
>
> *Discussion* — Reinforcing is often provided with organic fibrous materials such as straw.

In Oregon cob, the earthen material (clay-rich soil) is commonly mixed with sand to bring it to the appropriate strength and plastic state. For this work, soils were amended with sand and reinforced with wheat straw.

2.6.1 Soil Characterization

The need for robust soil characterization methods for reliable construction and agriculture has created a large set of standards characterizing many aspects of soil behavior. Catagorization and comparison of soils can be done using a formal classification system, as discussed in ASTM D2487 “Classification of Soils for Engineering Purposes (Unified Soil Classification System)” [11], or in more qualitative and descriptive terms, as in ASTM D2488 “Standard practice for description and identification of soils (visual manual procedure)” [7]. Both of these standards evaluate various texture, color, cohesion, and water retention properties to approximate the sand, silt, and clay contents of a soil and determine suitability for different uses. These also establish a common set of descriptors by which soils from different sites can be directly compared.

The behavior of many soils is tightly linked to the size of particles involved. Particle size provides the definition for distinctions between sand, silt, and clay, for example, though clay also differs chemically from sand and silt. Three test methods were used for determination of particle size distributions in this work. The first, ASTM C136 “Standard Test Method for Sieve Analysis of Fine and Coarse Aggregates,” was used to determine the particle size distribution of masonry sand added to the cob mixtures [19]. Second, ASTM D422 “Standard Test Method for Particle-Size Analysis of Soils” provides a general test method for using wet sieve methods to determine the particle size distribution of soils [12]. The use of mechanical sieves limits this method’s use for testing clay rich soils, which contain many fine particles. To address this deficiency, ASTM D1140 “Standard Test Methods for Amount of Material in Soils Finer Than the No. 200 (75-um) Sieve” can be used to test clay-rich soils effectively [6]. This test uses density measurements of the soil when agitated and while settling to the bottom of the vessel to determine particle size distribution.

Angularity and sand shape can have significant influence on strength of concretes [21] and therefore are likely to influence cob strength. ASTM D5821 "Standard Test Method for determining the percentage of fractured particles in coarse aggregate" provides a method of visually classifying fracture surface area of particles [18].

Water content can play a significant role in the behavior of soils. Determination of water content in a given soil is performed according to ASTM D2216, "Standard Test Methods for Laboratory Determination of Water (Moisture) Content of Soil and Rock by Mass" [17]. The description of soil behavior at various water saturation states is typically accomplished using the Atterberg limits of plastic limit and liquid limit. Plastic limit is the minimum water content at which a soil will behave plasticity. The liquid limit is the water content at which soil will flow at a specified rate when the test vessel is agitated. These two water contents are then used to calculate the plasticity index of the soil, which can be used for predicting behavior across a range of water contents. ASTM D4318, "Standard Test Methods for Liquid Limit, Plastic Limit, and Plasticity Index of Soils" provides the standard method of performing these tests [8].

2.6.2 Material Strength

Material strength characterization is critical for any construction material. Earthen materials, like cob, also require consistent methods of describing strength for each of the various loading methods: compression, bending, shear, and tension. This work examined only compression and three point bending (flexure) of cob specimens.

Compression testing was performed in accordance with ASTM D2166, "Standard Test Method for Unconfined Compressive Strength of Cohesive Soil," for testing cylindrical specimens [17]. Elements of testing from ASTM D2166 were combined with the required elements of the New Mexico adobe code for testing prismatic specimens.

Three-point bending was performed according to ASTM C78 "Standard Test Method for Flexural Strength of Concrete (Using Simple Beam With Center-Point Loading)" [13] and ASTM C1609 "Standard test method for flexural performance of fiber-reinforced concrete (using beam with third-point loading)" [14]. These standards govern the design of bend testing fixtures, test machine operation, and data analysis, including stress calculation. ASTM C1609 also includes standards for evaluating residual strength induced by fiber bridging of the fracture in concrete, similar to the behavior seen in cob. Toughness of materials can also be tested in bending by ASTM C1018, “Standard Test Method for Flexural Toughness and First-Crack Strength of Fiber-Reinforced Concrete (Using Beam With Third-Point Loading)” [5]. In the case of unreinforced concretes and earthen materials without fiber reinforcement typically exhibit very low fracture toughness.

2.7 Conclusion

Earthen construction, including cob, has been used for housing for hundreds of years. When such construction was common, best practice was passed on by oral tradition and experience gained under master builders. As industrialization changed housing, these more ancient materials were exchanged for manufactured goods, like milled timber and fired brick. However, at various points through the 20^{th} century, earthen construction was examined seriously as a lower cost and more available option for the mass housing needs created by destruction from war and a booming population. However, only in the past 30 years have serious, scientific examinations of earthen construction become more frequent. These include academic research both in the United Kingdom and the United States, where methods of cob construction have diverged somewhat.

Building codes governing earthen construction are inconsistent and largely completely absent in the United States. Various national standards governing earth construction are available, but these do not unify material requirements and design recommendations. A proposed International Residential Code amendment would provide a model code for adoption by US states and national governments.

ASTM standards provide a basis for most experimental tests in this work. These test methods make data from this work repeatable between researchers and add to the body of work supporting the careful and safe use of earth for residential construction.

CHAPTER 3

CHARACTERIZATION OF CONSTITUENT MATERIALS

3.1 Overview

This chapter discusses the evaluation of the constituent materials (sand, clay, and straw), used for experimental cob testing throughout this work. The physical and mechanical properties of the constituent materials may have a significant influence on the behavior of the final composite material. This chapter describes the characterization of the sand, clay, and straw using a broad range of characterization techniques, including both quantitative ASTM standards and qualitative traditional field methods.

3.2 Introduction

One of the challenges in both cob research and cob construction is the variability in constituent materials. Clay-rich soil is often sourced from the construction site itself. Such soils vary widely in clay content and other qualities. Finding suitable sand on-site is less common, often requiring sourcing from commercial quarries. In either case, variability in source rock, grading, and washing procedures may alter sand grain behavior in cob. Straw employed for cob construction may have widely differing properties based on variety and treatment. Winter wheat is generally recommended as having the highest strength and clay adhesion, while maintaining low thermal conductivity [38], but other materials with varying properties are used as well [92, 38].

3.2.1 Traditional Field Tests

Throughout the centuries of traditional cob construction, builders have used several qualitative tests to evaluate soils for use in cob structures. Builders engage as many senses as possible to understand the materials, such as rolling sand across the tongue to estimate roughness or listening to the sound created when malleable cob is squeezed to evaluate ratios of sand to clay. Even playing tug-of-war with a small bundle of straw can provide an understanding of fiber breaking strength. These qualitative tests provide low-cost and rapid evaluation of site materials with little reliance on equipment. They are limited, however, in their ability to quantify material properties for regulatory agencies.

3.2.2 Test Standards for Construction Materials

The need for quality control in concretes, gravels, and many road-building materials has led to the development of tests standards for sands and soils. These tests typically evaluate the geometric characteristics of a sample or provide metrics for predicting load-bearing capacity. While routine for many labs and plants around the world, these tests are often expensive or inaccessible for owner-builders or on-site material evaluation. Three central ASTM standards provide quantitative and qualitative methodologies for describing soils used in this work. ASTM D2487, "Classification of Soils for Engineering Purposes (Unified Soil Classification System)" [11], determines particle size distribution, plasticity limit, and liquid limit quantitatively and employs specialized laboratory equipment for precise determination of these characteristics. ASTM D2488, "Standard practice for description and identification of soils (visual manual procedure)" [7], provides a mix of qualitative and quantitative tests for sands and soils. Many of the tests described in this standard are designed to be carried out in the field with little specialized equipment. These test methods use visual classification methods for sand particle angularity, soil dry strength, and soil plasticity, among others. Both of these test standards are applicable to sand-, clay-, or organic-material-rich soils, but ASTM D2488 is most directly comparable to traditional cob builder's field test methods. As a balance between the two, clay content determination can also be accomplished with minimal equipment through ASTM D422, "Standard Test Method for Particle-Size Analysis of Soils" [12]. This test determines particle size distribution for particles passing a No. 200 sieve using sedimentation testing augmented with a hydrometer to provide solution density data at several points during sedimentation. The inclusion of the hydrometer removes much of the ambiguity from the traditional settlement test process while relying on the same underlying physical mechanism.

Tests from cob construction tradition and ASTM standards were applied to the sand, clay, and straw used throughout this work. Test descriptions, methodologies, and results, are described for both qualitative material descriptions and quantitative material property evaluation.

3.3 Sand

3.3.1 Angularity Evaluation

Angularity of sand grains determine angle of repose and structural properties of sand as an aggregate. Microscope images were used to evaluate representative sand grains for geometric properties according to ASTM D2488. Figure 3.1 shows the scale presented in ASTM D2488 for evaluating sand grain geometry.

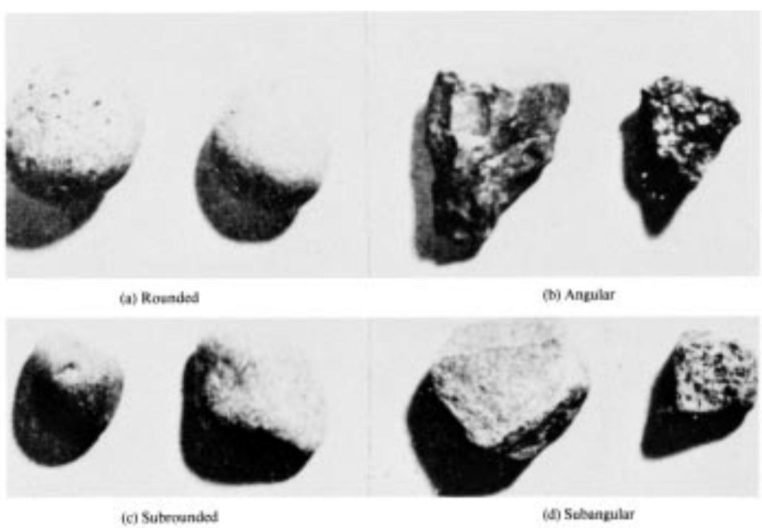

Figure 3.1: Four classes of sand grain angularity. Source: ASTM D2488.

Sand grains sampled from quarried masonry sand purchased for this work were primarily semi-angular, as shown in Figure 3.2. Though faces showed significant fracture surface, edges were significantly worn and few sharp points were observed.

Figure 3.2: Representative sample of sand grains observed under light microscopy.

3.3.2 Sieve Test

Sand particle size characterization was carried out through sieve screening. Six screen sizes were selected to provide directly comparable sieve data to Pullen [68]. Test procedure was according to ASTM Standard C136 [19]. Table 3.1 summarizes the sieve sizes and percent passing each sieve by mass. Two industry standard shape parameters, the Coefficient of Uniformity (C_u) and Coefficient of Curvature (C_c), were calculated for the sample.

Coefficient of Uniformity is calculated by Equation 3.1 and the Coeffient of Curvature is calculated by Equation 3.2. The variables D_x refer to the particle diameter that allows x percent of the sample to pass.

$$C_u = \frac{D_{60}}{D_{10}} \tag{3.1}$$

$$C_c = \frac{D_{30}^2}{D_{10}D_{60}} \tag{3.2}$$

According to ASTM D2487"Standard Practice for Classification of Soils for Engineer-

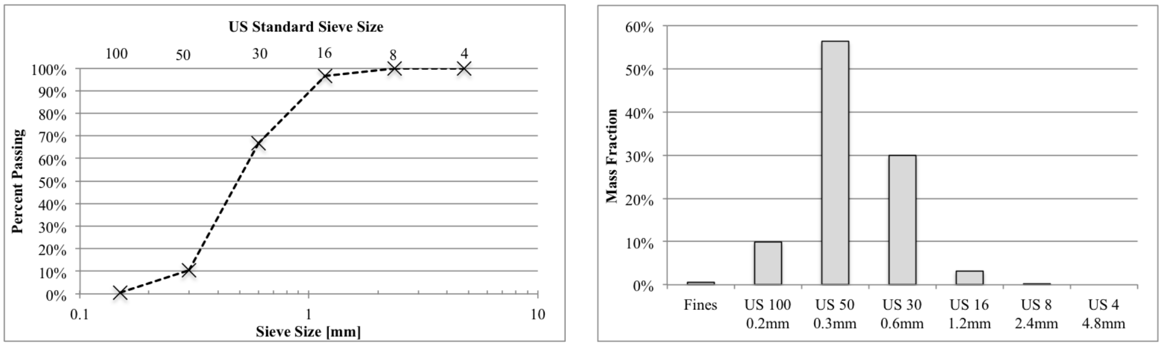

(a) Percent passing plot of sand sieve test. (b) Grain size histogram of sand sieve test.

Figure 3.3: Sand sieve test results.

ing Purposes (Unified Soil Classification System)" [11], the sand sample is classified as silty sand ($C_u \leq 6$ and $C_c < 1$).

Figure 3.3 shows the graphical representation of this particle size data. Figure 3.3a is the standard percent passing plot, while Figure 3.3b presents the particle size distribution curve.

3.4 Soil Analysis and Clay Content

3.4.1 Overview

Cob building often reflect both the aesthetic and structural properties of the earth from which they are built. Thorough characterization of the soils used for cob research allows data to be compared across various studies. Because no single best practice has emerged for characterization of soils for cob research or construction, a wide range of tests was conducted. This section presents a robust description of the soil used in this work for comparison against past and future studies.

3.4.2 ASTM Description

The clay-rich soil used throughout this work was obtained from a clay deposit near Chandler Park, Tulsa, OK[1] and was evaluated using ten descriptive properties, each in accordance with ASTM D2488. This soil is compared with several others in Chapter 7.

[1]Location of material source is recorded as 36° 7.51366980'N, 96° 5.44882980'W by GPS

Angularity The soil is composed of fine particles without an observable fraction of coarse sand. Therefore, sand angularity in the sample could not be characterized according to Figure 3.1.

Color Color ranges from rusty brown to umber, as shown in Figure 3.4. The umber layer was a distinct layer above the rust color layer.

Figure 3.4: Two distinct colors within the collected clay sample, shown dry.

Odor The odor contains mild decaying organic notes and wood odors.

Moisture When the sample was obtained from the site, entrained moisture was moderate. The outermost inch of soil was hard and dry, while soil below was moist but firm.

Calcium Content Hydrochloric acid was used to determine the presence and relative concentration of calcium carbonate. ASTM D2488 states that hydrochloric acid be applied to the soil and the rate of reaction be observed through surface bubble formation and classified as “none (no visible reaction)” , “weak (some reaction, with bubbles forming slowly”), or “strong (violent reaction, with bubbles forming immediately”). No reaction with 1M hydrochloric acid was observed. This indicates that the soil is not cemented with calcium carbonate.

Consistency Soil consistency and cementation were evaluated using a crushing and indentation test with bare hands. Soil consistency is classified by ASTm D2488 from very soft to very hard, based on the indentation of a thumb. The dry soil consistency was very hard, specified as "thumbnail will not indent soil."

Cementation Soil cementation describes the grain-bond strength rather than bulk hardness. Cementation is described as weak, moderate, or strong based on difficulty to crumble under finger pressure in bending. The soil cementation in this sample was moderate, requiring considerable finger pressure to crumble or break in bending.

Compressive Strength Soil dry strength is classified from none to very high based on strength in compression. The dry strength of the soil is very high, which means that samples cannot be crushed between a thumb and a hard surface.

Structure The structure of the soil is blocky. Large particles can be broken down into smaller angular lumps which resist further breakdown. Cracking seems to propagate between these smaller hard lumps, which are composed of clay, not stone aggregate. In situ, the soil exhibited some stratification, between colors of clay. A dark brown clay layer was observed close to the surface and between 12 and 24mm thick. The red clay was found beneath this brown clay.

Dilatancy No dilatancy was observed in the specimen, meaning that no water visibly accumulated on the surface of a whetted specimen when shaken horizontally. Likewise, no water was observed to be absorbed or released when a sample was squeezed.

Toughness Toughness testing of soil requires rolling the soil into a 1/8 inch diameter "thread" and repeatedly folding and re-rolling this thread. The thread of soil will crumble when it has reached the soil plastic limit. This test could not initially be performed at high water contents because the whetted soil was very sticky, adhering to both the rolling surface and the operators hands, preventing the forming of any thread. Plastic Limit, according to

ASTM D4318 is evaluated in Section 3.4.9. Toughness is classified as high from behavior in plastic limit testing, meaning that “Considerable pressure is required to roll the thread to near the plastic limit. The thread and the lump have very high stiffness.”

Plasticity Based on the soil behavior in plastic limit tests, the plasticity of the sample is high. According to ASTM D2488, “It takes considerable time rolling and kneading to reach the plastic limit. The thread can be rerolled several times after reaching the plastic limit. The lump can be formed without crumbling when drier than the plastic limit.”

Classification The above tests, all of which are specified by ASTM D2488, suggest a classification of the soil as “fat clay (CH)” from ASTM D2488 standard soil types. This class of soil sample is characterized by “high to very high dry strength, no dilatancy, and high toughness and plasticity.”

3.4.3 Visual Sedimentation Evaluation

Sedimentation testing, also known as the “jar test,” is described by both traditional cob builders and ASTM D2488 (Section X4.1). The purpose of the test is to visually estimate the proportions of sand, silt, clay, and organic matter present in a soil. In this test, a sample of soil is soaked and dispersed in water. The vessel is thoroughly shaken to distribute the sample throughout the volume, then left stationary while particles settle.

Measurements of the height of settled material on the bottom of the measurement vessel are performed at specified times, correlating to the volume of each class of particle sizes. Gravel is expected to settle first, followed by sand, silt, and finally clay. From Stokes law, particle settlement terminal velocity is proportional to the square of the diameter of the particle, for approximately round particles [61]. ASTM D2488 gives a settlement time of 20-30 seconds for sand to fall out of suspension. Michael Smith, in The Hand Sculpted House, states that coarse sand typically settles after 5 seconds, silt settles after 10 minutes, and clay settles out when the water clears, up to several days or weeks. Smith also recommends adding a small amount of soap or salt to the test as a deflocculant. A salt content of approximately

2-4% of the total soil and water volume has yielded positive results. A deflocculating agent, such as sodium hexametaphosphate, can be used for clay-rich specimens. A straight-sided jar is recommended by both Smith and D2488 so that the volume fractions of the sample can be estimated by measuring the height of each sediment layer. Smith advises marking the jar during the test with the sediment height after sand and silt have each mostly settled because a clear line between sediment layers is not guaranteed when the test is complete. When measuring relative volume proportions in this process, clay will have an artificially inflated volume due to the expansion of clay in the hydrated state, unlike silt, which undergoes no significant expansion in water. The quantity of expansion depends on the type of clay and the local soil, but hydrated expansion of over 50% is common for monmorolinite and illite clays [57]. Likewise, differences between sand and clay density prevent direct measurement of mass fractions, restricting results to volume fractions. Measurement of solution density using a hydrometer can mitigate this error and are discussed in Section 3.4.10.

A sample of soil was allowed to soak in water until the sample was fully hydrated. Sample was vigorously stirred to ensure no sediment remained on the bottom of the vessel. As soon as stirring stopped, the settlement time began. Thickness of the sand was difficult to observe because of the coloring and opacity of suspended silt and clay. Measured thicknesses and resulting volume percent are summarized in Table 3.2.

3.4.4 Palm Test

The palm test is a simple semi-quantitative test used for evaluating the clay content and behavior of a potential natural soil. This test is described in The Hand Sculpted House [38] and is common practice for many traditional cob builders. Water is added to the sample until it has a plastic and sticky consistency. If the sample does not become sticky no matter what, the clay content is likely too low to consider as a building material. When plastic and sticky, a golf-ball sized lump is pressed into the palm and the edges smoothed onto the palm. The hand is then turned palm-down and the fingers cycled from flat to perpendicular to the palm and back. This cycling of fingers is repeated until the sample delaminates and

Table 3.1: Sand sieve test results.

Sieve Size		Weight Percent Passing
U.S.	Metric (mm)	
4	4.75	100
8	2.36	99.9
16	1.18	96.7
30	0.6	66.8
50	0.3	10.5
100	0.15	0.6
Coefficient of Uniformity, C_u		1.93
Coefficient of Curvature, C_c		0.99

Table 3.2: Layer thickness results from jar sedimentation separation test.

Layer	Thickness [mm]	Volume %
Clay	13.7	26.9%
Silt	23.3	45.7%
Sand	14	27.5%

falls off the palm. A higher number of cycles generally indicates a higher clay content and more plastic and sticky soil.

Two samples of clay-rich soil were evaluated. One sample was taken primarily from each of the two color strata of clay observed, described in Section 3.4.2. Dry samples were moistened overnight and formed into test balls. Eight replicates of the first sample and nine replicates of the second sample were performed. The results of palm cycle testing are shown in Table 3.3.

Table 3.3: Cycles to sample delamination for the clay palm test.

	Average	Std. Dev.	COV
Overall	12.06	10.74	89%
Sample 1	8.75	4.30	49%
Sample 2	15.00	13.92	93%

These test results had large scatter. Though the clay was sticky to the touch for all of these tests, factors such as quantity of clay bonded to the palm prior to the test, moisture loss during repeated tests, and bonding pressure of clay to the palm reduced repeatability of test results. For example, the two initial tests of sample 2 had 8 and 51 cycles to delamination, respectively. The high variability of the test as currently performed reduces the precision of the resulting cycle count.

Water was added to the first sample after completing the eight standard tests and resulted in 221 cycles to delamination. This modification underscored the sensitivity of clay stickiness to water content. With sufficient water content, the clay cannot be formed into discrete lumps but acts as a paste capable of supporting its own weight and adhering to most surfaces.

The test is useful as a qualitative comparison of clay content and soil bonding ability between soils considered for construction. Plasticity, workability, and adhesion can all be quickly ascertained using a small sample of soil. Quantitative determination of plastic limit, discussed in Section 3.4.9, provides a more repeatable test method.

3.4.5 *Crack Test*

Like ASTM evaluation of soil toughness, the crack test, described in The Hand Sculpted House [38] states that soil whetted to a plastic state and rolled into a pencil-sized cylinder should be capable of being wrapped halfway around an index finger without cracks forming on the outer surface. Like the palm test, this simple test is rapidly assessed but us sensitive to water content and operator actions.

Exterior stresses are caused by bend radius of the cylinder of soil, rather than purely angle of deflection around the finger. Therefore, both a pinky and middle finger were used as mandrels of different diameters. Soil tested here performed moderately well in the crack test, breaking in four of six tests being bent over a pinky finger of diameter 14mm but breaking in none of the six tests bending over a middle finger of diameter of 16.5mm. Initial cracking before breaking is shown in Figure 3.5.

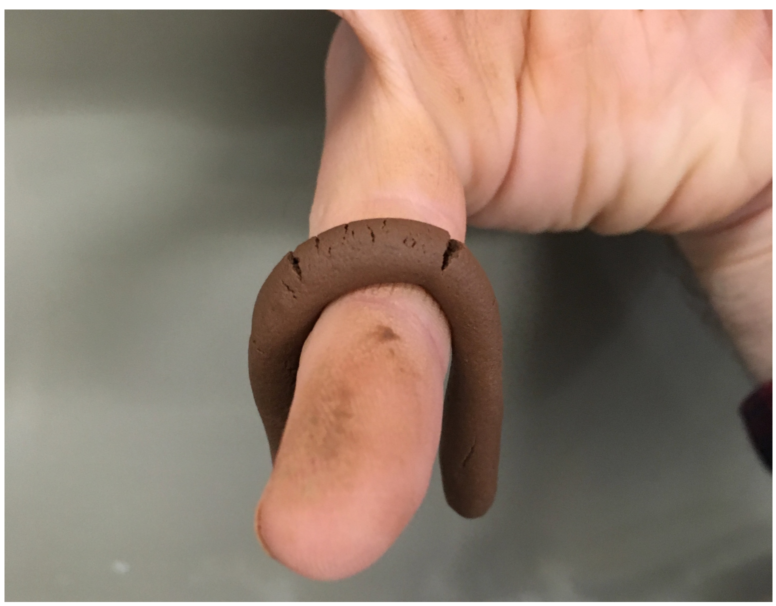

Figure 3.5: Soil characterization bend test performed on baseline soil.

3.4.6 *Wet Sieve*

Sieve testing provides quantitative particle size distribution data for a sample of sand or soil. Wet sieving is used for samples of containing fine particles or exhibiting cohesion when dry. Wet sieving of soil was performed in accordance with ASTM D-1140 [6].

Soil was dried at 110°C and dry weight was measured. Soil was then soaked in 350 mL of water and 4 drops of 5% solution of Calgon (active ingredients: zeolite, polycarboxylate) as a de-flocculating agent. Soil was soaked while stirring for 5.5 hours before wet sieving.

The soil-water admixture was slowly poured through the sieve stack. Additional water was added to capture all soil from the stirring vessel. Clean water was poured through the sieve stack until water was running clean from the bottom of the stack.

Each sieve was oven dried at 110°C while holding retained material. Sieves were dried to constant weight to determine dry weights of each soil size fraction.

The minimum sieve size used was 38μm. Clay particles are defined as those less than 2μm by ISO 14688-1:2017 [48]. Therefore, this test alone cannot distinguish between a region of the fine slit range (2–6.3 μm) and clay particles. Figure 3.6 shows the mass fraction of soil captured in each sieve. Fine soil fraction was calculated by subtracting captured soil from initial dry weight.

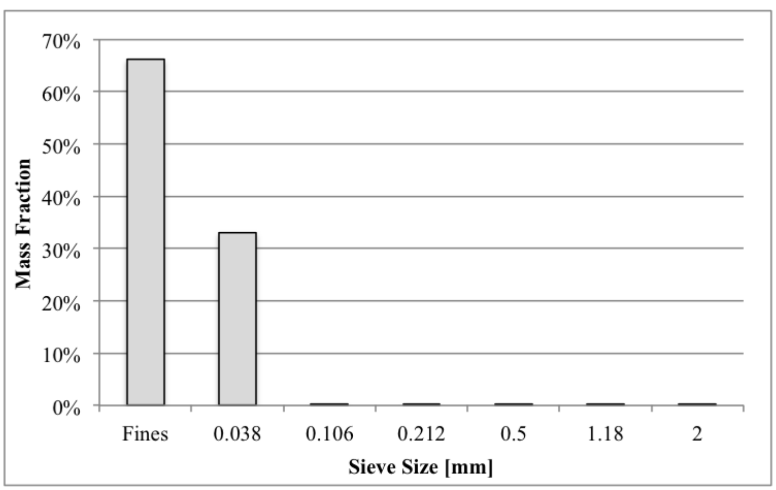

Figure 3.6: Mass fraction captured in each sieve for Chandler Park soil sample.

The particle size distribution plot reveals little about the characteristics of the soil because of the high concentration of fine and 38μm particles and almost complete lack of larger grains. Table 3.4 provides quantitative mass fractions from the wet sieve test.

Table 3.4: Mass fraction distribution in Chandler Park soil sample.

Size [mm]	Weight Fraction
Fines	65.96%
0.038	32.95%
0.106	0.41%
0.212	0.23%
0.5	0.23%
1.18	0.05%
2	0.16%

3.4.7 Dynamic Light Scattering

To determine clay fraction within fine materials passing through the $38\mu m$ sieve, dynamic light scattering (DLS) measurement was used. DLS measures particle accelerations from Brownian motion through light scattering to determine a particle size distribution of particles suspended in a solution. A sample of the fines from wet sieving were thoroughly re-hydrated and stirred to ensure even distribution of clay and silt particles.

The DLS specimen receptacle was calibrated to zero using tap water from the same faucet used for re-hydration of fines. Drops of fines suspended in water were added to the specimen receptacle until target opacity was achieved (as determined by the DLS control software). Analysis was performed quickly to prevent settlement of silt and clay particles in the suspension.

Figure 3.7 shows the particle size mass distribution observed under DLS. Using this, mass of all clay particles as a fraction of the total soil mass could be calculated.

Typical soil particle size distributions show fewer sharp discontinuities, casing doubt on the repeatability of this method of particle distribution measurement. High reflectance warnings also reduced confidence in this method. Surface treatments may improve particle size measurements by DLS, but the relatively complexity of this analysis method makes it less desirable than the alternatives presented here for clay content determination.

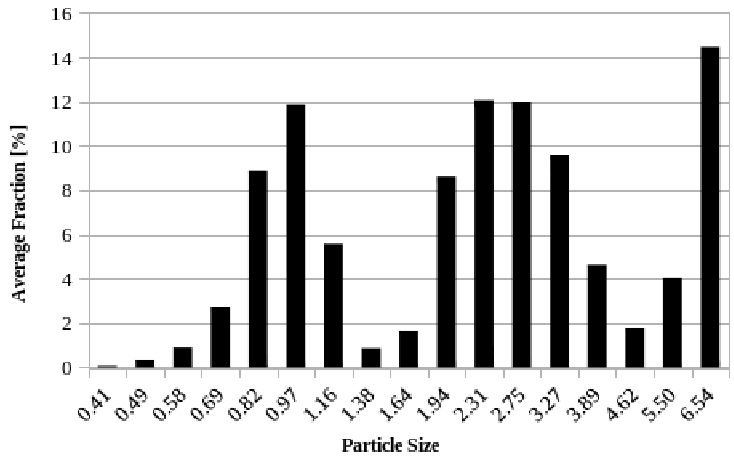

Figure 3.7: Particle size distribution calculated by DLS.

3.4.8 X-ray Diffraction

X-ray diffraction was used to determine mineralogical contents of the clay-rich soil used for testing in Chapter 4. Fine particles passing a number 400 sieve (38 μm diameter) were dried, powdered, and packed for x-ray exposure. A sweep between 3 and 20 degrees was used for wide-spectrum identification.

Modeling software Winmax was used to fit known responses of standard minerals to the observed response curve. The fitted model accounted for 76.74% of the observed response. Table 3.5 shows the materials identified during modeling.

X-ray diffraction modeling calculated a clay fraction of 72.3% in particles passing the 38 μm sieve from baseline soil wet sieving. When x-ray diffraction and wet sieving results are considered together, the resulting clay content is 47.69%.

3.4.9 Plastic Limit

Procedure for determining plastic limit is specified in ASTM D4318 [8]. Plastic limit is determined by repeated rolling of a soil specimen into $\frac{1}{8}$-inch cylinder until material fails to be sufficiently deformable to be rolled to the target diameter. At this point, the material is placed in a closed container. After more than 20g of soil have been collected in this manner, the soil and vessel are weighed and oven dried at 110°C, as specified in ASTM D2216 [15].

Table 3.5: XRD model results for baseline clay soil fine particles.

Mineral	Weight Fraction
Illite (di-octahedral)	23.7%
Smectite (di-oct) - 2 H2O layers	20.9%
Smectite (di-oct) - 1 H2O layer	13.4%
Quartz	12.5%
3:1 I:S Mixed Layer Clay	7.6%
Kaolinite	6.7%
Orthoclase	5.8%
Na>Ca Plagioclase	5.7%
Hematite	1.4%
Calcite	1.0%
Biotite - 1M	0.8%
Dolomite	0.4%

Plastic limit is given by the whole number moisture content average of two trials. Plastic limit for baseline (Chandler Park) soil tested throughout this work was found to be 33%.

3.4.10 Hydrometer Sedimentation

ASTM D422 specifies a procedure for performing sedimentation testing using a hydrometer to determine solution specific gravity at various points throughout the procedure. Direct measurement of solution density provides quantitative results without the limitation of correctly recording the top surface of settled material through poor solution visibility noted in Section 3.4.3. Correction for temperature variation and reading values at the top of the meniscus are performed simultaneously to calibrate the hydrometer to actual materials used. Soil is stirred with a fixed amount of sodium hexametaphosphate for a minimum of 16 hours before the start of testing to thoroughly separate clay particles from the surface of sand and silt particles.

Measurements are to be taken approximately 2, 5, 15, 30, 60, 250, and 1440 minutes after start of the test. Particle diameter is determined by the duration since the start of

Table 3.6: Clay content measured for baseline (Chander Park) soil.

Method	Calculated Clay Content
Visual Sedimentation	26.9%
X-ray diffraction	47.69%
Wet sieve + DLS	35.4%
Hydrometer Sedimentation	25.95%

the test and depth of the hydrometer bulb. Percent passing is determined by the mass of soil in solution as measured by the effective solution density at the depth of the hydrometer bulb. These measurements combine to produce a standard percent passing plot, as shown in Figure 3.8.

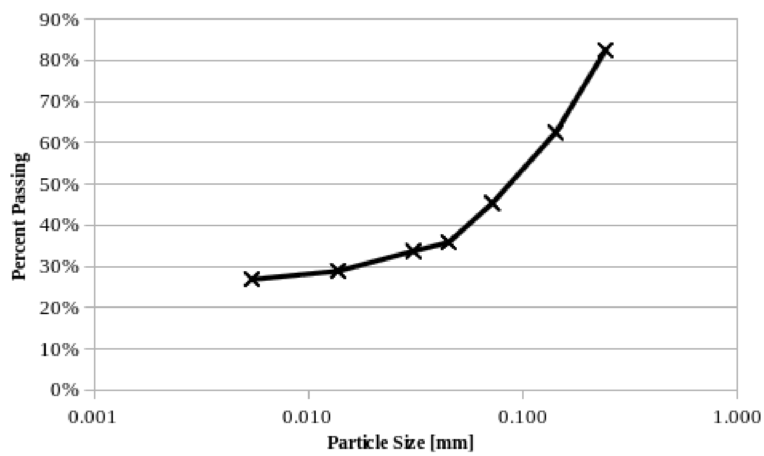

Figure 3.8: Percent passing plot from hydrometer sedimentation testing.

Soil shows smooth curvature of the percent passing plot, typically indicating low-noise measurements.

3.4.11 Results

Clay content was estimated using four techniques, with clay contents summarized in Table 3.6.

Average clay content calculated from the four methods was 33.98%.

X-ray diffraction analysis showed the highest calculated clay content. Because clay particles are created on, and adhere strongly to, the surfaces of eroded rock particles that make up a large fraction of subsoil [57], composition analysis will reveal a higher clay particle fraction than methods requiring separation of clay particles from the bulk material. Difficulties reading the top surface level of settled material and selection of times used for each portion of sedimentation testing are suspected as primary sources of error in this method. While useful for field testing, visual reading of sedimentation testing should be validated by more robust quantitative methods such as hydrometer sedimentation testing.

3.5 Straw

3.5.1 Pull Test

Single fiber hand-breaking tests can provide qualitative understanding of straw strength. Poor quality straw will be easy to pull in half, while fresh or well stored straw will be difficult. A simple pass/fail test proposed by Evans et. al. is a pull test of five straw stalks between two people [38]. Each person holds one end of the bundle and pulls. If the straw cannot be broken in tension in this way, the straw is of acceptable quality. Of six trials of the straw used for this test, one survived the test, indicating poor straw strength. Straw had been stored indoors for 2.5 years at the time of this test and may have experienced some degradation.

3.5.2 Bend Test

Brittle straw is traditionally less desirable for cob building because results in shorter average fiber length due to fracture during mixing. Single straw stalks can be tested for brittleness by wrapping them around a finger to observe flexibility and toughness. In 10 straw fibers tested, 7 broke apart while being wrapped around a pinky finger of 14mm diameter. This indicates that the straw used for this work is not very fresh and may experience breaking during the mixing process, shortening the average in-situ fiber length.

3.5.3 Length Distribution

Prior to mixing, straw length was measured manually to the nearest 1/16 inch (1.5 mm). A portion of straw was removed from the center of a straw bale and 500 stalks were measured. Isolated grain heads or non-stalk elements, such as leaves, were excluded from this analysis. Figure 3.9 shows a histogram of lengths measured. Table 3.7 presents the distribution statistics for the straw lengths.

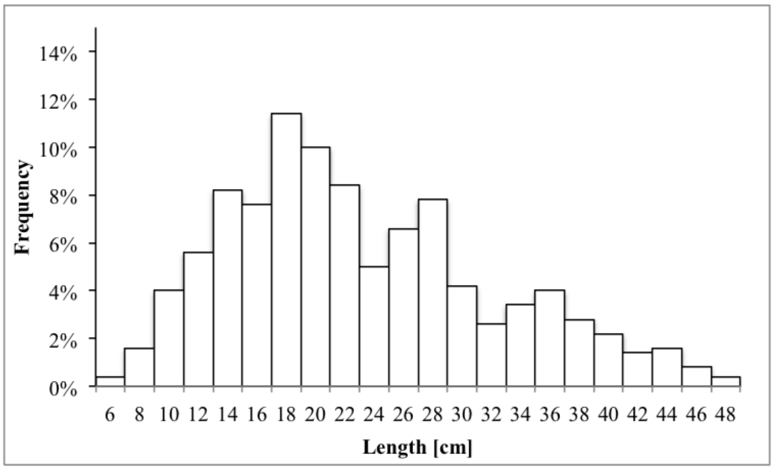

Figure 3.9: Histogram of straw stalk lengths.

Table 3.7: Straw stalk length statistics, all measurements taken in cm.

Average Length	22.0
Standard Deviation	9.0
Coefficient of Variation	41.0%
Fitted Weibull Parameters	
λ	2.456435178
k	9.161558511
R^2	0.8944

From the distribution of lengths found in the sample analyzed, the likely method of straw harvesting appears to be by a standard rotary mower, rather than cutter bar. Rotating mower cutters have a higher rate of secondary cuts on straw stalks, while cutter bars can operate closer to the ground and typically result in longer remaining stalks. The bundle of stalks measured for this data set is shown in Figure 3.10.

Figure 3.10: Bundle of straw stalks used for length distribution characterization.

A Weibull distribution was fitted to the straw length data. Fiber reinforced composite mechanical property models are is often dependent on fiber length distribution, and fitting a standard particle size distribution model to experimental data will provide greater modeling flexibility.

3.5.4 Single Fiber Strength Testing

Tensile testing of single straw stalks was performed to determine typical peak strength values. Straw stalks were selected from the same bale used for cob specimen testing. Stalks had outer leafy sheathing removed and only stalks without visible damage on an 8-inch span were selected. Specimens were cut to length and ends bonded in rigid tabs with hot melt adhesive. Tabs were used to distribute tensile load into the straw stalk and prevent crushing in traditional tensile testing grips. Tab design, a straw stalk encased in the tab end, and a specimen mounted in the tensile grip, are shown in Figure 3.11

Straw was tested to failure at a displacement rate of 0.005 mm/s. Straw stalks typically demonstrated a linear loading curve and a brittle fracture, as seen in the load-

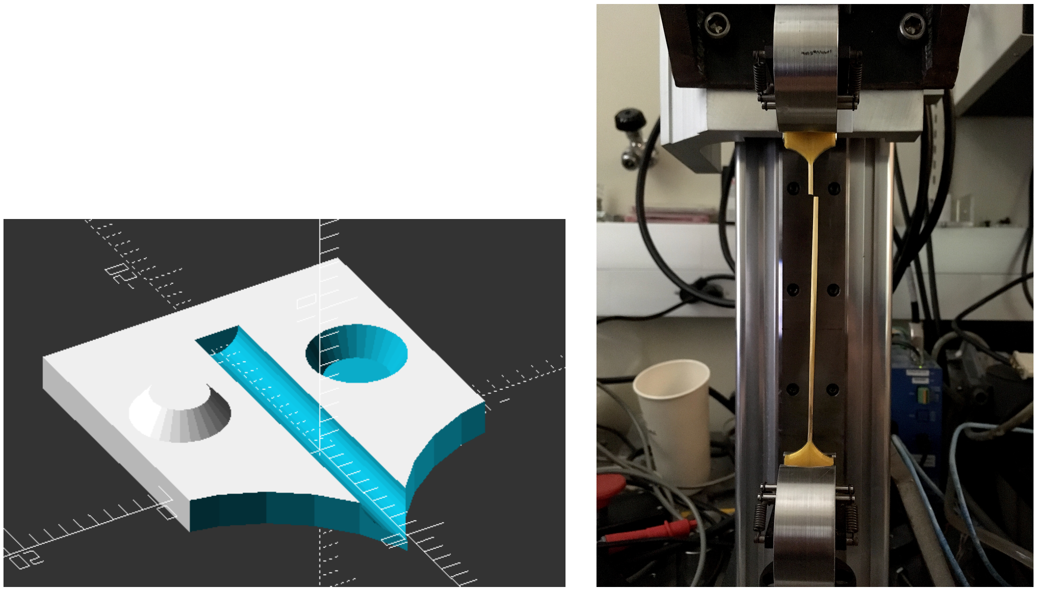

(a) CAD design of tensile testing tab for straw stalks.

(b) Tested straw specimen and tab mounted in tensile testing grips.

Figure 3.11: Straw stalk testing process.

displacement curve shown in Figure 3.12.

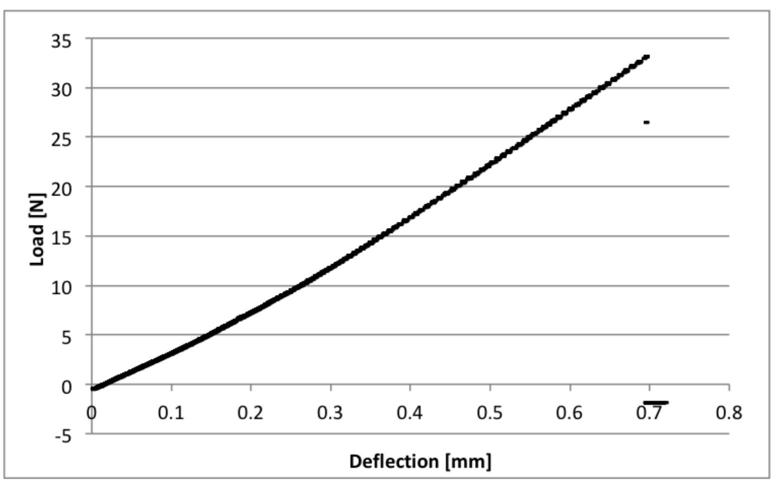

Figure 3.12: Typical load-displacement curve for straw stalk in tension.

Straw stalks have a hollow tubular structure. After tensile failure, the straw fiber was flattened and thickness and width of the resulting flat section measured. Flattening and measurement of thickness was performed with a micrometer, and width was measured with calipers. Dimensions taken and calculated are shown in Figure 3.13. Measurement of wall thickness and diameter were calculated from these flattened measurements. Width of the flattened straw stalk approximated as half the circumference of the round stalk, shown in Equation 3.3.

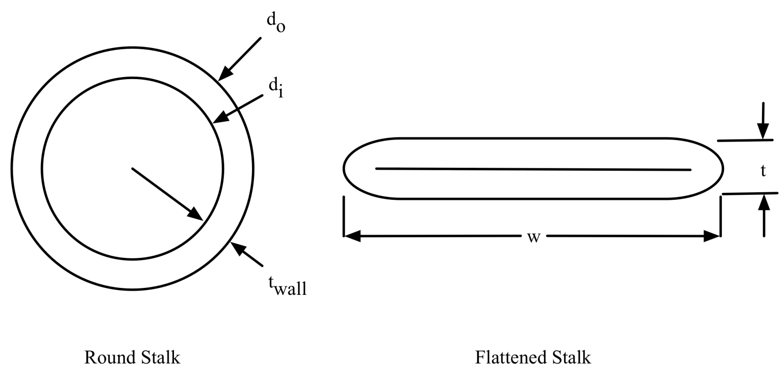

Figure 3.13: Dimensions measured on flattened straw and calculated for round straw.

$$c_o = 2 * w \tag{3.3}$$

Wall thickness was calculated from the measured thickness of the flattened stalk, as shown in Equation 3.4.

$$t_{wall} = t/2 \tag{3.4}$$

21 stalks were measured and tested to failure. A summary of the geometry and strength results obtained is shown in Table 3.8.

Table 3.8: Straw stalk geometry and strength statistics.

	d_o [mm]	t_{wall} [mm]	Peak Stress [MPa]
Mean	1.84	0.34	21.44
Std. Dev	0.31	0.08	9.42
COV	17.2%	25.5%	44.0%

Strength of straw stalks exhibited wide scatter, ranging from 10.7 to 41.1 MPa. Neither outer stalk diameter (p=0.204) or stalk wall thickness (p=0.368) significantly influenced breaking stress.

3.6 Conclusions

These tests robustly described the properties of the constituent materials used in cob samples tested. The key observations of these tests were:

- The sand was poorly graded and sub-angular.
- The natural clay-rich soil had an average of 36.7% clay across all methods employed.
- Hydrometer sedimentation testing was found to the best method of evaluating clay content in soil, producing repeatable quantitative results with a minimum of specialty equipment.
- The soil was classified by ASTM methods as a fat clay soil with high strength.
- By both ASTM and field classification methods, the soil is very well suited to cob construction, exhibiting high clay content and high strength.
- The straw had predominantly round stalks and an average length of 22 cm.
- The straw had an average fiber strength of 21 newtons, but was brittle after storage. Fresh straw or straw harvested with a cutter bar may exhibit more desirable mechanical properties for cob building.

CHAPTER 4

TRANSIENT PROPERTIES OF COB TEST COUPONS

4.1 Overview

This chapter discusses the characterization of cob mechanical properties as a function of drying time and estimated moisture content. Weight measurements provided moisture measurements, which fitted well to an exponential decay curve. Destructive testing in 3-point bending and compression provided measurements of material properties throughout the drying process.

4.2 Introduction

Safe building rates and the durability of cob during extreme weather events are significantly influenced by the effect of moisture content on material strength and stiffness. The goal of this experiment was to provide empirical correlations between moisture content and cob structural properties. These results are necessary for safe construction guidelines and understanding of material behavior during severe weather.

The New Mexico Earthen Building Materials Code is the most well-established building code for earthen materials in the United States [62]. Envelopes for test specimen geometry, fixture geometries, testing rates, and data analysis are detailed in these codes. Strength testing methods for this paper's research were designed to conform to the New Mexico code in all relevant parameters. The cob specimens for the work described in this paper are classified as "unstabilized adobe" by the New Mexico Adobe code. Unstabilized adobe is any earthen construction material which does not contain any cement, lime, fly ash, or asphaltic emulsion as a secondary strengthening agent. The two primary metrics for mechanical strength of earthen construction materials in the New Mexico code are compressive strength and bending strength (modulus of rupture). Therefore, flat plate compression testing and three-point bend testing were used for strength evaluation of specimens during drying.

New Zealand also developed building codes governing earth construction [94]. Similar to English tradition, New Zealand homes are often built of cob. Due to frequent severe earthquakes on the small island nation, seismic survivability is a prominent feature of the New Zealand codes. Many New Zealand homes are built of cob, similar to the English style.

The procedures for correlating material strength and moisture loss required validation to ensure accuracy of results. Figure 4.1 shows the dependency tree of experiments leading to correlation of moisture and strength. Direct measurements of material strength and block weight throughout the drying process were combined to correlate strength and moisture content.

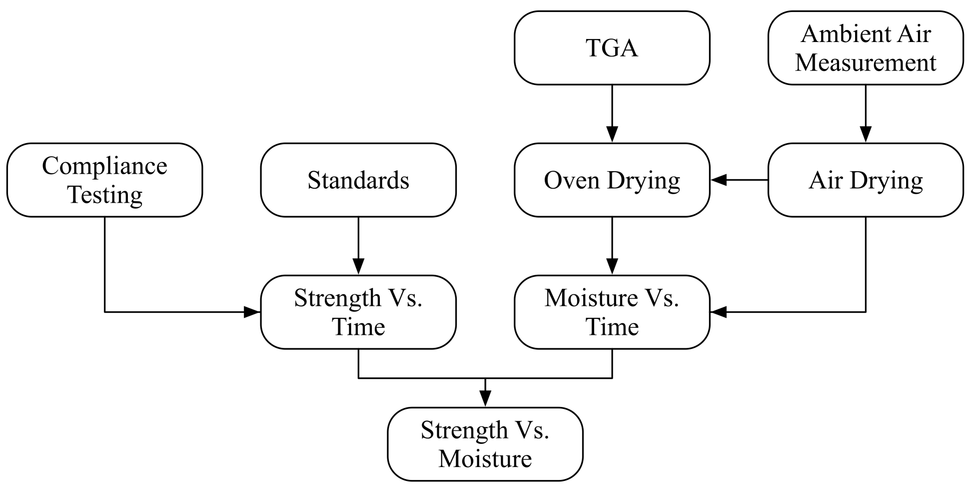

Figure 4.1: Experiment dependency tree required for correlating material strength and moisture content.

Moisture content was calculated by observing specimen weight change while drying at ambient conditions, then further oven drying specimens to remove all shrinkage and pore moisture, as defined by Grim [44]. Thermogravimetric Analysis (TGA) was used to ensure that oven drying did not cause oxidative degradation to straw within the cob. Ambient temperature and humidity were recorded during air drying of cob samples.

4.3 Specimen Preparation

The materials used for this work were intended to replicate methods used in full-scale cob construction. Clay-rich subsoil was sampled near Chandler Park, Tulsa, OK, at coordinates 36° 7.5137'N, 96° 5.4488'W. The sand used was screened and washed masonry sand purchased from a local quarry. The straw used was purchased in bales of wheat straw from a local outdoor supply store.

Cob batches were mixed using a nominal 2 parts sand to 1 part clay soil by volume. Water was added to bring the mix to a stiff plastic state and clay and sand were mixed until the material became homogeneous. Approximately 10 liters of straw was spread over the surface of each batch of 28.4 liters (7.5 gallons) sand and clay. Straw was then mixed into the sand-clay mix until the straw was well distributed and the material became stiff. The traditional process of treading cob by foot was used to maintain comparability with extant cob test data. Specimen molding order was randomized to distribute any difference between batches among test groups.

The cob was then molded into 10x10x30cm prismatic specimens. Molds were hand-packed using similar processes and pressures to in-situ cob manufacturing. These specimen measurements comply with the New Mexico Earthen Building Materials Code [62]. Specimens of this geometry were used for both weight and strength data acquisition.

4.4 Moisture Measurement

Eight cob blocks were selected randomly from a total of 70 manufactured specimens for weight tracking measurement. These blocks were not tested to failure during ambient drying but instead were measured periodically for weight loss. All weight loss observed was assumed to be from moisture loss. Care was taken to avoid any abrasion of blocks during moving and weighing.

Ambient air drying and elevated temperature oven dying were used to calculate moisture content for specimens during ambient drying.

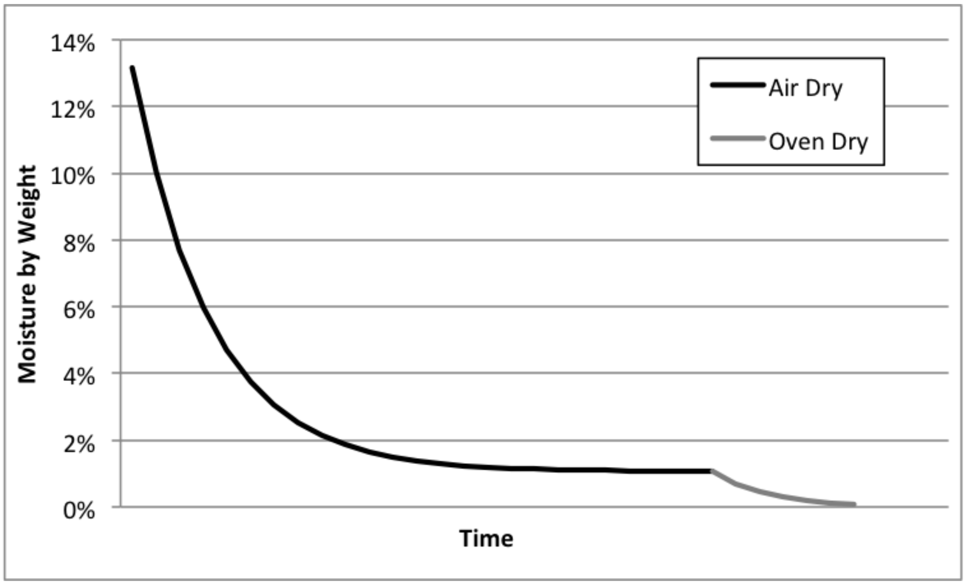

Figure 4.2: Example weight loss curve for drying specimen.

4.4.1 Ambient Conditions

Ambient temperature and humidity were recorded during the initial 32 days of specimen drying and are shown in Figure 4.3. An Adafruit DHT22 humidity and temperature sensor was used to collect data using a Raspberry Pi. Average values are given in Table 4.1.

Table 4.1: Average ambient drying conditions.

	Average	Standard Deviation
Temperature [°C]	23.99	2.17
Relative Humidity [%]	39.75	10.48

Temperature controlled by laboratory building HVAC and remained in a reasonable "room temperature" range of 20 to 28 °C. Humidity was left uncontrolled and typically remained between 25 and 55 % relative humidity.

4.4.2 Air Drying

Blocks designated for weight testing were randomly selected from the total specimen list. Blocks were weighed daily for 9 days, then every four days until an age of 40 days. Two

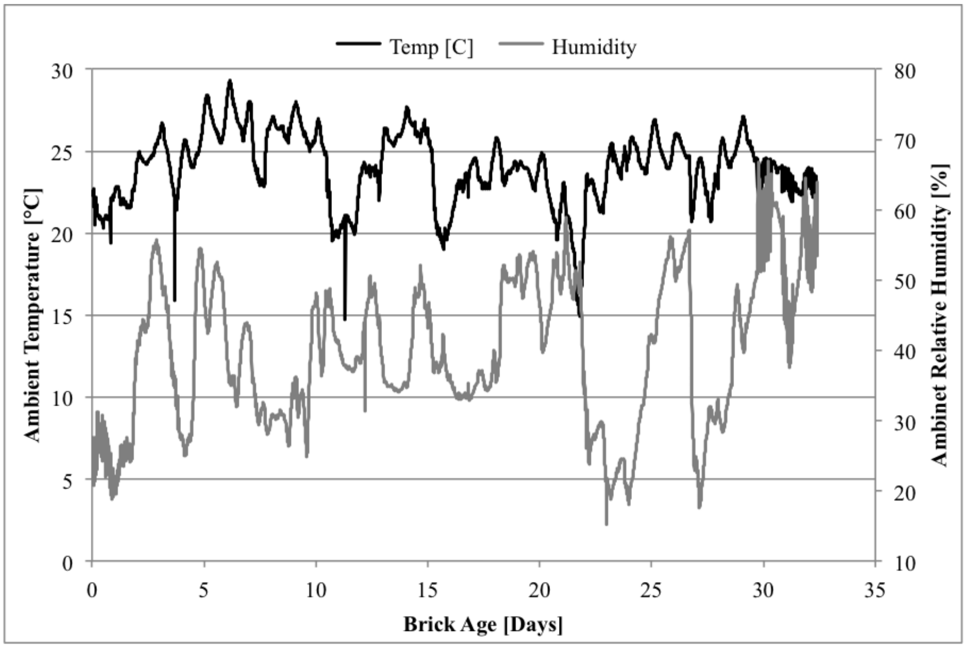

Figure 4.3: Ambient temperature and humidity during drying.

additional measurements were taken to ensure steady-state behavior. Like specimens tested for strength, weight measurement blocks were rotated on every measurement to maximize uniformity of surface exposure to air. Specimens on drying shelves are shown in Figure 4.4.

Weight data was normalized by dividing measured weight by initial block weight to compare moisture content among all blocks. After initial surface water evaporated, the rate drying as assumed to be proportional to the difference between the moisture content of the specimen and of the surrounding ambient air. The time-moisture relationship then becomes an exponential curve of the form

$$y = a\mathrm{e}^{-bt} + c \tag{4.1}$$

and was used to model the average drying behavior. The parameters were fitted to data using sum of squares minimization and resulted in the parameters shown in Table 4.2, where y is the percentage moisture and t is the age measured in days.

Parameter c in this equation is the modeled dry steady-state weight percentage of mixed cob. The data and fitted curve are shown in Figure 4.5.

Figure 4.4: Specimen drying shelves with specimens to break on the right and specimens for weight measurements on the left.

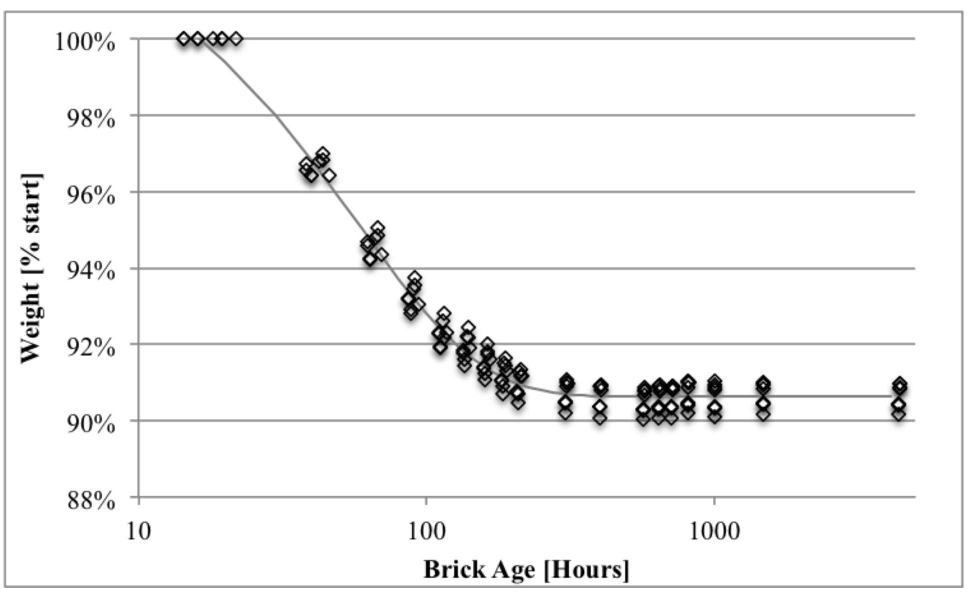

Figure 4.5: Normalized block weight data and fitted curve.

This model fits well with observed drying behavior of specimens, with an R^2 value of 0.9822. Model parameters are presented in Table 4.2. However,generalization of drying rate to other geometries and to other environmental conditions is beyond the scope of this experiment.

4.4.3 TGA

Thermogravimetric Analysis (TGA) was performed on straw stalk specimens to ensure that oven drying cob test specimens would not cause oxidative breakdown of the straw. Oxidative straw breakdown could lead to error in oven-dry weight, skewing moisture content calculations.

The TGA testing cycle consisted of an equilibrium step at 40 °C, a ramp at 10 °C per minute to 120 °C, a 20 minute dwell at 120 °C, and finally a ramp at 10 °C to 300 °C. This range was intended to capture anticipated residual water loss up to 100 °C and initial oxidative breakdown, anticipated between 200 and 300 °C. Oven drying without oxidative degradation was validated by the isothermal dwell at 120 °C. The testing was performed in an air environment. Four samples of straw stalk were selected from straws of varying sizes.

On average, straw samples lost 7.42%±0.65 of starting weight during the initial ramp to 120 °C. This weight loss was assumed to be purely water loss. Oxidative breakdown threshold was defined as a 2% weight reduction from oven dry weight. Average oxidative breakdown onset was observed at 242.35°C±1.73. From these results, oven drying at 120 °C can be safely performed on cob specimens without oxidative breakdown of straw samples.

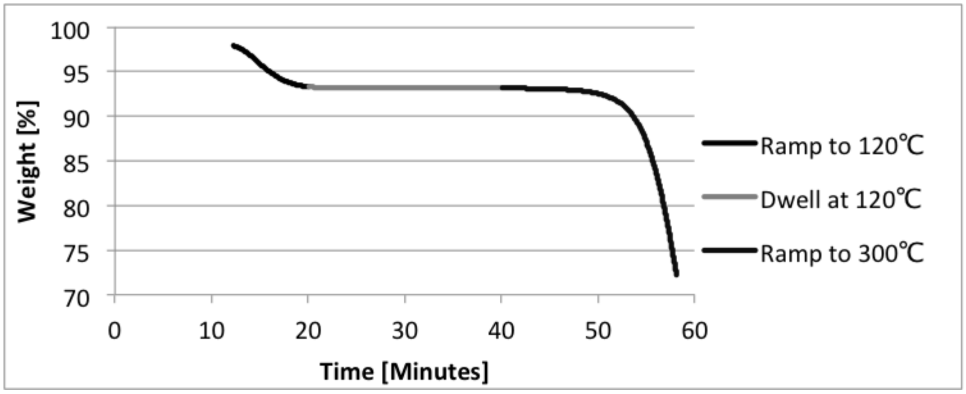

Figure 4.6: Straw weight verses time under TGA.

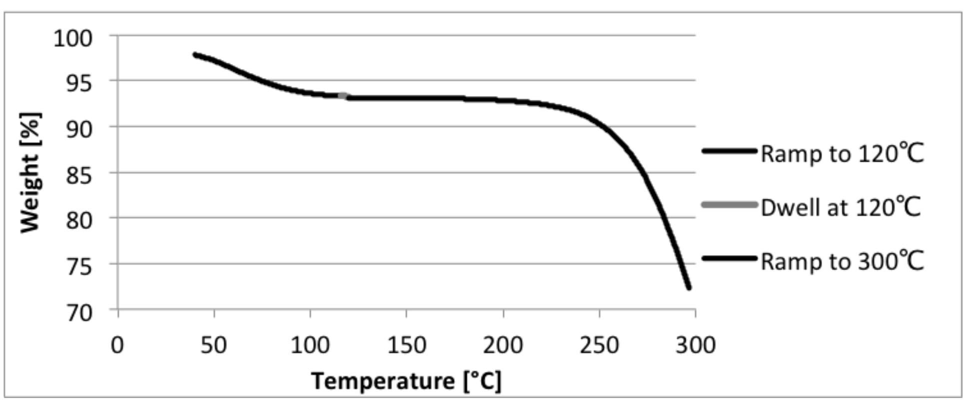

Figure 4.7: Straw weight verses temperature under TGA.

4.4.4 Oven Drying

Oven drying was used to drive out remaining mobile moisture from cob weight monitoring specimens. Oven drying took place at 120°C to ensure complete pore moisture release. This is slightly above the baseline temperature of 110°C used for testing by the Bureau of Standards for testing dehydration of clays [23]. From the similarity of cob to the drying of clay-based ceramics before firing, specimens were assumed to be sufficiently porous to allow for remaining pore moisture vapor transport from unmodified specimens. TGA testing verified that oxidative degradation of straw would not take place at this temperature.

Weight measurements were used throughout the oven drying to verify complete drying. The curves of weight loss during oven drying are shown in Figure 4.8.

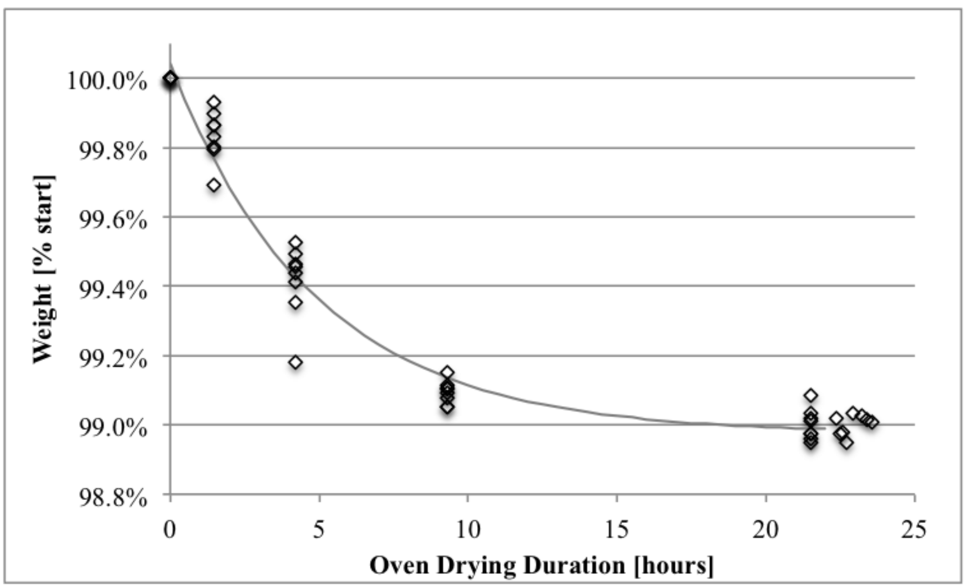

Figure 4.8: Weight loss during block oven drying.

On average, specimens lost 1.0% of air dried weight during oven drying. Block weight was observed to stabilize after approximately 24 hours of oven drying, corresponding with a release of all pore water [44]. Their oven-dried weight was used to calculate moisture content before oven drying and at manufacturing time. After complete drying, specimens were tested to failure to establish strength values at 0% moisture.

4.4.5 Moisture Results

Absolute moisture content was calculated by measuring residual weight loss through moisture transport of oven-dried blocks after ambient air-dry was complete. The moisture was calculated by Equation 4.2.

$$w_{\%} = \frac{w - w_{dry}}{w} \tag{4.2}$$

where w is the weight of the specimen as recorded and w_{dry} is the weight of the specimen after oven-drying. Equation 4.2 is equivalent to equation 4.3

$$w_{\%} = \frac{w_{water}}{w_{total}} \tag{4.3}$$

Figure 4.9 shows the percentage of moisture calculated for each block through the duration of ambient drying. Initial moisture content for the specimens was an average of 10.33%±0.34 by weight. Average water content after ambient drying was 1.07%±0.05.

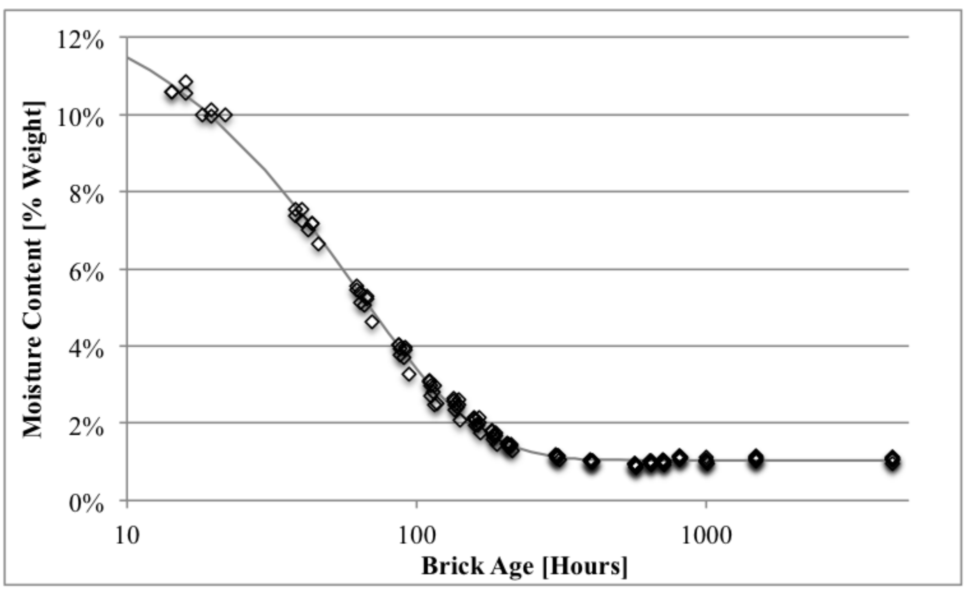

Figure 4.9: Calculated block moisture content data and fitted curve.

The exponential Equation 4.1 was used to model drying behavior of the specimens during each stage of drying. Fitted parameters and fit quality are presented in Table 4.2. Time values (t) are measured in hours. For ambient weight and oven weight, Equation 4.1's y value is weight of a specimen as a fraction of initial weight. For the ambient moisture content equation, y is the estimated specimen moisture content.

Table 4.2: Parameters and model fit for exponential model of block weight change and moisture content of the form $y = a\mathrm{e}^{-bt} + c$.

Parameter	Ambient Weight	Oven Weight	Ambient Moisture Content
a	0.1244	0.0106	0.1230
b	0.0174	0.2036	0.0164
c	0.9063	0.9898	0.0104
R^2	0.9822	0.9579	0.9974

Using this model, moisture content of destructively tested specimens may be estimated.

4.5 Strength Results

The strength experiment was structured as a two-factor factorial test with replication. The two factors were drying duration and breaking method. Three replicates were used for each level and factor. Because an exponential drying curve was expected, time steps were selected at a variable spacing to maximize experimental resolution at points of anticipated maximum rate of change of moisture content.

4.5.1 Overview

The compressive and bending strength of cob test samples were tested regularly throughout the drying duration. Because of surface roughness, linear load-deflection response was not observed until significant load had been applied in some cases. Applied load and cross-head deflection were directly recorded. Calculations of stress and strain were performed after machine compliance was removed from deflection measurements. Specimens were tested using a displacement-controlled test fixture using a crosshead displacement rate of 2 mm per minute.

Sufficiently dried specimens typically demonstrated four loading phases in either compressive or three-point bending testing:

1. Initial non-linearity as the fixture made more complete contact with the rough specimen surface

2. Linear load-deflection response

3. Rounded ultimate stress curve as internal cracking developed

4. Smooth reduction of stress as damage became more extensive

Linear load-deflection response became steeper and ultimate strength increased as specimens dried. Compressive specimens demonstrated a rounded curve around peak stress, while three-point bending specimens produced a sharp peak. Example curves for both compression and bending can be seen in Figures 4.10 and 4.12.

4.5.2 Compliance Testing

Test machine compliance curves were created for each test fixture. Machine deflection was subtracted from observed crosshead deflection during testing of specimens to accurately measure specimen behavior.

Table 4.3 shows the combined machine and fixture compliance testing results. Compliance testing for flat plate compression was performed with the two opposing flat plates in direct contact. Three-point bend test compliance was tested with a 1/2-inch steel plate substituting for a test specimen.

Table 4.3: Compliance testing parameters and results.

	Max Test Load [N]	Average Test Slope [mm/N]
Flat Plate Compression	66723.3	1.04×10^{-5}
Three Point Bending	4448.2	5.92×10^{-5}

True specimen deflection for each data point in future tests can be calculated by Equation 4.4, where δ_{true} is the calculated true displacement of the specimen, $\delta_{measured}$ is

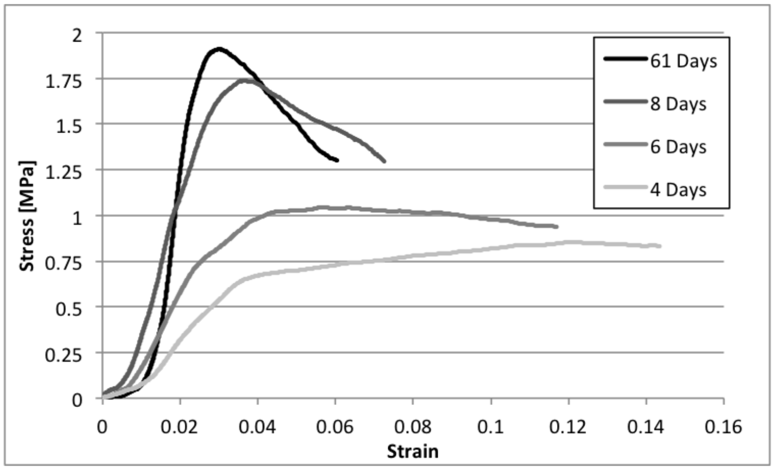

Figure 4.10: Typical stress and strain response curves for flat plate compression.

the observed displacement, S is the compliance slope from Table 4.3, and P is the measured load on the specimen.

$$\delta_{true} = \delta_{measured} - SP \tag{4.4}$$

4.5.3 Compression

Compressive strength is calculated using Equation 4.5 where P is the applied load and A is the specimen cross sectional area perpendicular to the loading axis.

$$\sigma_{comp} = \frac{P}{A} \tag{4.5}$$

Maximum compressive strength was calculated using the maximum applied compressive load for each specimen. Typical test curves for four ages of test specimens are shown in Figure 4.10.

The ultimate compressive strength of cob specimens is shown in Figure 4.11 with respect to the age of the sample. Difference between successive ultimate strength values was only significant between the consecutive data sets aged 160, 215, and 310 hours (p=0.0047, 0.0040).

New Mexico Earthen Building Materials Code stipulates that "Cured units shall have

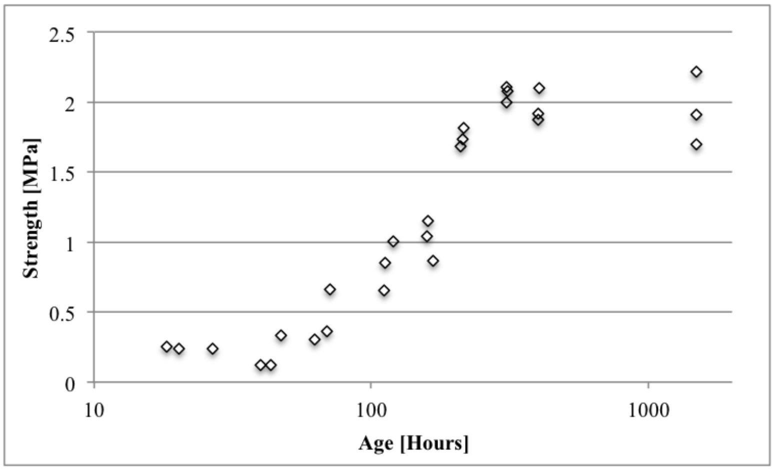

Figure 4.11: Ultimate strength of cob in compression with respect to time.

an average minimum compressive strength of three hundred (300) pounds per square inch [2.07 MPa] when tested. One (1) sample out of five (5) may have a compressive strength of not less than two hundred fifty (250) psi [1.72 MPa]." Average compressive strength over the final three durations tested at 300, 400, and 1480 hours was 1.99 MPa. The minimum strength observed was 1.70 MPa and the maximum was 2.22 MPa. These air-dried specimens thus do not meet either of the requirements for compressive strength in the New Mexico code. Specimens did achieve over 96% of the required strength.

4.5.4 Bending

Bending strength was calculated and reported in accordance with the New Mexico Earthen Building Materials Code and is reported in terms of rupture stress, calculated using the Equation 4.6 where P is the maximum applied load, L is the length between supports, W is the specimen width, and t is the specimen thickness. σ_{bend} represents the maximum tensile stress experienced in the beam.

$$\sigma_{bend} = \frac{3PL}{2Wt^2} \tag{4.6}$$

Bending strain was calculated by Equation 4.7 where t is the specimen thickness, δ is the

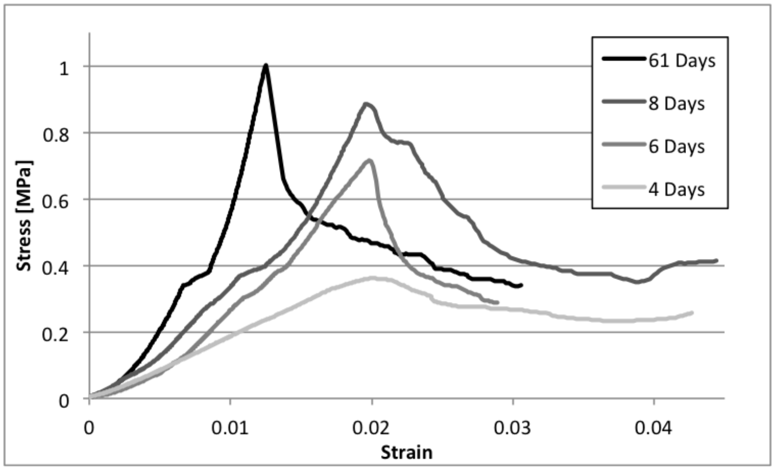

Figure 4.12: Typical stress and strain response curves for three point bending.

center-point displacement, and L is the length between stationary supports.

$$\epsilon_{bend} = \frac{6t\delta}{L^2} \tag{4.7}$$

Similarly to σ_{bend}, ϵ_{bend} represents the maximum strain experienced by the beam in bending. These equations are given in the New Mexico Earthen Building Materials Code.

Typical bending test curves for four ages of test specimens are shown in Figure 4.12. Sufficiently dried specimens typically demonstrated a small initial non-linearity, a linear loading response, a sudden initial fracture, and a slow decay of residual strength. The increase in steepness of linear loading and peak strength with more extensive drying is similar to specimens tested in compression.

Data for rupture stress is shown in Figure 4.13. Significant increase in rupture strength occurred between 80 and 200 hours after manufacturing.

New Mexico Earthen Building Materials Code states that "Cured units shall average fifty (50) psi [0.345 MPa] in modulus of rupture" when tested correctly. Average bending strength over the final three durations tested at 300, 400, and 1480 hours was 1.085 MPa. The minimum strength observed was 0.872 MPa and the maximum was 1.412 MPa. These air dried specimens meet the New Mexico building code requirements.

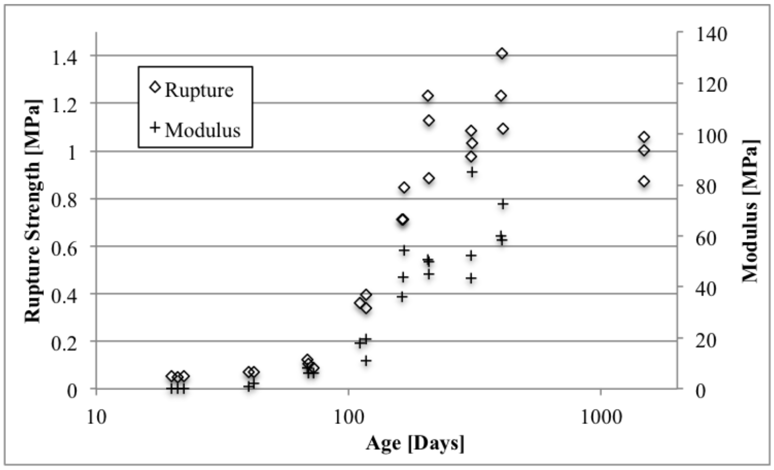

Figure 4.13: Bending strength and stiffness of cob with respect to time.

4.6 Correlation of Strength to Moisture Content

Having established models for the moisture content for cob test samples throughout the duration of drying, correlations of strength with respect to moisture content are now possible. The moisture contents of each tested sample was estimated using the exponential curve fit for moisture content in Equation 4.1 and parameters in Table 4.2. Figure 4.14 plots the strength results of specimens tested in flat plate compression.

Least squares minimization was used to model equations of strength with respect to moisture content to experimental strength data. An exponential equation of the form shown in Equation 4.8 was selected, where σ is the material strength and m is the moisture content by weight. Model curves are displayed in Figures 4.14 and 4.15, and equation parameters are reported in Table 4.4.

$$\sigma = a\mathrm{e}^{-bm+c} + d \tag{4.8}$$

Ultimate strength of specimens tested in compression exhibited high sensitivity to moisture contents in the low moisture region between 1% and 3% moisture. Lower sensitivity to moisture was observed at moisture contents over 3%, though strength was significantly reduced compared to the low moisture specimens.

Four specimens were tested in compression after oven drying. However, three spec-

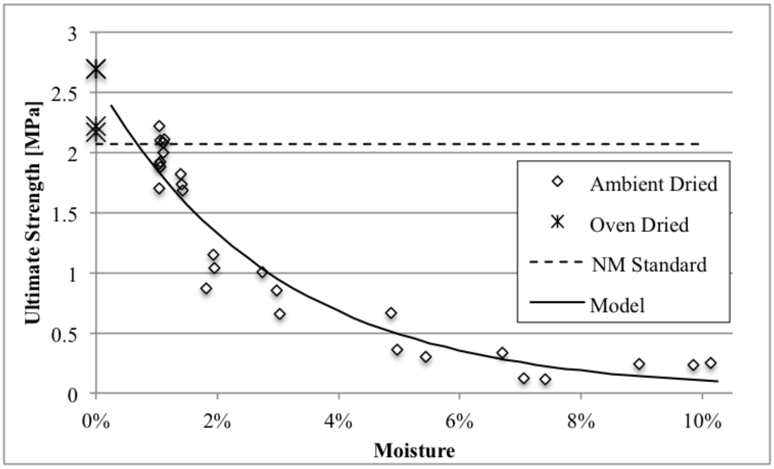

Figure 4.14: Ultimate compressive strength of cob with respect to moisture content.

imens exceeded the maximum load of the test frame, resulting in invalid peak stress measurements. The successful test specimen exhibited a peak stress of 2.69 MPa at 0% moisture content. The remaining specimens exhibited an average peak stress of greater than 2.36 MPa, but were excluded from all further analysis. All of these specimens meet New Mexico adobe building standards for compressive strength of 2.07 MPa. The high sensitivity of compressive strength to moisture content at very low moisture levels, less than 2%, suggests that ambient humidity experienced shortly before testing may influence observed compressive strength.

Figure 4.15 shows the strength data for three point bending tests. Blocks demonstrated brittle failure at less than 7% moisture and a more plastic failure above this threshold. Ultimate strength in bending was not significantly affected by changes in moisture contents at 5% and above. Below this value, the increase in ultimate strength was significant as moisture was reduced ($p=0.0040$).

Average bending strength of four oven dried specimens (0% moisture content) was 1.26 MPa. The minimum strength observed was 1.17 MPa and the maximum was 1.39 MPa. Both ambient dried specimens with moisture less than 3% and oven dried specimens meet New Mexico adobe building standards for bending strength of 0.345 MPa.

The selected exponential model exhibited strong correlation to compressive strength data ($R^2 = 0.9554$). Model fit for bending data was slightly weaker ($R^2 = 0.8980$) and did not fit the high-moisture region as well as the model for compressive tests.

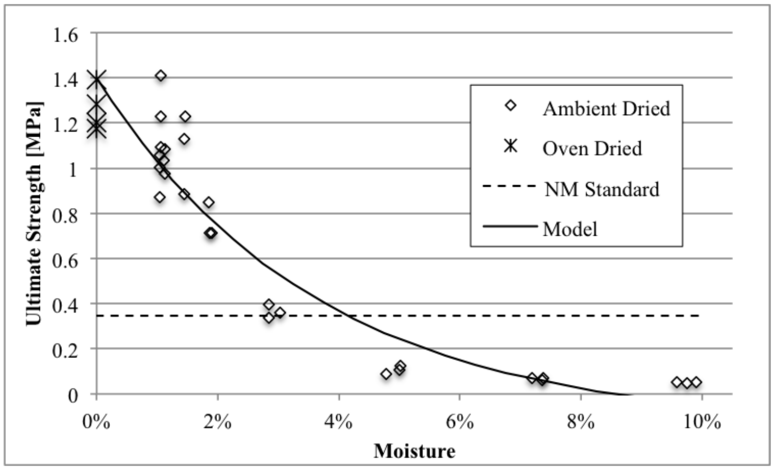

Figure 4.15: Ultimate bending strength of cob with respect to moisture content.

Table 4.4: Parameters and model fit for exponential model of cob strength with respect to moisture content of the form $y = a\mathrm{e}^{-bt+c} + d$.

Parameter	Compressive Strength	Bending Strength
a	1.2040	0.6770
b	45.0370	27.5757
c	0.8643	0.8255
d	0.1247	-0.1456
R^2	0.9554	0.8980

4.7 Summary and Conclusions

4.7.1 Summary

Moisture content was calculated using weight loss of specimens during ambient and oven drying. Models of moisture content with respect to time were developed with strong correlation to experimental data. The calculation of absolute moisture content improved model fit compared with simple weight loss data.

Strength testing was performed on test specimens to produce curves of strength with respect to specimen age. Specimen strength reached steady state for peak strengths in both compression and bending, validated by t-test comparisons of consecutive tests at high drying durations. These tests failed to show a significant difference between specimens dried for 17 and 62 high days, indicating that the specimens had achieved steady-state ($p=0.8968$ for peak compression strength and $p=0.0798$ for peak bending strength).

Specimen mobile moisture content was then modeled, facilitating estimation of mobile moisture content in specimens tested in both compression and three-point bending. Models for strength as a function of moisture content for a single geometry were developed.

4.7.2 Conclusions

These tests provided several conclusions to inform the design of future experiments:

- Future specimens of the same geometry should be dried in indoor air ambient conditions for a minimum of 18 days to be considered fully dried.
- Specimens were shown to be typically manufactured with slightly over 10% water content by weight.
- Ambient air drying for 18 days or more reduced the steady-state moisture content to slightly over 1% on average.
- Elevated temperature drying at 120°C is required to remove the remaining pore water.

- Air dried specimens met the New Mexico building code for bending strength but failed for compressive strength.
- Oven dried specimens passed New Mexico building code standards for both compressive strength and bending strength.
- Exponential models fit strength data to both age and moisture content data.

CHAPTER 5

EFFECT OF SPECIMEN GEOMETRY ON APPARENT MECHANICAL PROPERTIES

5.1 Overview

This chapter discusses the characterization of cob mechanical properties as a function of specimen geometry. Three prismatic geometries were compared. Strength results from compression and three-point bending were not statistically different for the three geometries.

5.2 Introduction

Cob, like many composite materials, contains macroscopic inclusions and inhomogeneity in the form of large sand grains and straw stalks. Large composite specimens have been shown to be more likely to contain critically-sized flaws, lowering the observed average material strength.

Smaller specimens are desirable because they require less raw material, reduce fabrication time, facilitate more convenient storage and transportation, and require lower loads to test.

5.3 Design of Experiment

Three specimen geometries were selected for evaluation. The large specimen, used in Chapter 4, was a rectangular prism measuring 4x4x12 inches. The medium specimen evaluated measured 3x3x12 inches. Small specimens measured 3x3x10 inches. The purpose of these choices was to independently evaluate the effect of changing cross section and length on both apparent compressive and bending strength.

Twenty-six specimens of each size were manufactured. Four of each were selected for weight monitoring through the drying process. Once dry, these specimens used for monitoring were tested along with the others. The twenty-six specimens were randomly assigned to be tested in compression or three-point bending.

Eight "batches" of cob were needed to manufacture specimens. Specimen manufacturing order was random, distributing any differences between batches randomly between specimen sizes. Two-factor ANOVA was used to evaluate both the influence of batch and specimen size on strength results in Section 5.5.2.

5.4 Drying

Specimens with a smaller cross-section were expected to achieve a steady-state moisture content more quickly than specimens of a larger cross-section. Fitted curves of weight during drying showed a more rapid drying rate in specimens of smaller cross sections. A slightly higher drying rate can also be observed in the small specimen than the medium specimen, due to differences in length.

Steady-state moisture content was taken to be equal to the steady-state moisture content calculated in Chapter 4. Curves of calculated moisture content with respect to time are shown in Figure 5.1.

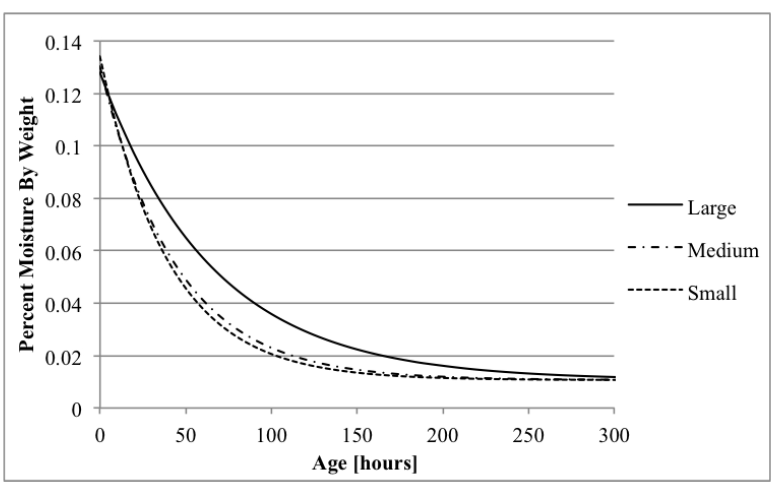

Figure 5.1: Drying curves of three specimen geometries tested.

Table 5.1: Flat-plate compression and three-point bending strength of cob geometries (Units in MPa).

	Large	Medium	Small
Compression			
Average	1.24	1.51	1.39
Std. Dev.	0.16	0.24	0.21
COV	12.5%	15.6%	15.1%
Bending			
Average	0.75	0.70	0.70
Std. Dev.	0.08	0.11	0.14
COV	10.5%	15.8%	19.7%

All specimens were dried for 87 days before testing.

5.5 Results

5.5.1 Strength

Average strength for each specimen size is shown in Table 5.1

Both specimens geometries with 3x3 inch cross sections showed significantly higher apparent compressive strength than specimens of 4x4 inch cross section. The hand-packing process used to produce specimens may have been capable of exerting higher pressures on smaller specimens, resulting in a more well-compacted specimen and higher strengths. However, the variation in compressive strength on specimens of 3x3 inch cross section was higher than 4x4 inch cross section, suggesting that smaller specimens were more sensitive to defects or inhomogeneities than larger specimens.

Though the bending strength of the three specimen geometries was not significantly different, the variation in the 3x3 inch cross section specimens was higher, as observed in results for compressive strength.

Table 5.2: ANOVA parameters from flat-plate compression test results.

	Df	Sum Sq	Mean Sq	F value	P
Batch	1	0.5209	0.5209	13.701	0.0007549
Size	1	0.04332	0.04332	1.1396	0.2932676
Batch:Size	1	0.08171	0.08171	2.1491	0.151839
Residuals	34	1.29264	0.03802		

If differences in pressure from hand-packing the specimen mold cause significant differences in specimen strength, two conclusions are evident. First, maximizing pressure used to consolidate material before incorporating cob into a wall will maximize the strength of the final structure, such as the methods seen in compressed earth block equipment. Second, specimen sizes used for testing and validation should match forming pressures used in in-situ cob construction. This second conclusion supports the use of larger specimens in future material tests to maintain process symmetry with full-scale cob construction.

5.5.2 ANOVA

Compression: Two-way ANOVA performed on ultimate strength of specimens tested in flat-plate compression shows significant influence of batch on peak strength but no significant influence of specimen size on peak strength. The ANOVA result parameters are shown in Table 5.2.

Specimen batch did show a significant influence on compressive strength. Batch-to-batch consistency is an important parameter in the production of any material, and future work should evaluate methods of reducing batch-to-batch variation in cob construction. However, no significant influence of specimen size was observed for compressive strength.

Three Point Bending: Two-way ANOVA performed on ultimate strength of specimens tested in three-point bending showed no significant influence of either specimen geometry or batch. The results of the ANOVA are shown in Table 5.3.

Table 5.3: ANOVA parameters from three-point bend test results.

	Df	Sum Sq	Mean Sq	F value	P
Batch	1	0.01598	0.015978	1.2429	0.2723
Size	1	0.01506	0.0150569	1.1712	0.2863
Batch:Size	1	0.00011	0.0001121	0.0087	0.9261
Residuals	36	0.4628	0.0128557		

Like the results of compression testing, the specimen size failed to show a significant influence on strength. No significant differences between batches were observed for bending strength.

5.6 Summary and Conclusions

5.6.1 Summary

Differing specimen sizes were compared to determine influence of geometry on apparent material properties. Three specimen geometries (4x4x12, 3x3x12, and 3x3x10 inches) were selected to test. Specimens of each size were tested in flat plate compression and three-point bending, with 13 specimens assigned to each test method. ANOVA testing showd that specimen size was not a significant factor on apparent specimen strength in either compression or three-point bending. ANOVA testing did show significant a significant influence of the batch of cob on the material compressive strength.

5.6.2 Conclusions

These tests provided several conclusions to inform the design of future experiments:

- Specimen size had no significant influence on apparent strength in either compression or three-point bending
- Specimen batch had significant influence on compressive strength specimens but had no significant influence on bending strength specimens.

- Future tests for this work will use specimens of the 4x4x12 inch geometry for consistency with prior tests.

CHAPTER 6

EFFECTS OF CONSTITUENT MATERIAL RATIOS

6.1 Overview

This chapter describes a set of single-factor experiments used to evaluate the properties of specimens made with various ratios of sand, clay-rich soil, and straw. Specimens were manufactured using cylindrical specimens intended to isolate sand-clay interaction behavior as well as the typical prismatic specimens used throughout this work. Physical, admixture, and mechanical strength properties of specimens were evaluated during specimen manufacture and after complete air drying.

6.2 Clay-Sand Mixes

Materials: Clay-rich soil used for this test was removed from the same sample as the soil used for transient material testing and raw material characterization as described in Chapter 3. As discussed in Section 3.4.11, the soil is approximately 36.7% clay by mass. The remaining mass of soil was approximately 0.8% sand and 63.8% silt by mass, based on wet sieving results.

6.2.1 Experiment Design

The goal of this experiment was to isolate the influence of clay content in the sand-clay mixture on mechanical properties of cob. Removing any influence from straw may simplify the modeling of material properties and allow more modular property functions.

Cylindrical specimens were selected according to ASTM D2166, "Standard Test Method for Unconfined Compressive Strength of Cohesive Soil." Because sand and clay were mixed together before molding, samples adhered to the "remolded specimen" specifications of ASTM D2166. Figure 6.1 shows the ratios of sand and clay soil used in this experiment.

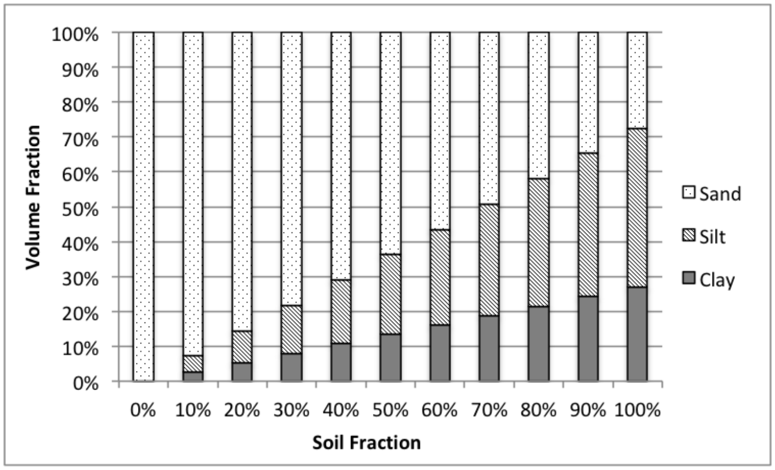

Figure 6.1: Ratios of constituent materials in specimen conditions.

Five replicates of each condition from 10% soil to 100% soil were manufactured for testing, resulting in a total of 50 specimens made. Pure sand specimens did not show the cohesion necessary for manufacture and testing.

6.2.2 Specimen Preparation

Specimens were prepared in accordance with ASTM D 2166, "Standard Test Method for Unconfined Compressive Strength of Cohesive Soil." A cylindrical mold of height 108mm and diameter 52.3mm was used to form specimens. A plunger disk was manufactured to eject specimens from the mold. The mold had a height-to-diameter ratio of 2.07, within the recommended geometry of the ASTM standard.

Clay soil had been stored indoors for over 12 months and was thoroughly air-dried. Hard clay lumps were broken up and ground using a steel cylinder to less than 3mm diameter particles. Stones and inclusions greater than 3mm were discarded.

For each ratio of sand and clay, material for all replicate samples was simultaneously mixed. The specified volume of sand and soil were measured into beakers and the actual poured volume was noted. The weights of sand and clay were each recorded, and density was calculated to monitor measurement reliability. A large and small beaker were used to measure volumes, with measurement markings at 50mL and 25mL increments, respectively. Measurements between the marks were read to the nearest 10mL in the large beaker and to the nearest 5mL in the small beaker.

Sand and powdered clay-rich soil were then mixed together while dry. A fixed volume of water was measured. Water was gradually added to the sand-soil mixture until the material achieved a stiff, plastic state suitable for specimen molding. Material was then mixed by hand until achieving a cohesive and uniform consistency. After water was added, the remaining water volume was recorded. The volume of wet material was then measured.

Material was packed into the mold in several layers to minimize the development of large voids. When the mold was filled, the plunger was placed on the top surface of the material and a 9.14 kg weight was used to compress the specimen, providing a mold pressure of 41.7 kPa. After compaction, any additional material was scraped from the top of the specimen. The specimen was then pressed out of the mold using the plunger onto a plastic membrane to air dry.

Specimen surface textures can be seen in Figure 6.2. Specimens of low clay content had a rough, crumbly surface, while high clay contents had a smooth surface. Specimens above 20% soil exhibited little or no surface crumbling.

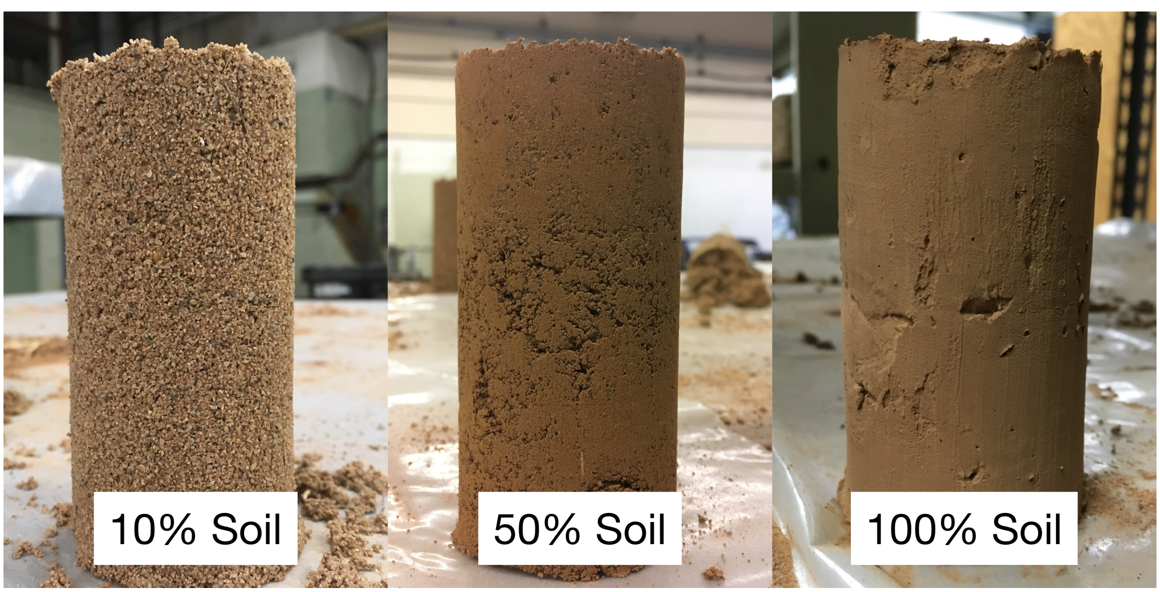

Figure 6.2: Cylindrical specimens showing three ratios of constituent materials in specimen conditions.

6.2.3 Physical Characterization

Description of densities and interactions of variously sized particles in both dry and plastic states is important for conversion between mass and volume fractions in admixtures and prediction of quantities of necessary raw materials to produce a desired mixed quantity. Physical characterization of mixed material compaction (mixed volume ratio), density, and specimen diameter provide benchmarks for behavior of sand-clay interaction without the complication of fiber (straw) reinforcement.

Mixed Volume Ratio Measurement: When combining particulate materials of different particle sizes, small particles may settle into gaps between large particles to occupy formerly unused interstitial space. The result is that one liter of sand added to one liter of fine clay particles produces less than two liters of mixed material. Mixed volume ratio is a measure of compaction of the final mix compared with the volumes of the ingredients. The mixed volume ratio will be defined using Equation 6.1, where v_i is the volume of each solid ingredient and v_f is the final volume of the mixture.

$$MVR = \frac{v_f}{\Sigma v_i} \tag{6.1}$$

The addition of water complicates the direct measurement of mixed volume ratio. Powdered clay is highly porous and compressible, but when whetted typically becomes dense, reducing in volume. However, many kinds of individual clay particles expand when exposed to moisture. When water saturates sand, buoyancy reduces normal forces between grains, which causes a correlating reduction in frictional forces between grains. Similarly, water between grains of unsaturated sand may act as lubrication, allowing grains to slide against each other more easily. This may allow sand grains to find a more compact structure, causing further compaction. This effect is evident when pouring out a small volume of water on a dry beach.

For measurement of mixed volume ratio, dry volumes and masses of each ingredient were recorded before mixing. Water was added until a stiff plastic state was achieved, and the volume of water added to each batch was recorded. The volume of the resulting mixture was then measured. Because of the previously mentioned effects of water on the volume of both sand and clay, the mixed volume ratio at neither extreme was 100%. The results of these measurements and calculations are shown in Figure 6.3.

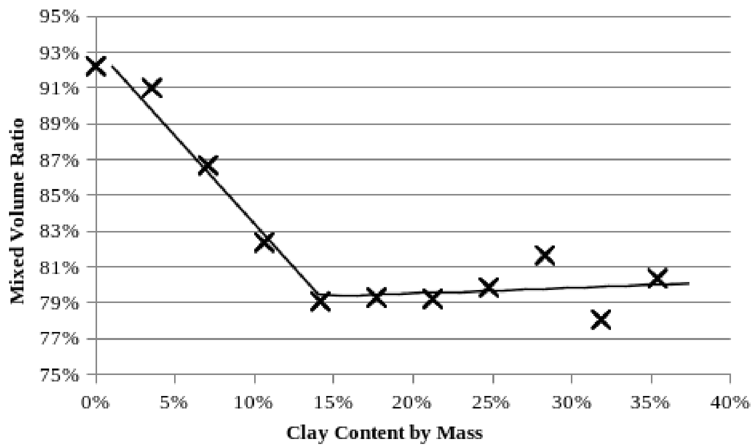

Figure 6.3: Mixed volume ratio of various sand-clay mix ratios.

Mixed Volume Ratio data appear to show a threshold behavior. Evaluation and modeling of this pattern are discussed in Section 6.2.5.

At low clay contents, mixed volume ratio decreased with respect to increasing clay content. An inflection point was observed near 15% clay content, above which mixed volume ratio slowly increased with increasing clay content. This suggests that sand-clay mixture behavior is significantly different when voids between sand grains are saturated with clay. Above saturation, the mixed volume ratio only changed slowly with respect to additional clay.

Density Measurement:

Weight and volume of constituent materials, combined materials, and dried specimens were measured. Apparent density was calculated by simple division of weight by volume. Density measurements of constituent materials were used to evaluate material consistency. Powdered dry soil had an average density of 1.25 g/mL and COV of 2.7%. Sand had an average dry density of 1.58 g/mL and COV of 3.6%.

Volumes of specimen mixes after water was added were also recorded. As discussed in earlier, the volume of whetted soil was used to calculate the mixed volume ratio. Bulk density, most comparable to specimen densities, was computed using Equation 6.2, where W is measured weight and V is measured volume. Density is reported in grams per milliliter or grams per cubic centimeter.

$$\rho = \frac{W_{soil,dry} + W_{sand,dry}}{V_{mix,wet}} \tag{6.2}$$

Water was assumed to be a transient component and not a significant fraction of the dried specimen mass. Therefore, the dry component mass divided by packed wet volume should be most comparable to the density of packed and dried specimens. Densities for specimens were calculated from specimen measurements and weights measured for each. Figure 6.4 shows the resulting distribution of specimen densities and single density measurement for each batch of material before specimen molding. Error bars are 1 standard deviation wide.

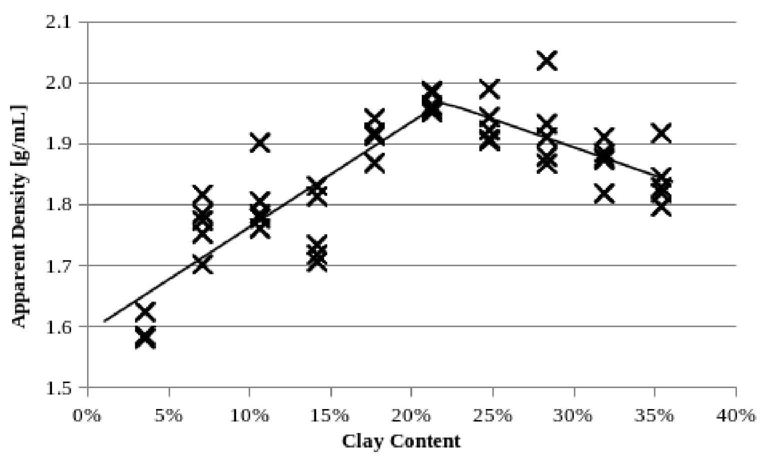

Figure 6.4: Densities of dried specimens and bulk material batches.

Correlation of bulk and specimen densities was good for the four mixes with lowest clay content. Above 40% soil content, apparent bulk densities became significantly lower than typical specimen observed densities.

Higher concentrations of clay particles in close proximity may retain appreciable amounts of water even after reaching an air-dried steady state. As seen in Chapter 4, elevated temperatures are required to drive out all pore water. The potential water retained in specimens of higher clay content may be responsible for the elevated apparent density.

As seen in Figure 6.4, specimen density showed steady increase with increasing clay quantity at lower clay contents. Above the saturation point of about 21%, density was reduced with increasing clay. This also supports the clay saturation model, in which clay is filling unoccupied voids between sand grains at low clay contents. Apparent specimen density was reduced as clay content increased above the clay saturation point, indicating that clay soil had lower bulk density than sand. More details on the behavior of swelling and hydrating clays have been discussed by Osipov [65].

Based on the success of the initial bi-linear fit model for density, the fit parameters were re-cast to directly describe physical properties of the material. Void, sand, and clay density were modeled, along with a void saturation clay content and an initial void content value. Voids were assumed to be linearly replaced by clay with respect to clay mass fraction, as described in Equation 6.3, where V_v is the void volume fraction, V_i is the void volume fraction at 0% clay, m_c is the clay mass fraction, and m_{crit} is the clay saturation mass fraction. Above the clay saturation point, voids were assumed to be filled with clay.

$$V_v = \left\{ \begin{array}{ll} V_i - \frac{Vi}{m_{crit}} m_c, & \text{for} \quad m_c \leq m_{crit} \\ 0, & \qquad \text{for } m_c < m_{crit} \end{array} \right\} \tag{6.3}$$

The density of the remaining solid material was calculated using a simple rule of mixtures, as shown in Equation 6.4, where ρ_c is the bulk density of pure clay, ρ_s is the density of sand excluding voids, and m_c is the clay mass fraction.

$$\rho_{solid} = \rho_c m_c + \rho_s(1 - m_c) \tag{6.4}$$

Because void density was assumed to be negligible when compared with sand and clay densities, the final mix density can be calculated using Equation 6.5.

$$\rho_{bulk} = \rho_{solid}(1 - V_v) \tag{6.5}$$

Figure 6.5 shows the calculated ratios of sand, clay, and voids along with measured specimen data and overall specimen density model. Least squares error minimization calculated a clay saturation point was 22.1% by mass, sand density of 2.17 g/mL, clay density of 1.25 g/mL, and a void fraction at 0% clay of 27.3% volume fraction. Model fit had an R^2 value of 0.7362

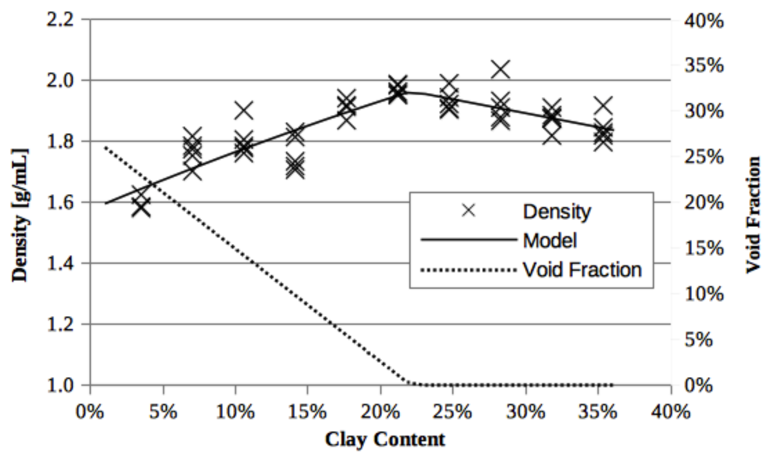

Figure 6.5: Densities of dried specimens and model of void content and bulk density.

Diameter: Diameter measurements were recorded immediately prior to specimen testing. Because all specimens were made in the same mold, a statistically significant correlation of diameter and clay content could be used to estimate shrinkage rate with respect to clay content. Specimen diameters are shown in Figure 6.6.

Diameter measurements indicate specimen shrinkage after drying. Low clay contents show small amounts of shrinkage, while above the bi-linear inflection point (approximately 21%) shrinkage became more significant with respect to increasing clay content. Single-factor ANOVA shows a significant reduction in diameter with higher clay contents (p=0.0000).

6.2.4 Mechanical Characterization

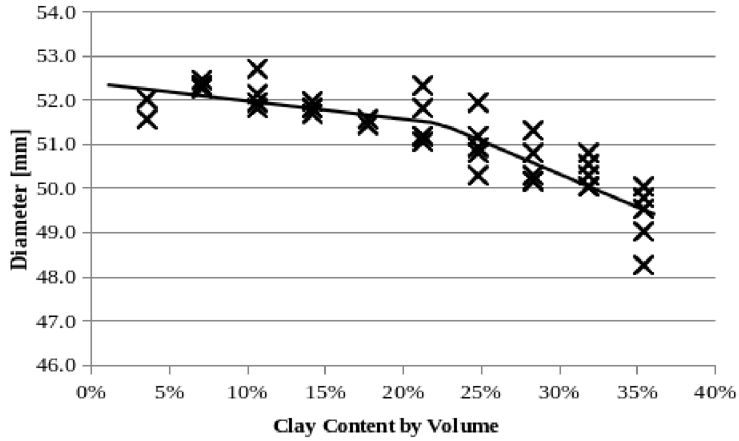

Figure 6.6: Diameters of dried cylindrical specimens.

Ultimate Compressive Strength: Ultimate strength was calculated from peak load from the testing file and dividing by cross-sectional area of the specimen being tested. Ultimate strength of all specimens tested are shown in Figure 6.7. Maximum ultimate strength observed was 3.45 MPa (500 psi).

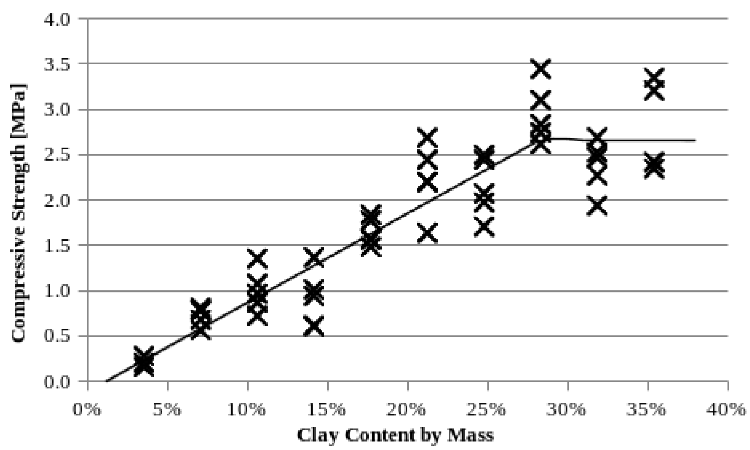

Figure 6.7: Ultimate strength for measured cylinders.

Specimens typically exhibited brittle failure, usually with fractures running along the entire axial length of the specimen. Specimen strength increased significantly with increasing clay content, as shown in Figure 6.8.

Elastic Modulus: Elastic modulus was calculated using the secant method on the linear portion of the load-displacement curve. Machine compliance was subtracted from

Figure 6.8: Cylindrical test specimen broken in axial compression.

deflection values before modulus calculation. Modulus data for all specimens are shown in Figure 6.9.

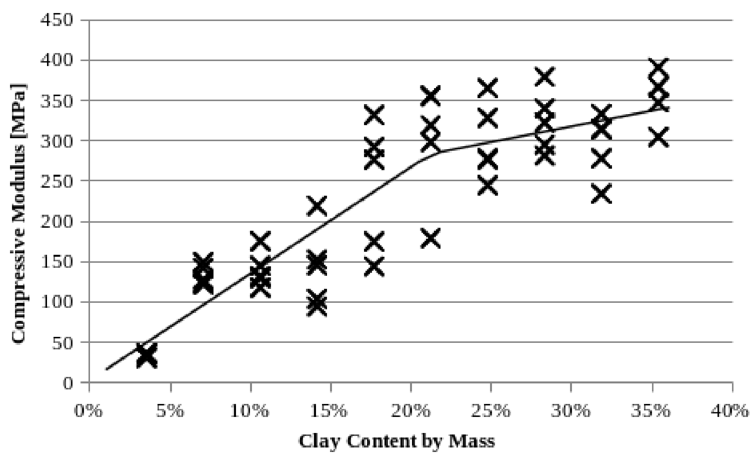

Figure 6.9: Elastic modulus for measured cylinders.

Elastic modulus steadily increased for specimens with low clay contents. However, high clay content (above 20%) specimens showed little change in modulus with changes in clay content.

6.2.5 Bi-Linear Regressioin

Specimens manufactured at 10% soil were delicate and crumbly. Two of these specimens collapsed during drying, resulting in three specimens remaining for strength testing.

Results of mixed volume ratio and elastic modulus testing most strongly indicate a bi-modal material behavior with respect to clay content. In low clay content samples, space may remain between sand grains. Above a critical quantity of clay, most voids between sand grains have been filled with clay and sand grains begin being separated by clay particles. As clay content increases, but below the point of clay saturation, sand grains are more tightly bound together, resulting in higher compressive strength and stiffness. Above clay saturation, increasing clay content will slightly separate sand grains but will have far less significant influence on strength and stiffness than additional clay below the saturation point.

Pure sand, well compacted, will exhibit air voids between sand grains. Sphere packing theory has proposed the upper bound of volumetric efficiency to be approximately 64% [27]. At low clay contents, clay particles will become bound by surface tension to the smallest voids between sand particles. As the clay content is increased, clay will fill a larger fraction of these voids, until the voids are totally saturated. Once saturation has occurred, additional added clay will force sand grains apart, reducing the frequency grain-to-grain contact. Additional clay added at this state will simply force sand grains further from neighboring sand grains. The point at which clay perfectly saturates sand voids is posited as the inflection point between otherwise largely linear behavior regions, as seen in Figures 6.3, 6.4, 6.6, 6.7, and 6.9.

Bi-linear least squares fitting was used to model material behavior for specimen diameter, density, mixed volume ratio, compressive strength, and modulus. These fits were 4-variable least squares optimization: slope and intercept for the first linear fit, slope for the second linear fit, and the threshold to select between the two linear fits.

Chapter 8 discusses the incorporation of this modeling method into prismatic cob specimen strength prediction. The two linear portions of each graph (for example: density vs. percent clay) were modeled by the standard line equation, $y = mx + b$, resulting in a total of four fit parameters for each property. A fifth parameter was the point of transition from one linear fit to the other: the void saturation point. However, the intercept of the second slope was constrained such that the two lines would intersect at the threshold point,

Table 6.1: Bi-linear fit parameters for clay content characterization.

Property	m_1	b_1	m_2	b_2	Saturation	R^2
Diameter	-4.11	52.39	-15.00	54.82	22.36%	0.8128
Mixed Volume Ratio	-0.98	0.93	0.03	0.79	14.16%	0.9591
Density	1.72	1.59	-0.93	2.17	21.90%	0.7367
Compressive Strength	9.83	-0.11	-0.16	2.72	28.32%	0.8520
Modulus	1321.67	3.04	388.08	201.31	21.24%	0.7842

ensuring a model without jump discontinuities. All fits were performed with respect to clay content by mass.

Bi-linear models were generated for each of the measured properties. Mean void saturation value across all modeled properties was 21.6% clay content by mass - the average fo the "saturation" column in Table 6.1.

Fit parameters and fit quality for each individual property are reported in Table 6.1. Physical properties (diameter, mixed volume ratio, and density) showed more clear bi-linear behavior. The two linear fit portions for mechanical properties (ultimate strength and modulus) were not as obvious in the raw data plots.

The calculated saturation point for MVR is significantly lower than the average saturation point across all parameters tested. The calculated saturation point for compressive strength was the highest of all parameters tested, at 28.3% clay. Specimen strength showed steady increases with clay until the saturation point, at which compressive strength remained stable or was slightly reduced.

Measures of density, required for conversions between volume and mass fraction, require knowledge of properties and ratios of five constituent ingredients in the matrix material: sand, clay, straw, water, and voids, assumed to be air-filled.

6.3 Prismatic Specimen Tests

6.3.1 Experiment Design

The purpose of this experiment was to investigate the respective influences of clay and straw content on the mechanical strength of cob. This both increases the known bounds of cob properties as a function of composition and produces data useful for informing future material modeling. Sets of specimens were chosen to separately vary the clay and straw contents to reveal mechanical property response curves across the full range of feasible ingredient ratios.

Four recipes of cob were chosen to test the effect of various sand-clay ratios on mechanical strength. A 102x102x305 millimeter (4x4x12 inch) prismatic specimen geometry as used throughout this work was chosen. Unlike the cylinder tests described previously, these specimens would include a constant amount of straw to maintain similarity to typical cob production. The straw content was selected to be consistent with the specimens testing in the specimen drying and size studies, as discussed in Chapters 4 and 5. The four levels of soil content were 20%, 55%, 75%, and 100%. These levels were intended to span the feasible region of soil content without duplicating prior test specimen ratios of 33% soil. Thirteen specimens were manufactured in each level. One specimen was used for correlation of straw fiber volume fraction with weight fraction. The remaining specimens were destructively tested using flat-plate compression and three-point bending, assigning six specimens to each method.

An additional four recipes of cob were selected to test the influence of straw content on mechanical properties. Quantities of added straw were determined during the first batch of specimen manufacturing by continuing to include additional straw until the batch was barely workable. The other three straw quantities were uniformly distributed between 0% straw and the maximum straw content found in the first batch. Weights of sand, clay soil, and straw were recorded to determine quantitative mass fraction of each ingredient. A constant ratio of two parts sand to one part soil by volume was used, the same as both the transient and specimen size studies. This is also the typically recommended ratio according to the traditional Oregon cob building methods. As with the sand-clay-variation specimens, 13 specimens of each straw level were manufactured, one for straw content analysis and the remaining to be divided between compression and three-point bend testing.

Figure 6.10 shows the locations of the new tests ratios of sand, clay, and straw along with the location of ratio used for testing transient drying behavior. These mix ratios approximately form two linear data sets through the design space. These lines are not perfectly perpendicular a constant mass of straw was added to mixes of varying clay content, resulting in increasing mass fractions of straw as specimen densities were reduced by high clay contents. However, the combination of these two test lines allowed material modeling to take place throughout the entire feasible region. this is discussed in Chapter 8.

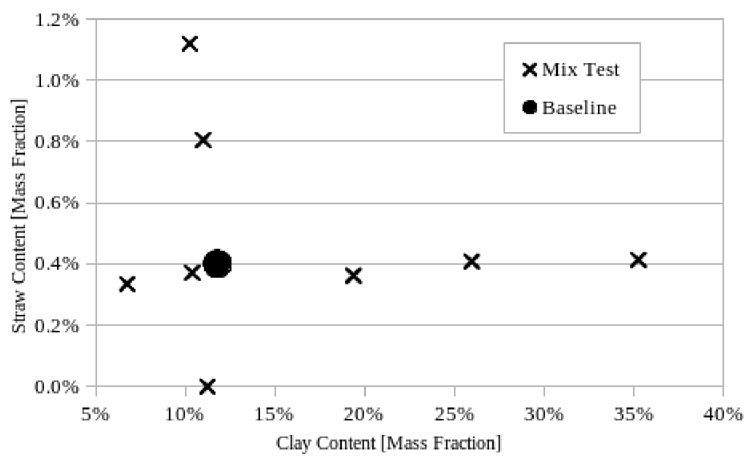

Figure 6.10: Mass ratios of cob mixes tested.

6.3.2 Specimen Manufacturing

Clay-variation specimens were manufactured on November 15, 2018, and straw-variation specimens were manufactured on November 27, 2018. Each batch of specimens was dried for 42 days before testing. All materials included were weighed prior to mixing. Straw content was calculated as a weight fraction. Sand and clay were measured to the nearest 100 grams, while straw was measured to the nearest gram. Nominal volume and density of sand and soil were each calculated for each batch to validate consistency of measurements and materials.

All specimens were manufactured in the same way as prior specimens in this work, as discussed in Section 4.3. Specimens were weighed periodically to verify complete drying before testing. Specimen test order and kind (compression or bending) were randomly assigned within each batch.

6.3.3 Straw Volume Fraction Calculation

Because many fiber-reinforced polymer (FRP) composite material equations are written in terms of fiber volume fraction, conversion from known fiber mass fractions to volume fractions was necessary. The highly compressible loose straw and unknown manufacturing compressive stresses applied made direct in-situ density calculations impossible. Three approaches for conversion of fiber mass to volume were tested: calculation of straw density in as-baled state, comparative density analysis of straw variation specimens, and visual analysis of cross-section surface.

Straw Density Estimation: Density of straw in the as-baled compressive state was estimated from measuring bounding dimensions and weights of a variety of straw bales. Eight bales of straw were measured, and the average density was 139.3±12.1 $\frac{kg}{m^3}$. The as-baled straw density provides a baseline against which to compare in-situ results.

Specimen Density Calculation: Specimens manufactured to test influence of straw content on strength were weighed and density of specimens after drying was calculated. As shown in Figure 6.11, increased straw mass fraction resulted in a lower average specimen density.

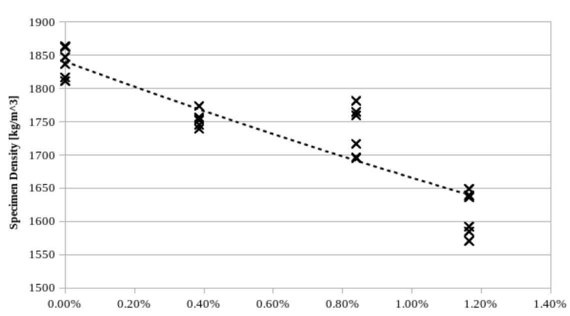

Figure 6.11: Specimen density with varying straw mass fractions.

ANOVA testing shows a significant influence of straw weight fraction on specimen density (p=0.0000). Conversion from mass fraction to volume fraction by relative densities can be accomplished by Equation 6.6, where V_f is the fiber volume fraction, M_f and M_m are the masses of fiber and matrix materials, respectively, and ρ_f and ρ_m are the densities of fiber and matrix materials, respectively.

$$V_f = \frac{M_f/\rho_f}{M_f/\rho_f + M_m/\rho_m} \tag{6.6}$$

Using Equation 6.6, a monotonic non-linear relationship between fiber mass fraction and volume fraction is expected. Least-squares optimization of fiber fraction, apparent matrix density, and apparent straw density resulted in an estimated in-situ straw density of 160.13 $\frac{kg}{m^3}$. In very low fiber mass-fraction regions, Equation 6.6 is nearly linear. Because of the substantial difference in density between the matrix (sand and clay soil) and the fibers (straw), the function rapidly increases at low fiber mass fractions. As fiber volume fraction grows, increasing fiber mass fraction has dwindling results for volume fraction. A portion of the mass and volume fraction relationship is shown in Figure 6.12 for a family of ratios of matrix density to fiber density.

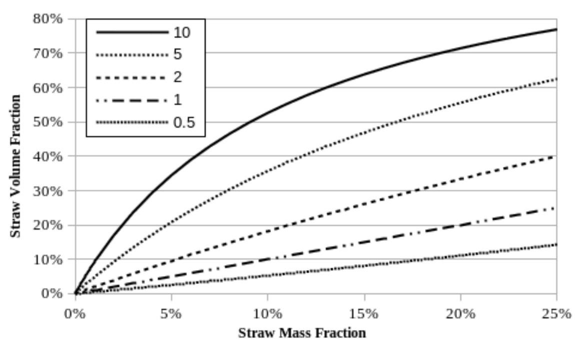

Figure 6.12: Theoretical relationship between straw mass fraction and volume fraction.

Macrostructural Straw Volume Fraction:

Specimens manufactured for straw content analysis were cut perpendicular to the long axis using a coarse-tooth reciprocating saw. Cut faces were ground flat. Specimen sections were then fired for two hours at 500°C to burn out straw and remove remaining soot. This process left clean voids visible in the surface of the cut face for visual analysis. The sample was then photographed for later processing, and one sample is shown in Figure 6.13.

Figure 6.13: Specimen cut face after straw fiber burnout, showing voids in previous fiber locations.

Images for analysis were created using image editing software GIMP [78]. Images for analysis were created with black pixels drawn over fiber void regions and the cut face of the specimen. The background image could then be hidden and the fiber areas isolated for simple analysis. The ratio of area of fiber regions to cut face area was calculated using the ImageJ distribution FIJI [72, 73]. The plot of apparent straw content volume fraction with respect to mass fraction in Figure 6.14 shows strong correlation of visual straw fraction with straw mass fraction.

Density estimation was performed by setting soil density equal to the mean soil density observed in Section 6.3.3. Equation 6.6 was used to model fiber volume fraction. Resulting fitted straw density was $477.52 \frac{kg}{m^3}$.

Straw Density Results: Baled straw density, specimen densities, and cross-section visual void content analysis were used to estimate in-situ straw density. Calculated straw

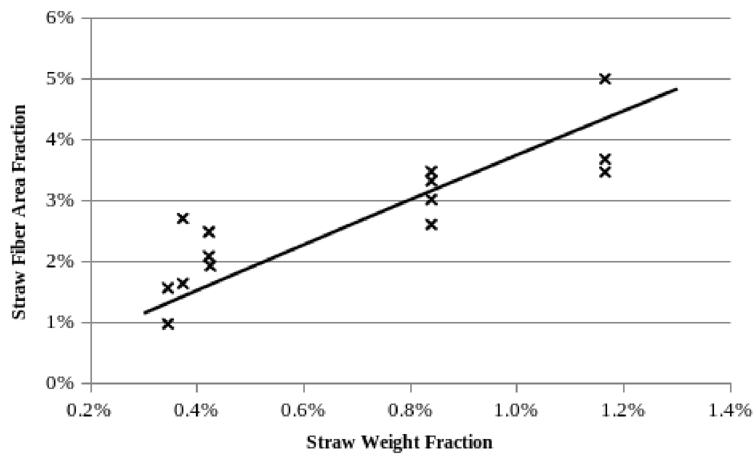

Figure 6.14: Straw fiber volume fraction with respect mass fraction.

density from specimen density measurement was 15% greater than the as-baled density measured. Cross-sectional visual analysis was 2.4 times larger than as-baled density. These results indicate that cross-sectional analysis may be under-reporting fiber volume fraction compared with specimen density measurements. Additionally, as straw content increases, more voids may be introduced into the specimen, resulting in a lower measured specimen density. From specimen molding pressures used for this work, straw density is likely similar to as-baled density, supporting the in-situ density estimation from bulk specimen measurements. Further process refinements may be necessary for optical fiber volume calculation methods to be viable for cob.

6.4 Strength Results

6.4.1 The Effect of Straw

On Compressive Strength: Figure 6.15 shows observed specimen strengths tested in flat plate compression.

Average compressive strength observed was highest in specimens using 0.84% straw by mass. The most straw-filled specimens showed the highest amount of variance, as can be seen in Table 6.2. Specimens without straw exhibited the lowest average strength.

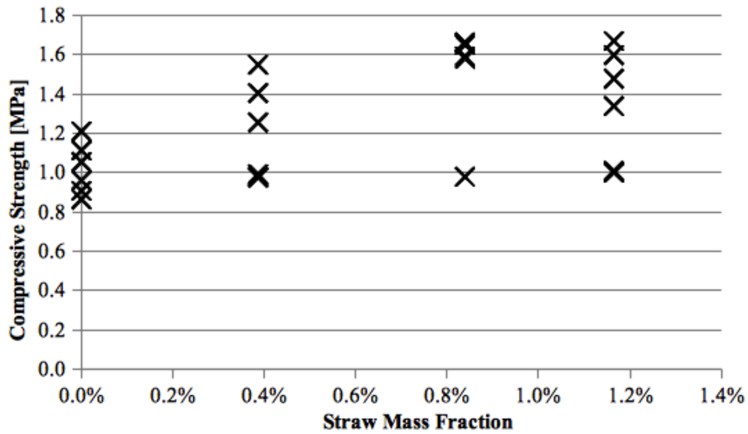

Figure 6.15: Specimen compression strength with respect to straw mass fraction.

Table 6.2: Compression strength results for straw variation specimens.

Straw Content	Average [MPa]	Std. Dev. [MPa]	COV
1.17%	1.35	0.29	21.4%
0.84%	1.53	0.27	17.6%
0.39%	1.21	0.25	20.5%
0.00%	1.03	0.13	12.4%

ANOVA shows significant influence of straw on compressive strength (p=0.0120). Higher straw contents generally increased compressive strength. However, the maximum straw content batch (1.17%) showed lower average strength than specimens with 0.84% straw.

Strength of prismatic specimens made with 33% soil and no included straw was compared to 30% soil cylindrical specimens tested in Section 6.2.4. A two-tailed t-test failed to show a significant difference (p=0.8678) between cylinder specimens (mean strength of 1.00 MPa) and prismatic specimens (mean strength 1.02 MPa). This supports the conclusion that cylinder testing to isolate sand-clay interaction produces comparable results to prismatic specimen testing.

On Bending Strength: Figure 6.16 shows bending strength results for specimens of varying straw weight fractions. As with compressive strength, maximum average bending

Table 6.3: Bending strength results for straw variation specimens.

Straw Content	Average [MPa]	Std. Dev. [MPa]	COV
1.17%	0.705	0.102	14.4%
0.84%	0.822	0.106	12.9%
0.39%	0.681	0.044	6.4%
0.00%	0.756	0.140	18.5%

strength was observed at 0.84% straw content by weight. Specimens without straw exhibited the highest amount of variation in bending strength. However, unlike compressive strength, the average bending strengths do not exhibit an obvious curvature or linear trend.

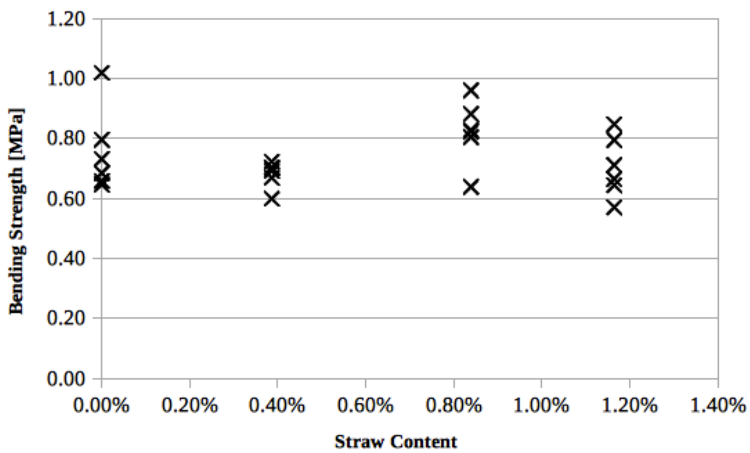

Figure 6.16: Specimen bending strength with respect to straw mass fraction.

ANOVA fails to show significant influence of straw on bending strength (p=0.1234) Table 6.3 shows descriptive statistical summaries of bending strength tests.

6.4.2 *Effect of Clay*

This experiment was designed to primarily test the independent influences of clay and straw on mechanical strength. Qualitatively, however, interaction between clay and straw content seems likely. During manufacture, a constant mass of straw was included in each batch. However, mixes of different clay contents had different senses of straw "capacity", the amount of straw able to mixed into the sand-clay matrix while maintaining mix-ability and coating of all straw fibers. The constant mass of straw felt like a significant fraction of the straw "capacity" of the most sand-rich mix, but felt almost negligible when mixed into the most clay-rich batch, despite equivalent mass fractions. From this observation, high-clay mixes are expected to accommodate higher quantities of straw before failing to be manufacturable. Additionally, specimen strength may reflect a significant interaction between clay and straw content, although this experiment is not designed to effectively test this interaction.

On Compressive Strength: Figure 6.17 shows material compressive strength with respect to changes in soil fraction when straw mass was held constant at 340 grams, or approximately 0.4% by mass. Specimens tested in Section 6.4.1 using 0.39% straw were included for analysis because straw content matched those in this test and provided a unique clay content. Specimens at low clay contents showed significant scatter and far lower average strength than other specimens.

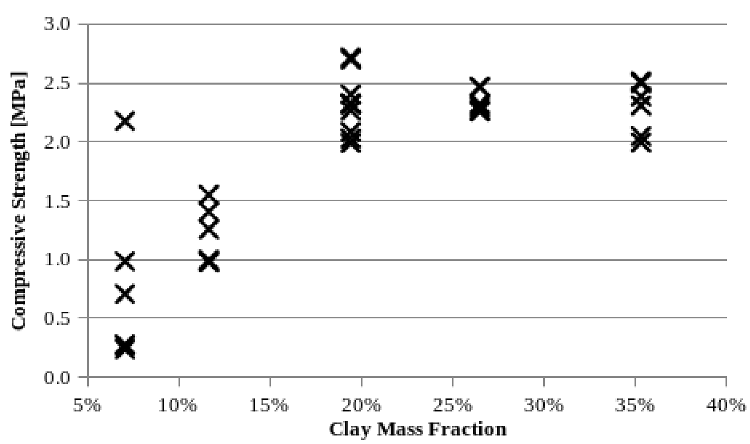

Figure 6.17: Specimen compression strength with respect to clay mass fraction.

Summary statistics for compressive strength of clay variation specimens are shown in Table 6.4. These show that sample specimens containing 55% soil exhibited the highest average strength. One specimen using 7.1% clay achieved a compressive strength capable of meeting New Mexico building code requirements (2.07 MPa), but was nearly ten times stronger than the weakest specimens of the same mix.

Table 6.4: Compressive strength results for soil variation specimens.

Soil Content	Clay Content	Average [MPa]	Std. Dev. [MPa]	COV
20%	7.1%	0.77	0.75	96.8%
55%	19.4%	2.45	0.20	8.2%
75%	26.5%	2.34	0.10	4.1%
100%	35.3%	2.29	0.22	9.8%

ANOVA results showed that clay content had significant influence on compressive strength (p=0.0000). The relative similarity of compressive strength among the three mixes of highest clay contents may indicate a threshold behavior of critical clay content for acceptable strength. Threshold behavior in behavior of clay-sand mixes has been noted already in this chapter. Further study of strength in specimens between 5% and 20% clay would be necessary to determine behavior in this region.

On Bending Strength: Figure 6.18 shows the bending strength of specimens of varying clay contents. Specimens made with 0.39% straw from the straw variation study were included here, as was done with the clay variation compressive strength.

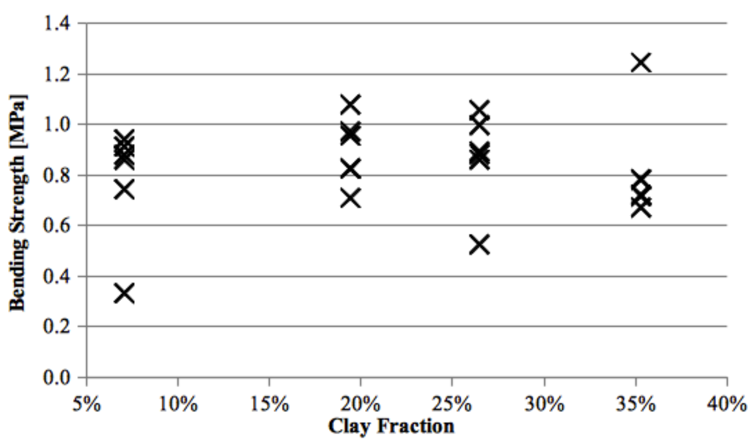

Figure 6.18: Specimen bending strength with respect to clay mass fraction.

Table 6.5 shows that sample specimens containing 55% soil exhibited the highest average strength, while both the lowest and highest clay content specimen groups had the

Table 6.5: Bending strength results for soil variation specimens.

Soil Content	Clay Content	Average [MPa]	Std. Dev. [MPa]	COV
20%	7.1%	0.779	0.229	29.4%
55%	19.4%	0.895	0.133	14.8%
75%	26.5%	0.870	0.185	21.3%
100%	35.3%	0.821	0.213	25.9%

two largest variances.

As was the case with straw content variations, ANOVA failed to show a significant influence of clay content on bending strength (p=0.25940). Additionally, second-order linear regression fitting an equation of the form $y = ax^2+bx+c$ resulted in no statistically significant parameters.

6.5 Damage Tolerance Results

Although the straw content of specimens failed to show statistically signification influence on peak bending strength, the failure behavior of specimens in both flat plate compression and three point bending was notably different with increasing quantities of straw.

6.5.1 Compression

Specimens tested in flat-plate compression without straw demonstrated small fractures throughout the loading. These fractures occurred at load levels significantly below the typical peak load for specimens with straw tested previously, but the load recovered quickly after such a fracture was observed. However, the loading slope would become more shallow after each successive fracture event. This is contrasted with samples including straw, which universally showed a smooth loading ramp and gradual non-linear failure arc. A representative curve selected from each of the four mix ratios is shown in Figure 6.19.

The proposed mechanism causing this behavior is effective load re-distribution through

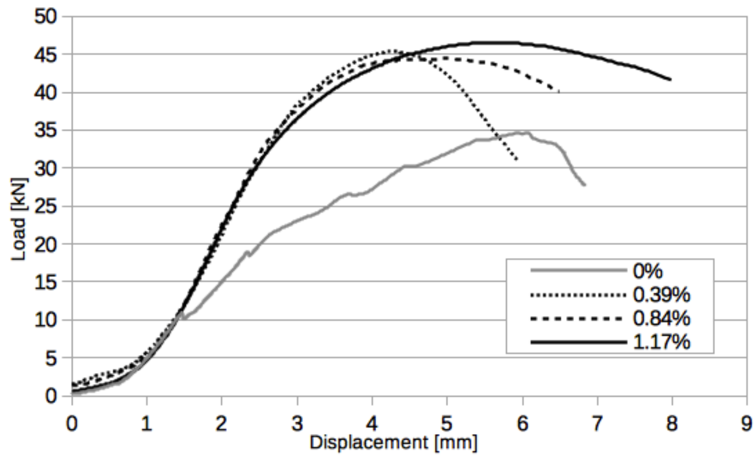

Figure 6.19: Typical compressive testing curves from tests of varying straw fiber mass fractions.

straw fibers. Stress risers present from non-planar surfaces or internal structural non-homogeneity experience premature failure in specimens without straw, leading to small fracture events and a reduced observed stiffness. However, in the presence of straw, load is transmitted from stress risers and distributed more uniformly throughout the specimen. This creates a more gradual loss of strength at the onset of failure. With increasing quantities of straw, residual strength after failure initiates increases. However, as straw quantity increases, non-linear load response is induced at lower loads. Because the matrix material is more brittle than the straw, matrix failure at lower loads is expected at high fiber fractions.

6.5.2 Bending

Loading curves observed in three-point bending primarily differed in the post-peak-load specimen behavior. Similarly to compression testing curves, the primary difference in behavior of specimens occurs after initial damage. In the case of three point bending on earthen materials, the failure behavior is usually a single sudden fracture initiating from the tensile side of the beam. The quantity of straw altered the quantity of residual strength after initial fracture and the speed at which the specimen lost residual strength with continued displacement. Representative curves are shown in Figure 6.20.

While straw content may not always have statistically significant influence on the peak

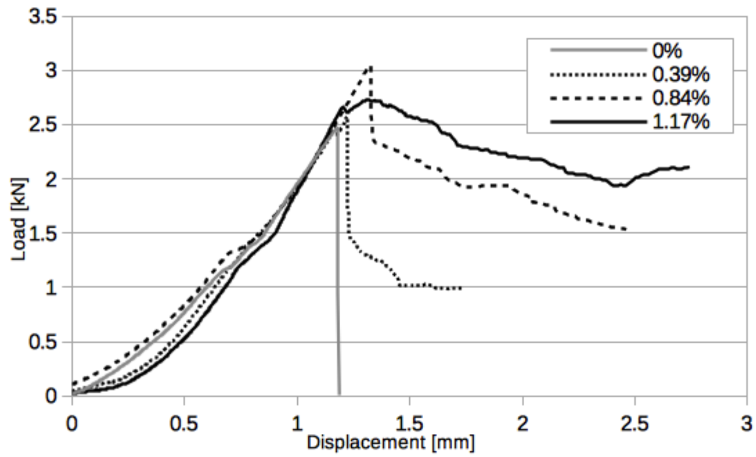

Figure 6.20: Typical three point bend testing curves from tests of varying straw fiber mass fractions.

strength of cob, the influence on failure behavior suggests that including straw in residential construction materials would significantly improve structural safety in the event of damage, such as might be induced by an earthquake.

6.6 Conclusions

- Sand-clay mixtures show a bi-linear response to changes in clay content behavior across the parameters evaluated.
- Apparent straw density in specimens was similar to as-baled density when calculated from measurements of specimen densities and fiber mass fractions.
- Compressive strength was sensitive to both clay and straw content.
- Maximum average strength while varying straw content in both flat plate compression and three point bending was observed using 0.84% straw by weight.
- Bending strength failed to show statistically significant sensitivity to either clay or straw content.
- A wide range of mix ratios can produce cob of sufficient compression strength to meet New Mexico Adobe Code standards.

- Peak strength in both compression and bending was observed when using 55% soil and 0.84% straw.
- Material behavior after initial damage is significantly altered by straw content for both compressive and three point bend testing.

CHAPTER 7

INFLUENCE OF DIFFERING REGIONAL SOILS ON MECHANICAL STRENGTH

7.1 Overview

This chapter discusses the influence of local differences in clay-rich soil on the final strength of cob. Clay soils from Taos, NM, Longivew, TX, and a secondary site in Tulsa, OK were evaluated for particle size distribution, clay content, and plastic limit. Specimens were manufactured to maintain a similar final clay content in all specimens. Specimens were tested in both compression and three-point bending to evaluate differences between regional clay properties, rather than simply clay content present in specimens. Patterns of clay content and strength were compared to prior single-soil testing.

Understanding the sensitivity of constructed materials to local ingredient properties is vital to establishing national guidelines for earthen construction. While performance-based standards provide safety for each new construction, such testing is also expensive and of limited availability. Understanding the influence of regional differences in clay soils on final material strength, if any, will minimize unnecessary burdens on construction while maintaining safe standards.

7.2 Soil Sources

Soil specimens selected to capture a diversity of natural clay content and clay type. Samples were taken from Taos, New Mexico, Longview, Texas, and second site in Tulsa. Taos has over 1,000 years of earth construction history, most notably constructed by the Red Willow People. Pueblo tradition uses soil removed from the mountainsides for construction and maintenance of the Pueblo buildings. The sample used in this work was taken from the high plains due to restrictions on access to traditional adobe digging locations. Longview soil was taken from a site known for highly sticky soil with iron oxide contents. The second Tulsa location soil is a dark brown heavy clay taken from the Coal Creek watershed. The soil source used throughout the rest of this work will be referred to hereafter as the baseline soil.

7.3 Soil Characterizations

7.3.1 Particle Size Analysis

Wet Sieving: Wet sieving was performed for each soil. Each soil showed a majority of fine particles, as expected from clay-rich sub-soils. Particle mass fractions captured in each sieve are shown in Figure 7.1. Soils taken from sites in Tulsa, OK (both "Baseline" and "Tulsa") showed the highest fraction of particles passing the finest sieve of 0.038mm.

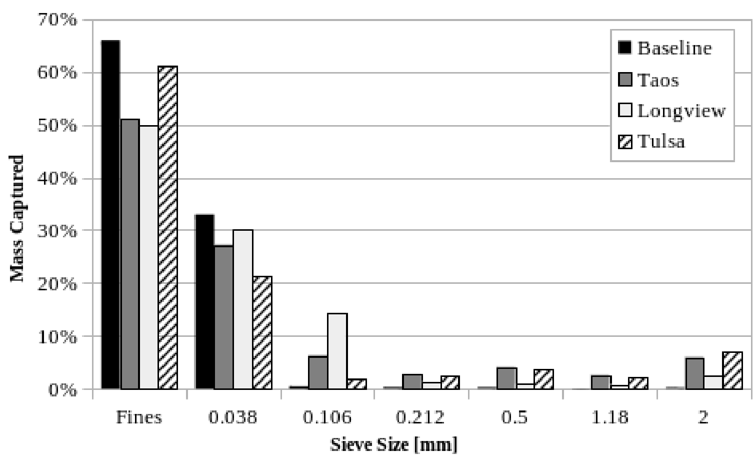

Figure 7.1: Particle size mass fractions captured during wet sieving.

Data from wet sieving can be used to calculate the more traditional percent passing plot, shown in Figure 7.2. Percent passing plots show that the baseline soil contains the highest fraction of fine particles of any sample tested. Longview soil shows the next largest fraction of fine and medium particles, with only small changes in the percent passing coarse sieves.

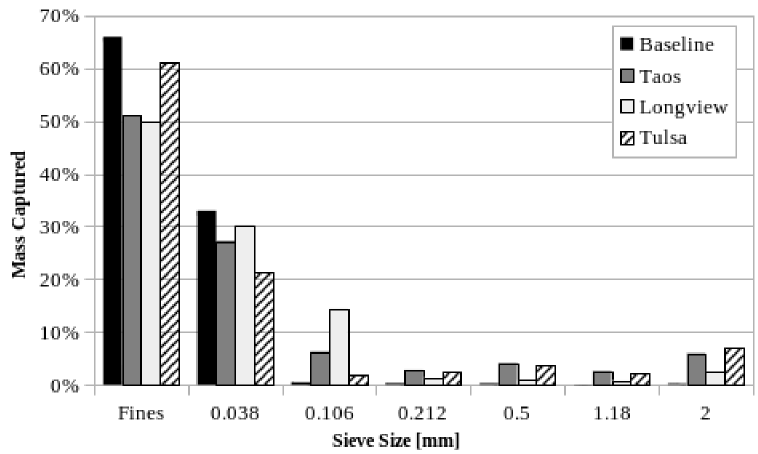

Figure 7.2: Particle size mass fractions captured during wet sieving.

Dynamic Light Scattering: Dynamic light scattering was used to determine the particle size distribution of particles passing the 0.038mm sieve, the "fines" from Figure 7.1. These particles were soaked in water with a small quantity of sodium hexametaphosphate as a deflocculating agent. The particles did not remain in suspension permanently but would settle slowly enough to allow data collection. A Microtrak dynamic light scattering instrument was used for data collection. For each soil sample, a total of ten measurements were taken on two different subsets of the fine particles. The ten measurements were averaged to create a particle size distribution and percent passing curve for each soil's fine particles. The percent passing curve for all four soil samples is shown in Figure 7.3. Longview and Tulsa soils show the highest quantity of particles passing less than 2μm

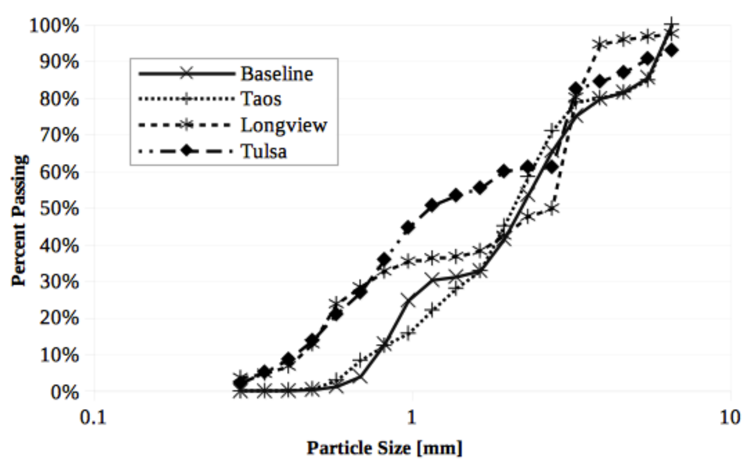

Figure 7.3: Particle size mass fractions of fine particles of each soil as measured by DLS.

Particle size distributions for the same specimen calculated by DLS were inconsistent run-to-run. The presence of particles up to 38μm, larger than the nominal particle size range of the instrument, may have contributed to data fluctuations. The average of several collection runs began to resemble a smooth distribution.

Sedimentation Test: A sedimentation test using a hydrometer for suspended particle mass density was performed according to ASTM D422 [12]. The only modification of the test procedure from the standard was the substitution of a magnetic stirrer for an approved agitation chamber. Hydrometer 152H was used for the measurement of mass of particles suspended per liter of solution. Hydrometer reading and solution temperature were recorded at specified times over a period of 24 hours as particles settled in a graduated cylinder.

Figure 7.4 shows the percent passing plot from sedimentation measurements, and Table 7.1 shows the calculated fractions of sand, silt, and clay for each soil.

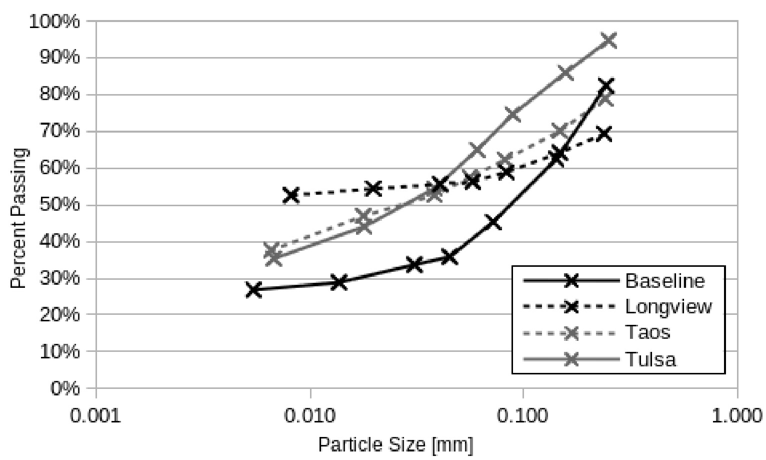

Figure 7.4: Percent passing plot for soils measured using hydrometer-based sedimentation testing.

Baseline soil shows the highest content of sand and a steep drop in percent passing in the large particle region. This indicates a particle size distribution that is less uniform than the other three samples, whose percent passing curves are more linear when plotted on a semi-log scale.

Table 7.1: Hyrometer-assisted sedimentation testing soil composition results.

Location	Sand (63μm-2mm)	Silt (2μm-63μm)	Clay (<2μm)
Baseline	57.84%	16.20%	25.95%
Longview	43.18%	5.25%	51.58%
Taos	41.27%	24.95%	33.78%
Tulsa	34.25%	34.11%	31.64%

Clay Content Determination: The clay fraction of each soil was calculated by multiplying the fraction of particles smaller than 2μm calculated by DLS and the fraction of fine particles from wet sieving. Table 7.2 shows the calculated fractions of sand, silt, and clay in each soil. Because clay shows both swelling and adhesion properties when hydrated, clay content will be the primary characteristic of interest in each soil. Differences between the effects of silt and sand on strength of cob is left for later experiments. Particle size definitions from ISO 14688 are used for classifications of sand, silt, and clay [48].

Table 7.2: Soil particle size mass distributions calculated from sieving and DLS.

Location	Sand (63μm-2mm)	Silt (2μm-63μm)	Clay (<2μm)
Baseline	0.6%	71.8%	27.4%
Tulsa	10.6%	46.5%	35.9%
Taos	15.8%	55.3%	23.0%
Longview	17.4%	47.4%	32.7%

The calculated clay content by hydrometer testing does not agree with with wet sieve and DLS testing for clay content. As shown in Table 7.3, the calculated clay contents by hydrometer testing differ from DLS in both the absolute quantity of clay and the identification of samples with highest or lowest clay contents.

No statistically significant correlation was observed between calculated clay content resulting from wet sieve clay + DLS and hydrometer-assisted sedimentation testing methods (p=0.8602). Because of the inconsistent results returned by DLS for determining particle

Table 7.3: Comparison of clay content calculated by wet sieving + DLS and hydrometer-assisted sedimentation.

Location	Wet Sieve Clay Content	Hydrometer
Baseline	35.40%	25.95%
Longview	35.28%	51.58%
Taos	29.80%	33.78%
Tulsa	44.57%	31.64%

size distribution of particles passing the 38μm sieve, the hydrometer-based methods outlined in ASTM D422 are taken to be more reliable.

7.3.2 Plastic Limit Determination

Plastic Limit was determined in using the method described in Chapter 3.4.9. Table 7.4 shows the two tests of plastic limit for each soil sample and resulting average rounded to an integer percentage as specified in ASTM D4318 [8].

Table 7.4: Plastic limit test data.

Location	Trial 1	Trial 2	Plastic Limit
Baseline	45.5%	21.1%	33%
Taos	27.7%	23.7%	26%
Longview	21.5%	21.8%	21%
Tulsa	22.3%	23.3%	23%

Plastic limit showed statistically significant changes with respect to clay content ($p=0.0417$). However, more than four data points would be necessary to show the shape of the curve relating these properties. With sufficient data, plastic limit testing may be able to serve as a low-cost material evaluation method for cob construction.

7.4 Design of Experiment

The experiment was designed using a random single-effects model. Taos soil contained the lowest clay content, requiring the highest soil fraction to hold clay content constant across all batches. The amount of soil available from the Taos site limited the total number of specimens manufactured for each location to 14. These were divided equally between flat-plate compression and three-point bend testing. Each specimen's test method was randomly assigned.

7.4.1 Specimen Preparation

Specimens were prepared as described in Chapter 4.3. Because the purpose of this test was to isolate the influence of different kinds of clays on mechanical strength, rather than confirming the influence of clay content on strength, clay content of the manufactured cob was held constant across all batches. Differing amounts of sand were added to achieve a final clay content of 12% by mass. Due to time constraints, clay content was calculated using data available from wet sieve and DLS methods, although hydrometer-based sedimentation testing was later considered more reliable. A target straw mass fraction of 0.56% was also selected. Target mass ratios of sand, clay and straw were chosen to exhibit similarity prior experiments and maximize the number of specimens manufactured from limited materials. Desired and actual mass ratios included in this test, as recalculated using soil clay contents from hydrometer testing, are shown in Table 7.5.

Table 7.5: Material volume ratios tested.

Location	Sand	Clay	Straw
Target	87.44%	12.00%	0.56%
Baseline	63.69%	9.50%	0.56%
Longview	63.15%	18.98%	0.57%
Taos	64.66%	12.07%	0.41%
Tulsa	70.16%	9.50%	0.55%

Differences between batches will be compared with modeled influence of clay on strength for evaluation of differences in strength caused by regional differences, rather than clay content.

7.5 Results

7.5.1 Compressive Strength

Compressive strength was testing using seven specimens per clay source. Table 7.6 shows the summary statistics for the peak strengths of each location.

Table 7.6: Material volume ratios tested.

Location	Average [MPa]	Std. Dev. [MPa]	COV
Baseline	1.35	0.13	9.6%
Longview	1.00	0.16	15.6%
Taos	1.02	0.16	16.1%
Tulsa	1.37	0.12	9.0%

All specimens showed moderate scatter in strength results. Both sets of specimens from Tulsa ("Baseline" and "Tulsa") showed the highest average strengths. ANOVA testing shows significant differences between the compressive strengths of the soils (p=0.0000).

7.5.2 Bending Strength

Bending strength was also evaluated for seven specimens per clay source. Table 7.7 shows the summary statistics for peak bending stresses on tested specimens for each location.

Table 7.7: Material volume ratios tested.

Location	Average [MPa]	Std. Dev. [MPa]	COV
Baseline	1.05	0.09	8.15%
Longview	0.64	0.05	7.06%
Taos	0.57	0.02	4.30%
Tulsa	0.66	0.07	9.95%

Bending strength results showed smaller statistical scatter than compressive strength results. Baseline soil bending strength exhibited much higher strength than any other soil source. ANOVA testing shows significant differences between the bending strengths of the soils (p=0.0000).

7.6 Analysis

Strength results from different regions were compared to other more easily measured properties. If a property of a local soil correlates well to mechanical strength, this property could provide a method of showing on-site or local soils acceptable for structural applications to regulators.

Despite not showing the highest compressive strength, baseline soil strength in three point bending shows significantly stronger behavior than any other soil source. The shape of the percent passing plot calculated from hydrometer testing (Figure 7.4) shows the baseline soil having less well-graded particle sizes. The low silt content and balanced clay and sand ratios may contribute to creating high bending strength. However, the influence of silt-sand ratios on mechanical strength are beyond the scope of this experiment.

7.6.1 Correllation to Clay Content

Linear regression was performed on both compressive and bending strength with respect to clay content calculated by hydrometer-assisted sedimentation. Because hydrometer-based clay content measurements differed from those calculated by wet sieving and DLS, the clay content of the batches differed from each other. Strength data with respect to calculated mix clay content is shown in Figure 7.5. As discussed in Chapter 6, clay content showed a bi-linear behavior with respect to compressive and bending strength. At low clay contents (between 5% and 20%), clay is expected to cause an increase in compressive strength. Bending strength showed no significant correlation to clay content in prior testing. However, correlation of both compressive and bending strength to clay content calculated by hydrometer testing showed statistically significant reductions in strength. Table 7.8 shows the fitted

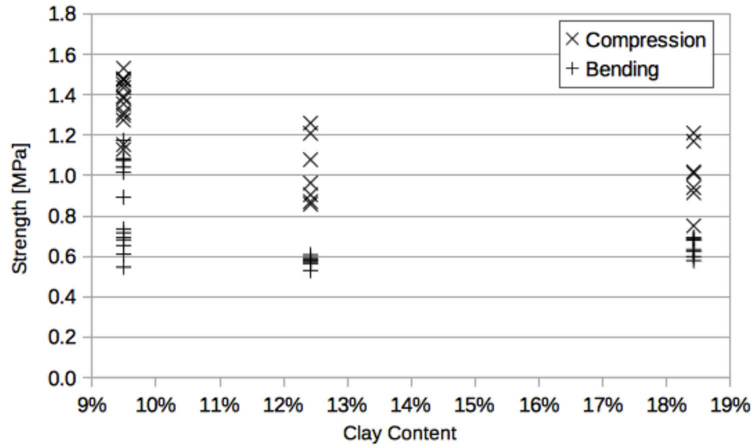

Figure 7.5: Compression and bending strength of location comparison specimens with respect to calculated mix clay content.

values of linear regression coefficient for slope of the fitted line.

Table 7.8: Linear regression results for slope of strength vs. clay content (confidence interval of 95%).

	Lower Bound	Estimate	Upper Bound	p
Compression	-5.91	-4.07	-2.23	0.0001
Bending	-4.32	-2.39	-0.47	0.0169

These results indicate that, if clay generally increases compressive strength, other features of the soils also significantly contribute to strength.

7.6.2 Correllation to Plastic Limit

A potential relationship between plastic limit and mechanical strength was also explored. Linear regression between plastic limit and compressive strength showed no significant influence, but the relationship between bending strength and plastic limit was significant. Regression results for the slope coefficient are shown in Table 7.9.

Unlike correlations between clay content and strength, the relationship between strength and plastic limit was generally positive. As Figure 7.6 shows, this relationship is not linear, but driven primarily by the high-plastic-limit data points from the baseline soil source.

Table 7.9: Linear regression results for slope of strength vs. clay content (confidence interval of 95%).

	Lower Bound	Estimate	Upper Bound	p
Compression	-0.01	1.81	3.63	0.0512
Bending	2.65	3.58	4.51	0.0000

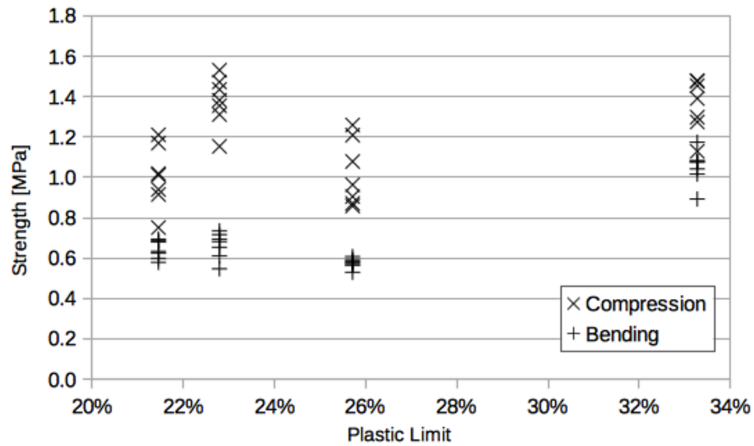

Figure 7.6: Compression and bending strength of location comparison specimens with respect to plastic limit.

Future study may show a more reliable relationship between plastic limit and mechanical strength.

7.7 Conclusions

- Soils from different regions or watersheds exhibit differing ratios of sand, silt, and clay.
- Wet sieving is effective in determining the particle size distribution of coarse particles, but dynamic light scattering is not well suited to the large particles remaining after wet sieving.
- Hydrometer-assisted sedimentation testing from ASTM D422 proved to be direct and easy to implement.
- Hyrometer-assisted sedimentation testing results did not agree with wet sieve and DLS results, and the hydrometer method was selected for high-clay-content soils.

- Plastic limit was compared for each soil.
- Compressive strength was highest on average for the Tulsa specimens, though Baseline specimens were nearly the same strength.
- Baseline specimens were approximately 60% stronger in three-point bending than any other soil.
- Linear regression testing showed a statistically significant, negatively sloped influence of clay content on both compressive strength and bending strength. This means that higher clay contents are expected to produce lower strength specimens, contrary to what prior experiments have shown.
- Linear regression testing showed a significant influence of plastic limit on bending strength, but failed to show a significant influence on compressive strength. The slope of this relationship was positive, indicating higher plastic limits would be expected to produce higher strength specimens.
- Without comparing further soil samples or controlled soil mixes, attempting to predict specimen strength by only clay content or plastic limit is premature.
- Because higher clay content mixes produced lower strength specimens, when prior studies predicted higher strength specimens, other properties of the soil likely have significant influence on the strength of specimens. The modeling conducted in Chapter 8 reflects a likely general shape of response surface and fitted parameters for a single source of soil.

CHAPTER 8

MODELING OF COB COMPRESSION STRENGTH

8.1 Overview

The goal of this chapter is to describe several modeling efforts designed to predict the compressive strength of cob as a function fo clay, straw, and sand content. Prior qualitative models describing the effects of clay and straw content are discussed and equations for these models are proposed. Three models are presented to describe material compressive strength based on available data. The first two are both additive independent effects models. The first was fitted to all available data at the time: the constituent material mix ratio experiment and baseline data from the moisture content study. New data was gathered from the theoretical maximum strength mix from the first model and a separate mix from the regional clay study. These new data sets required re-fitting the independent effects model. The potential interaction between the effects of clay and sand also drove the development of a more general additive effects model. This model allows the influence of added straw to change with respect to clay content, capturing potential interaction between these parameters. All models are compared and recommendations for future validation are discussed.

8.2 Theoretical Background

Ideally, a model of bulk material behavior can be built up from an analytical description of micro-mechanical behavior. In the case of cob, the dual composite nature (an aggregate composite of clay and sand mixed with fiber reinforcement), such modeling rapidly becomes complex. The variability of including natural soil in the material increases the difficulty of producing accurate first-principles mechanical models.

The discussion in this section is instead intended to provide some fundamental behavior and equations by which the strength and stresses of cob may be bounded. An analysis of the stresses developed by a clay shell around a spherical aggregate particle may provide analytical upper bounds on inter-granular friction, governing bulk material shear strength, and the peak clay shrinkage rate before cracking from hygroscopic strain becomes likely. The effect of straw on drying shrinkage and loading stresses is discussed in general terms. Future work may be able to develop fundamental material models to accurately describe bulk material behavior, including stiffness and failure envelopes. However, insufficient data is currently available to validate a model correlating intrinsic soil conditions and micro-mechanics to bulk cob properties.

8.2.1 Spherical Aggregate Analysis

Research by Charles Augard suggests that earth-based construction materials gain their strength from the shrinkage of clay driving sand particles against each other [49]. Clay is hygroscopic, binding strongly to available water. Many kinds of clays also swell when bound to water and shrink when dried [57]. As clay dries and shrinks, internal stresses constraining the motion of entrapped aggregates develop. Shrinkage of clay also can increase normal forces on the surfaces of aggregate particles, increasing static friction between clay and aggregate, thereby increasing bulk shear strength.

In the most simple case, a surface of clay surrounds a spherical aggregate particle. The schematic shown in Figure 8.1 shows relevant dimensions. The aggregate (usually quartz-rich sand grains) is assumed to have no hygroscopic behavior. The clay soil is applied to the surface in a wet plastic state and allowed to dry. If the total amount of shrinkage from drying (hygroscopic strain) is denoted as η_h, the inner diameter of the clay ring, if unconstrained, can be given by Equation 8.1.

$$1 = \frac{D_{dry}}{D_{wet}} + \epsilon_h \tag{8.1}$$

Because the diameter of the inner surface of the clay ring is constrained by the

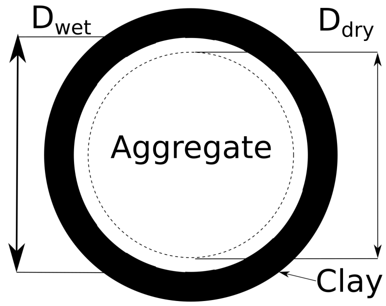

Figure 8.1: Shrinkage of clay shell if unconstrained by aggregate.

aggregate surface, radial pressure at the surface is generated and strain from this pressure will be equal to ϵ_h. The stress in each in-plane axis of the clay material taken from the spherical pressure vessel equations and shown in Equation 8.2.

$$\sigma = \frac{Pr}{2t} \tag{8.2}$$

Because both directions of the sphere contain hoop stresses, $\sigma_x = \sigma_y$. Therefore, the equivalent stress in the volume of the clay shell, from the von Mises criterion, is given in Equation 8.3.

$$\sigma_{eq} = \sqrt{\sigma_x^2 - \sigma_x \sigma_y + \sigma_y^2} = \sqrt{2\sigma(\sigma - 1)} \tag{8.3}$$

Cracking of the clay surface will begin when this stress exceeds the tensile strength of the clay soil.

The circumferential strain in the clay shell will be given by Equation 8.4.

$$\epsilon_{hoop} = \frac{\sigma}{E} - \nu\frac{\sigma}{E} = (1 - \nu)\frac{\sigma}{E} \tag{8.4}$$

Because the internal surface of the clay shell is bonded to the surface of the aggregate particle, shrinkage strain will be exactly equal to strain from pressure exerted by the aggregate. Therefore, internal stress of the clay can be calculated from the shrinkage rate and material properties, as shown in Equation 8.5.

$$\sigma = \frac{\epsilon_{hoop} E}{1-\nu} = \frac{\epsilon_h E}{1-\nu} \tag{8.5}$$

Substituting the function for σ from Equation 8.2 into Equation 8.5 and solving for the resulting pressure exerted on the contact surfaces generates Equation 8.6.

$$P = \frac{2t\epsilon_h E}{R(1-\nu)} \tag{8.6}$$

Therefore, pressure exerted on aggregate surrounded by clay is proportional to the rate of shrinkage in the clay species. The residual compression caused by clay shrinkage increases contact forces between aggregate particles, increasing maximum force exerted by static friction. Residual tension in the clay matrix can lead to cracking if overall shrinkage stresses are greater than clay tensile strength.

Hygroscopic and shrinkage behavior of clay soils is also indirectly measured by matric suction measurements of soil voids at various moisture contents. Work to predict shear strength of soils from the soil-water characteristic curve was successful for predicting shear strength from a two-parameter model after experimental measurement of the characteristic curve [2]. Tests that correlate soil properties with bulk material strength may be used in future to reduce the need for destructive testing.

8.2.2 The Effect of Straw on Shrinkage and Cracking

Empirical evidence shows that straw does not eliminate cracking in a clay-rich soil but can distribute the cracking and reduce the maximum defect size [43, 45]. The analysis in this section assumes that no stress relief occurs during drying due to plastic deformation of the clay when still damp. The potential for included natural fibers to exhibit hygroscopic strain as well complicates the modeling of bulk residual stresses created during drying. As such, the equations above should be considered an upper bound on residual stress purely from hygroscopic strain between clay and aggregate.

8.2.3 Critical Fiber Volume Fraction Calculation

Theoretical models of tensile performance of uniaxial fiber reinforced composites are used to calculate the critical fiber volume fraction, which is the volume fraction of fibers at which the resulting composite has equivalent properties to the pure matrix material. Models have been discussed by Agarwal et. al for typical descriptions of longitudinal strength of uniaxial fiber composites [1]. The typical model assumes that all fibers fail at the same strain and that the failure strain of the fibers is lower than the failure strain of the matrix material. In three-point bend testing, clay-sand specimens without straw exhibited twice the failure strain of uniaxially tested straw stalks. At low fiber volumes, fibers are expected to fail before the matrix, causing the matrix material to carry all the remaining load, where σ_{cu} is th logitudinal strength of the composite, σ_{mu} is the ultimate strength of the matrix, and V_f is the volume fraction of the fiber reinforcement. This behavior is described in Equation 8.7.

$$\sigma_{cu} = \sigma_{mu}(1 - V_f) \tag{8.7}$$

At high fiber volume fractions, the matrix is not expected to be able to sustain the load after fibers fail, causing the entire composite to fail. This behavior is described in Equation 8.8, where σ_{fu} is the ultimate strength of the fiber, $(\sigma_m)_{\varepsilon f}$ is the stress developed in the matrix at the failure strain of the fibers.

$$\sigma_{cu} = \sigma_{fu}V_f + (\sigma_m)_{\varepsilon f}(1 - V_f) \tag{8.8}$$

Critical fiber volume fraction is the point at which Equation 8.8 equals the initial matrix strength at 0% fiber volume fraction, shown in Equation 8.9.

$$V_{crit} = \frac{\sigma_{mu} - (\sigma_m)_{\varepsilon f}}{\sigma_{fu} - (\sigma_m)_{\varepsilon f}} \tag{8.9}$$

From the calculated properties of the matrix and fibers shown in Table 8.1, the calculated critical fiber volume fraction was 2.65%. Tensile composite properties of cob were calculated from three-point bending tests.

Table 8.1: Cob tensile properties as a fiber-reinforced composite.

Parameter	Calculated Value
σ_{mu} [MPa]	0.756
E_m [MPa]	25.15
ε_m	1.21%
σ_{fu} [MPa]	21.4
E_f [GPa]	3.13
ε_f	0.765%
$(\sigma_m)_{\varepsilon f}$ [MPa]	0.192

Bending strength data did not align well with this model. First, data tensile strengths were calculated from three-point bending tests, inducing shear and bending stresses rather than pure tension. Second, and more importantly, these models assume uniaxial fibers aligned with the tensile stresses, while specimens tested used random oriented long fibers. Therefore, the fibers imparted significantly less strengthening than the model predicted, as can be seen in Figure 8.2.

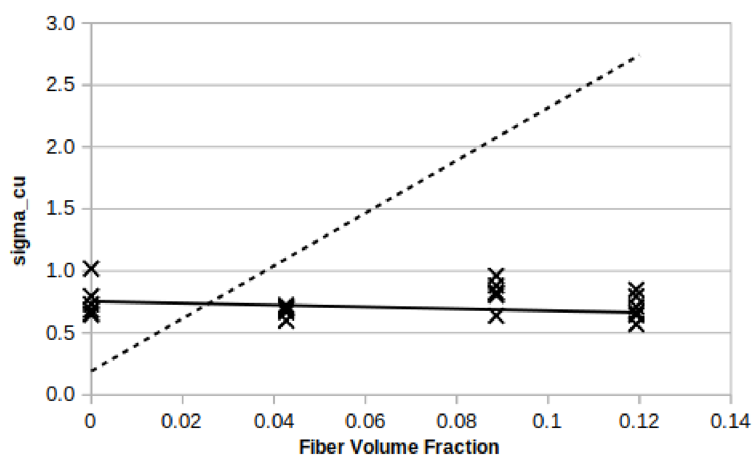

Figure 8.2: Bending strength experimental data compared with Equations 8.7 (solid) and 8.8 (dashed).

Compression testing data was compared to models for longitudinal compression strength. Like the tensile models, the primary difference between model assumptions and the test specimens is the alignment of fibers. Compression strength of uniaxial fiber composites are modeled by Equation 8.10, where σ_{lu} is the longitudinal compression strength, E_f is the modulus of elasticity of the fiber reinforcement, V_f is the fiber volume fraction, E_m is the modulus of elasticity of the matrix, V_m is the volume fraction of the matrix, ν_f is the poison's ratio of the fiber, and ν_m is the poison's ratio of the matrix.

$$\sigma_{lu} = \frac{(E_f V_f + E_m V_m)(1 - V_f^{1/3)})\varepsilon_{mu}}{\nu_f V_f + \nu_m V_m} \tag{8.10}$$

Compression strength data showed the same shape as Equation 8.10 but showed significantly smaller response than the model predicted and response at lower fiber volume fractions than predicted.

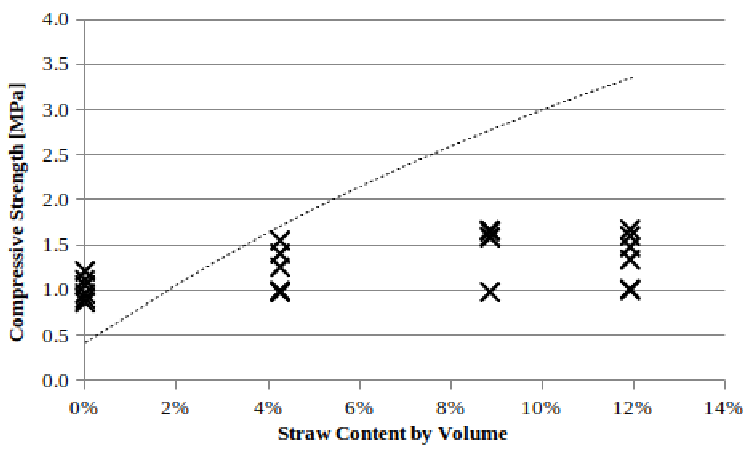

Figure 8.3: Compression strength data compared with Equation 8.10 (dashed).

Aside from fiber alignment, properties possibly influencing the fit of theoretical models to experimental data include a non-ideal bond between fiber and matrix material, the hollow straws displacing more matrix material than solid fibers, or the wider statistical distribution of straw ultimate strains than manufactured fibers. Further research is necessary to reconcile experimental data with established composite performance models.

8.3 Initial Model

Data from Chapter 6 was fitted with an additive independent-effects model for compressive strength. Because no statistically significant trends were observed for bending strength in Chapter 6, predictive modeling of bending strength was not performed. An additive model was chosen to describe the separate influences of clay and straw content on bulk strength. The forms of model equations were selected to best fit the experimental data while minimizing fit parameters. Materials were assumed to behave continuously across the feasible region of mix ratios, though differentiability at all points was not assumed.

Because the experimental points selected for the mix ratio experiment were nearly perpendicular in the design space, interaction between the two independent variables of clay and straw content was not observable. The initial model simply summed the terms describing the influence of clay and the influence of straw on strength without considering any interaction. The following equations are fitted to experimental data and the model quality evaluated in Section 8.3.4.

8.3.1 Sand-Clay Matrix Behavior

Clay Saturation Calculation: From testing of sand-clay specimens in Chapter 6, a bi-linear behavior for sand-clay compressive strength was observed (Figure 6.7). It was postulated that the inflection point in the bi-linear fit was the point at which clay saturated the voids between sand particles and began to displace sand grains.

Sphere packing theory has shown that an ideally packed set of randomly-sized spheres will leave approximately 36% of the bulk volume empty [27]. Regression modeling on the inflection point of the matrix specimen experiment demonstrated an inflection point at 21.6% clay by mass. Equation 8.11 shows the form of the bi-linear equations used for modeling strength influence of clay, where m_1,m_2, b_1, b_2, and m_c are parameters for model fitting, and σ_{matrix} is the resulting strength of the sand-clay mixture which forms the matrix for cob when viewed as a fiber-reinforced composite.

$$\sigma_{matrix} = \begin{cases} m_1 m_c + b_1, & \text{if } m_c \leq m_{crit} \\ \\ m_2 m_c + b_2, & \text{if } m_c > m_{crit} \end{cases} \tag{8.11}$$

The primary constraint on this set of equations was that $b_2 = b_1 + m_1 m_{crit} - m_2 m_{crit}$, ensuring that the two linear portions intersect at the clay saturation point.

8.3.2 Straw Augmentation Behavior

Straw performs multiple roles in the behavior of well-made cob. It distributes stresses through the volume of the cob, reduces severity of cracking from clay shrinkage, and improves the damage tolerance of cob, even providing behavior that can appear similar to plastic deformation in metals. Each of these mechanisms is important for safe and feasible construction but do little to directly alter material strength. Effective re-distribution of stresses from points where load is applied or around stress risers can improve the apparent strength in buildings and test specimens.

Experimental data presented in Section 6.4.1 shows statistically significant trends of compressive strength with respect to straw mass fraction. Specimens with included straw were stronger than samples without straw. Increasing straw quantity at low straw mass fractions (less than approximately 1% by weight) tended to increase specimen strength. Highest straw fraction specimens (1.17% by mass) showed a reduced strength, as shown in Figure 6.15.

A second-order polynomial fit was selected for modeling the influence of straw on compressive strength. Based on the trends outlined above, the fit is expected to be concave down with the parabolic peak near 1% straw mass fraction. Even though straw does not change the compressive strength of cob as significantly as clay does, the influence of straw on damage tolerance, as discussed in Section 6.5, demonstrates the value of straw inclusion in earthen materials like cob.

Combining the straw and clay behavior equations, the model to fit to existing data is represented in Equation 8.12, where m_c is the clay mass fraction and m_s is the straw mass fraction, and all others are fit parameters. The one constraint applied to the model is that $b_2 = b_1 + m_1 m_{crit} - m_2 m_{crit}$.

$$\sigma_c = \begin{cases} m_1 m_c + b_1, & \text{if } m_c <= m_{crit} \\ m_2 m_c + b_2, & \text{if } m_c > m_{crit} \end{cases} + a m_s^2 + b m_s + c \tag{8.12}$$

After the reduction of one degree of freedom by the single constraint, Equation 8.12 has seven degrees of freedom. The two inputs are independent within the bounds that neither is negative and that the sum of m_c and m_s is never greater than 1 (100%). The quantity of sand for a given mix can be calculated by $m_{sand} = 1 - m_c - m_s$.

Model fitting and quality testing were performed using a Differential Evolution and Particle Swarm Optimization (DEPS) algorithm implemented in the Solver function of LibreOffice [77].

8.3.3 Gaussian Process Regression

In addition to analytical modeling, Gaussian process regression (GPR) was used to fit a model to experimental data using machine learning. GPR is a non-parametric kernel-based modeling method which can return both predicted behavior and model confidence for both interpolation and extrapolation tasks. The kernel, provided to the GPR routine on initialization, is a transformation function which distorts the problem space so that the model becomes a linear function. GPR was selected because of the statistical nature of sample testing and straightforward model use and interpretation in comparison with more complex machine learning techniques.

The GPR model was trained on the average and standard deviation of each test set of fully dried cob of the 101.6x101.6x304.8mm (4x4x12 inch) geometry specimen. A radial basis function (RBF) kernel was selected for kernel with an initial length scale of 20%.

The inputs to the GPR training were the ratios of sand, clay, and straw used for each batch of specimens. After training, models could be queried with a test recipe to predict resulting strength and uncertainty bounds. GPR modeling was then compared with analytical models.

GPR modeling presents advantages of flexibility as data sets grow and quantitative uncertainty bounds on model results. The kernel is treated as a black box, eliminating the ability to clearly communicate the model in printed form. In this work, GPR results will be shown and analyzed, but the trained model itself will not be represented, but is available as a digital file (`https://github.com/Wright4TheJob/CobModelGPR`)[90]. This practice is common when working with "black box" machine learning models.

8.3.4 Results

Analytical Model: Analytical modeling, using equations from Section 8.3, was performed on all data points from the mix ratio study. The resulting model parameters and goodness of fit are shown in Table 8.2. The model showed good agreement with the experimental data.

Table 8.2: Analytical model initial parameters and fit.

Parameter	Fit Value
m_1	18.1400
b_1	-0.2368
m_2	-0.4629
b_2	2.3073
m_{crit}	0.1368
a	-5889.55
b	110.46
c	-0.252
R^2	0.7934

Figure 8.4a shows the raw data means from each test batch and the fitted model surface.

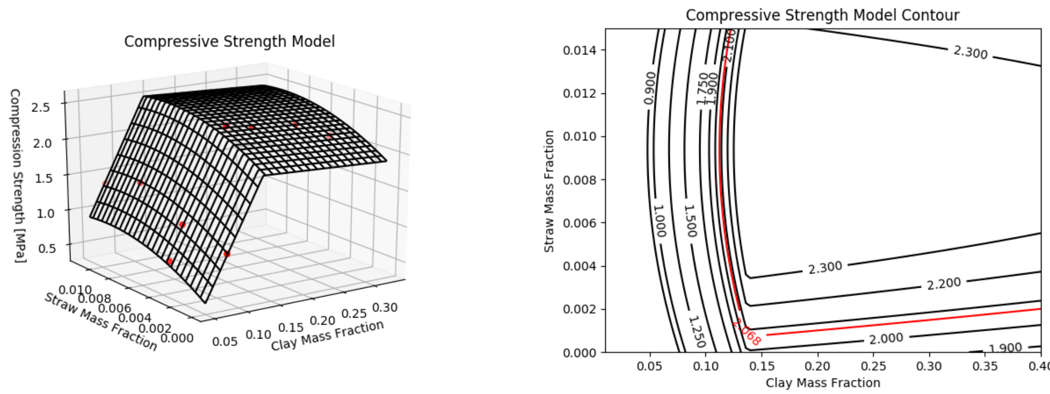

(a) Estimated response surface for compressive strength of cob mixes according to Equation 8.12.

(b) Contour plot of analytical model with minimum strength of New Mexico Adobe Code in red.

Figure 8.4: Compressive strength data and analytical and GPR mode fits.

Two "cross-section" views show the mixes varying clay and straw, respectively, along with the mean strength predicted by the analytical model, and the mean and 95% confidence interval predicted by GPR. Changes to compressive strength with respect to clay content were captured well by both models. Changes to strength with respect to straw was captured by the analytical model but largely ignored by the GPR model.

GPR Model: GPR modeling showed a similar, smooth response surface when trained on the mix ratio experiment data. The response surface and raw data are shown in Figure 8.6. GPR model had an $R^2 = 0.9174$.

8.3.5 Experimental Validation

Analytical modeling provided a closed-form solution for calculating peak strength mix under certain model parameter conditions (generally that the model is concave down). A closed-form solution for a peak strength mix requires $m_1 > 0$, $m_2 < 0$, and $a < 0$. If these conditions are met, the peak strength mix is found such that:

- $m_{clay} = m_{crit}$

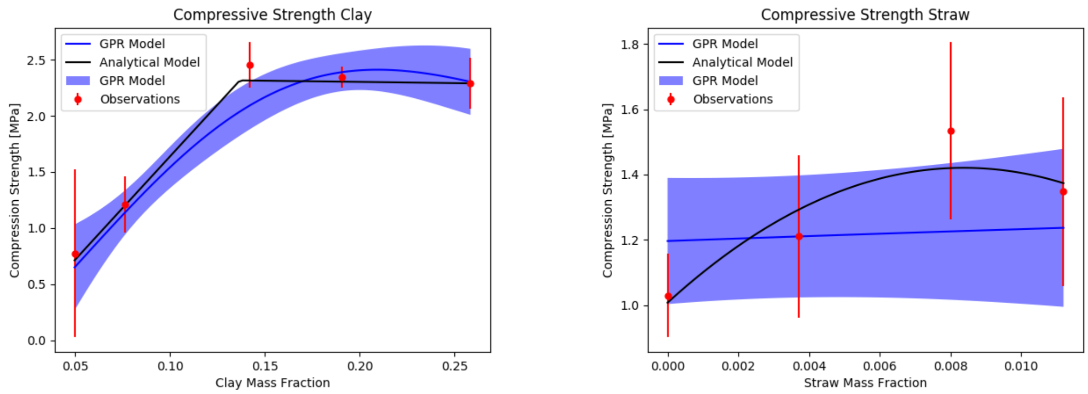

(a) Compressive strength with respect to clay content.

(b) Compressive strength with respect to straw content.

Figure 8.5: Compressive strength data and analytical and GPR mode fits.

- $m_{straw} = \frac{-b}{2a}$

- $m_{sand} = 1 - m_{clay} - m_{sand}$

These equations specify a clay mass fraction for a given mix, not a soil fraction. Clay fraction present in a particular soil must be quantified to calculate a soil quantity to use in a specified mix.

Using the analytical model and a soil clay content measured by wet sieving and DLS (approximately 35%), the maximum compressive strength mix was found to be 80.39% sand, 18.68% clay, and 0.93% straw by weight. Using the updated soil clay content from hydrometer testing, the theoretically peak strength recipe is 85.39% sand, 13.68% clay, and 0.94% straw by weight. When the model was created, hydrometer testing had not yet been performed. Therefore, the mix based on wet sieve clay content was created for validation of the model function. A mean compression strength of 2.51 MPa was predicted by the analytical model.

A total of 16 specimens were made to be divided equally between flat plate compression and three point bending tests. All specimens were made from a single batch of cob. Specimens were dried for 34 days before testing.

Table 8.3 shows the results of strength testing for both compression and bending. Both compression and bending strengths showed relatively low variance. The mean com-

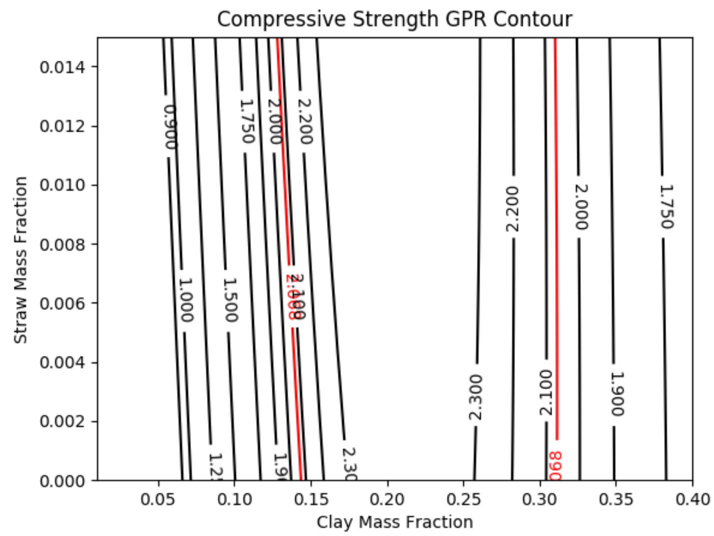

Figure 8.6: Estimated contour plot for compressive strength of cob mixes according to Gaussian process regression.

pressive strength is significantly lower than the predicted peak strength (p=0.0000 by a single-sample, two-tail t-test).

Table 8.3: Results of strength testing theoretical peak strength mix.

	Compression	Bending
Average	1.999	0.8006
Std. Dev.	0.034	0.0267
COV	1.72%	3.33%

Average bending strength was similar to that observed in the mix experiment. In addition to data collected from this peak strength study, the results of the clay source study provided another unique recipe to compare against the predictive model. These results included both compression and bending tests. All available data from bricks made with the baseline soil (Chandler park) were used to evaluate future models.

8.4 Revised Model

8.4.1 Analytical Model

The initial model captured the direct effects of clay and straw content on compressive strength observed in mix ratio experimental data. However, initial data was insufficient to draw inferences about interactions between effects of clay and straw content. Both peak strength and clay source comparison data exhibited significantly lower strength than the initial model anticipated (p=0.0000 and p=0.0014, respectively). These results suggest that an interaction of clay and straw is reducing the actual strength of specimens compared with the initial independent additive model. When the initial model was tested against all the data sets, rather than just the mix ratio experiment data, the goodness of fit was reduced from $R^2 = 0.7934$ to $R^2 = 0.6983$. Re-running parameter optimization increases the fit to $R^2 = 0.7448$.

A modification to the model may increase goodness of fit by allowing the influence of straw on the strength to change with respect to clay content. Rather than assign fixed constants to the parabolic model of influence of straw, each parameter was converted into a linear function whose independent variable is clay content. This modified form of straw influence is shown in Equation 8.13.

$$\sigma_{straw} = (a_1 m_c + a_2) m_s^2 + (b_1 m_c + b_2) m_s + c \tag{8.13}$$

When fitted, this model shows a fit quality of $R^2 = 0.7735$ with the addition of two parameters.

The response surface for this model is shown in Figure 8.7. The parabolic fit from variations in straw content changes at higher clay contents to reduce predicted strength at the test locations that showed lower strength than expected from initial fitting.

The contour plots for both forms of the model fitted to all available data shown in Figure 8.8 reveal little difference in strength in the part of the plot where the strength is above the of minimum compressive strength according to New Mexico Adobe Code.

Two-way ANOVA performed on all available data showed significant influences of

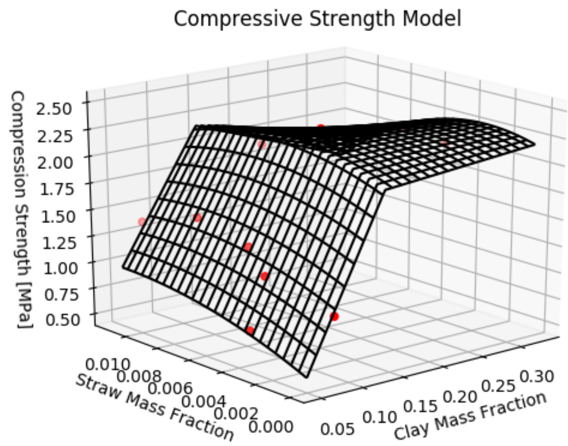

Figure 8.7: Estimated response surface for compressive strength of cob mixes according to revised analytical model with additional parameters.

clay and straw content. The influence of the interaction of clay and straw, while measurable, failed to show significance at a confidence threshold of 95%. Results of the two-way anova (type III sum of squares) is shown in Table 8.4.

Table 8.4: Influence of straw and clay on compressive strength by two-way ANOVA.

	Sum Sq	Df	F value	Pr(>F)
(Intercept)	0.2855	1	1.8430	0.17944
Clay	5.3691	1	34.6630	1.647e-07
Straw	0.7533	1	4.8631	0.03109
Clay:Straw	0.6063	1	3.9144	0.05225
Residuals	9.7583	63		

The design of experiments to test influences of clay and straw was primarily intended to test the independent influences of each ingredient. Specimens made at the predicted peak strength included more similtanious clay and straw than any single batch made during the mix ratio experiment, allowed limited testing of interaction between the influences of these ingredients. However, the effect of potential interaction between clay and straw contents

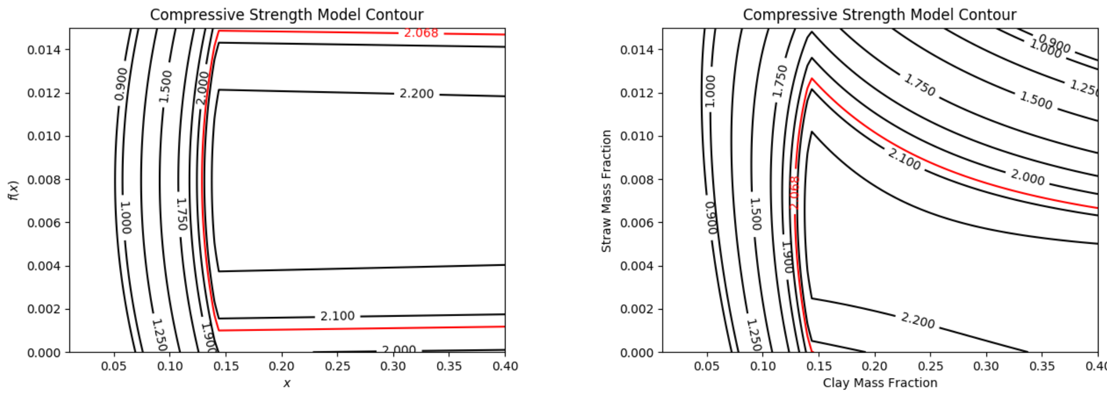

(a) Analytical model with independent clay and straw influences.

(b) Analytical model with variable straw influence with respect to clay content.

Figure 8.8: Contour plots of compression strength with respect to clay and straw mass fraction.

would magnified by testing a mix that maximizes both clay and straw content. This mix would provide more conclusive results on the statistical significance of any interaction. Future research should be designed to specifically examine the potential interaction of influences of clay and straw on compressive strength.

8.4.2 GPR Model

The Gaussian Process Regression model was re-fitted to all available data with the same parameters as initial fitting. The contour plot of GPR model is shown in Figure 8.9. The model showed an R^2 value of 0.9487. The model is less smooth than the analytical model, but fits the available data more closely. As more experimental data becomes available, machine learning models and refined analytical models would be expected to converge on an accepted function for predicting cob strength.

The roughness of this model reduces usability as a general model. The number of "folds" also throws suspicion on the accuracy of this model in capturing true material behavior instead of noise in the experimental data.

"Cross-section" views along the straw- and clay-variation mixes from the mix ratio experiment compare the values of the analytical and GPR models along with uncertainty bounds and experimental results. Figure 8.10 shows the analytical model re-fitted to all data

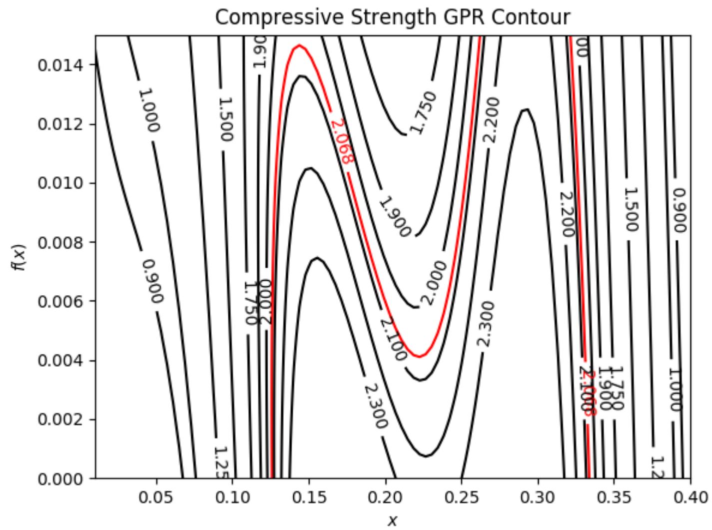

Figure 8.9: Contour plot of the GPR compressive strength model trained on all baseline soil data.

and including clay and straw interaction terms. The analytical model fits the data points shown less well than in Figure 8.5 because the model is fitted to additional data points outside the plane of the "cross-section."

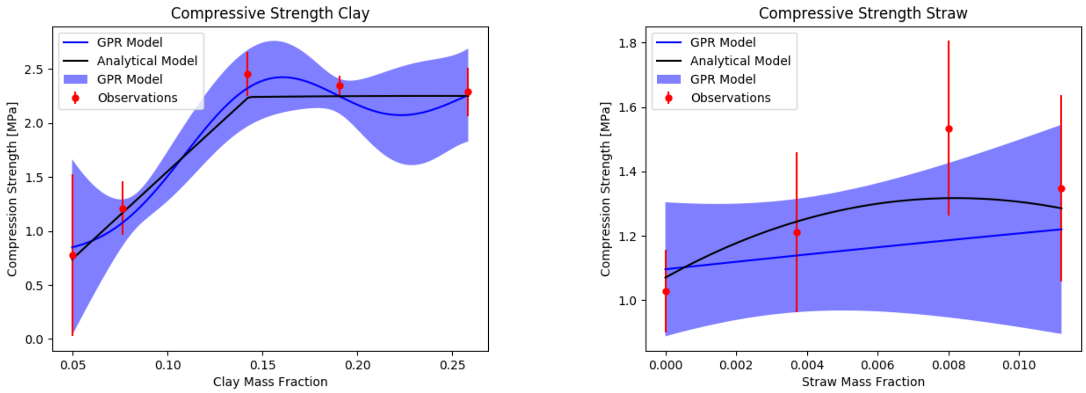

(a) Compressive strength with respect to clay content.

(b) Compressive strength with respect to straw content.

Figure 8.10: Compressive strength data, analytical model with interaction terms, and GPR model results.

8.5 Discussion

Comparison of the three tested models (initial independent, revised independent, and revised with interactions) is shown in Table 8.5.

Because the interaction of the influences of clay and straw failed to show statistical significance, the revised independent effects model is suggested as the best working model for strength predictions. Additional parameters may be required to model more complex behavior or interaction of behaviors as future data become available.

Contour plots show that a significant range of variation in clay and straw content can still produce cob that meets the compressive strength requirements of the New Mexico Adobe Code. Gaussian process regression showed good model fit ($R^2 = 0.9487$), but showed local variability likely to be caused by noise rather than underlying behavior. Cross section plots show generally good agreement between analytical and machine learning modeling methods, but analytical models result in smoother results.

Table 8.5: Analytical model, fit parameters, and quality for three evaluated models.

$$\sigma_c = \begin{cases} m_1 m_{clay} + b_1, & \text{if } m_{clay} \leq m_{crit} \\ m_2 m_{clay} + b_2, & else \end{cases} + (a_1 m_{clay} + a_2) m_{straw}^2 + (b_1 m_{clay} + b_2) m_{straw} + c$$

Parameter	Initial Independent	Revised Independent	Revised with Interaction
m_1	18.1400	15.0104	16.5285
b_1	-0.2368	-0.5010	0.9363
m_2	-0.4629	-0.0412	0.6877
b_2	2.3073	1.6474	3.1974
m_{crit}	0.1368	0.1427	0.1427
a_1	0	0	-21364.15
a_2	-5889.55	-4344.44	-2189.97
b_1	0	0	-83.96
b_2	110.46	68.89	78.82
c	-0.252	0.362	-1.230
R^2	0.7934	0.7448	0.7735

8.6 Conclusions

Analytical and machine learning modeling, experimental model validation, and model revision were performed for compressive strength data of cob made from the baseline soil (Chandler Park).

- Modeling was performed for compressive strength data only. Bending strength data failed to show statistically significant influence of mix ratio on strength.
- Initial modeling captured large-scale trends using a continuous, additive, independent effects model.
- GPR showed good agreement with both initial experimental data and analytical modeling.
- Closed-form solutions for maximum strength specimens are possible for certain parameter values of the analytical model. This form was used to calculate a theoretical peak

strength mix.

- The experimentally measured strength of the theoretical peak strength mix was significantly lower than predicted. The independent effects model was re-fitted to include new data, and a model including an interaction term was proposed.

- Interaction of influences of clay and straw failed to show statistical significance from the data currently available ($p=0.0522$) but the possibility of significant interaction remains open as new data are produced.

- The revised independent effects model is proposed as the best working quantitative model form for the compressive strength of cob to date. Fit parameters are expected to change from effects of different local soils, as discussed in Chapter 7.

- GPR modeling showed generally good agreement with experimental data and analytical models. However, limitations on model portability and sensitivity to small data sets reduce the effectiveness of GPR in comparison with current analytical modeling.

CHAPTER 9

CONCLUSIONS AND FUTURE WORK

9.1 Summary of Work Completed

The sand, clay soil, and straw used for almost all cob specimens were characterized by most relevant test methods. The Sand was a semi-angular silty masonry sand.

Clay soil sampled from near Chandler Park, Tulsa, Oklahoma was tested using a wide array characterization methods. The soil was almost devoid of coarse sand particles. Soil showed high stickiness and plasticity, typically indicating good properties for cob construction. Clay content evaluated differed between different test methods, with results ranging from 26% to 48% clay by mass. Hyrometer-based sedimentation testing (according to ASTM D422) was used as the primary method of comparing this baseline soil to other regional soils.

Straw was a wheat straw likely cut with a rotary mower, based on the length distribution. Straw stalks showed an average strength of 21 MPa Straw stalks failed typical field tests for strength after being stored indoors for three years, likely indicating entitlement from decay in open air.

The pattern of weight loss with respect to moisture content was measured and modeled using an exponential decay curve. Strength increased non-linearly with respect to both time and moisture content, achieving equilibrium after approximately 12 days. A minimum of 18 days of drying under typical indoor temperature and humidity conditions is recommended for specimens to considered fully dried and ready for strength testing. Longer drying periods show an increase in standard deviation of specimens strength and may indicate continued hardening and entitlement as drying continues. Weight loss measurements, however, were unable to show continued drying after 18 days.

Specimen geometry showed no significant influence of specimen size on observed strength. Smaller specimens may be used for larger statistical groups, but size of the straw fibers and potential inhomogeneity in the mixed material suggest that larger specimens will provide more reliable comparison to material strength when used in structures. Comparisons of brick-sized specimens to full wall-section tests would confirm the validity of miniaturized test specimens. Prismatic specimens for the remainder of this work were made with the 4x4x12 inch dimensions for consistency with earlier tests.

Various properties, including density, mixed volume ratio, and compressive strength, showed a bi-linear trend with respect to clay content in a sand-soil mix. Specimen strength was then tested with respect to ratios of sand, soil, and straw. Both clay and straw content had a statistically significant influence on compressive strength. Neither clay or straw content had a statistically significant influence on bending strength. Both clay and straw showed local peaks, with reduced observed strength at the high and low mass fractions of both clay and straw.

Soils from different regions were characterized for clay content and physical behavior. Various methods of clay evaluation did not agree on either value of clay or order of most clay-rich specimens. Hydrometer-based sedimentation testing was used to evaluate clay content as the most standard and well-suited method for clay-rich soils. Calculated clay content of each soil was used to create cob mixes of equal final clay content. Differences in strength of specimens from different regions could not be sufficiently explained by differences in clay content of the soils. Therefore, properties other than clay content, such as chemical or physical differences, can have a significant influence on the strength of resulting cob.

Predictive modeling was performed for experimental data on compression data. An additive independent effects model was applied to the mix ratio data. Available data was only able to test independent effects and did not show significant influence of sand and clay content interaction. This model fit existing data well. From this model, the peak strength mix was calculated and this mix was manufactured. However, the mix intended to show peak strength of this soil showed a lower strength than anticipated. Additional data from the location comparison study became available for analysis at this time as well. From these new data sets, the additive independent model was revised to fit all data, and a model including interaction terms was tested as well. Both of these models show good fits to the experimental data. The interaction between influence of clay and straw content on compressive strength was measurable not not statistically significant at 95% confidence. Therefore, the additive independent effects model is proposed as the best form for predicting compressive strength based on available data. Machine learning model fitting, performed by Gaussian process regression, initially performed well on fitting a small set of data, but the model results appeared over-fitted when additional data from location comparison testing and the calculated peak strength mix was added.

9.2 Key Deliverables

- Comparison of clay content soil tests (Section 3.4.11)
- Material drying curve (Section 4.4.5)
- Curve for strength reduction with respect to moisture content (Local soil dependent, Section 4.5)
- Pair of material compressive strength models (Section 8.5)
- Well-characterized cob strength data

9.3 Future Work

Many potential influences on the strength and safe use of cob as a construction material remain for further study. Presented below are some of the tests that show most promise of contributing to the reliable and safe use of cob for construction.

- Operationalization of mixing process: An study of the statistical influence of operator and batch-to-batch variance would clarify which elements of cob production are necessary to codify. Thorough study of influences of various production variables can also be used to produce a set of best practices by blending quantitative testing and traditional training.

- Influence of operator: Traditional mixing is performed underfoot and may change with the operator pace, force, and pattern of mix inversion and flattening. Likewise, mechanized production of cob, such as with a tractor, is subject to similar variability. Effective training practices may be able to reduce operator variance in strength of cob as well.
- Influence of mixing duration: Currently, cob is mixed until the soil and straw are well distributed and the batch shows cohesion. Evaluation of the influence of mixing time could explain difference between batches and establish a recommended process.
- Influence of added water content: Traditional methods suggest adding sufficient water to produce a mixable, plastic state for the batch of cob. Experiences shows that insufficient water may fail to mix the soil into sand, or the sand-soil mixture may fail to bond to straw fibers. Likewise, an overly wet mixture will take longer to dry and fail to hold the required shape when added to the wall. The sensitivity of the resulting cob strength to water added during mixing is desirable to understand for writing best practices

- Influence sand classification on strength: Sand grain shape shows significant influence on the strength of concrete. The influence of sand grain angularity and sand particle size distribution can help qualify many kinds of sands for use in earthen construction and may provide further insight into material strength.
- Influence of fiber orientation: Fiber alignment has significant influence on strength and stiffness properties of fiber reinforced composite materials. Although highly non-traditional, cob includes natural fibers to increase stress transmission and damage tolerance. In actual use, cob is assumed to have fibers randomly oriented through the

entire volume. However, significant quantities o oriented fibers may have significant influence on material properties, including strength, elasticity, and damage tolerance.

- Influence of soil suction: Matric suction is a property of soil used to measure the interaction of soil and moisture as soils dry. Initial work as evaluated the matric suction of soils of different strengths. If suction can provide strong correlation to mechanical strength, this may be viable as a method of testing for code compliance of construction materials using significantly less material and cost.

- Interaction of influences of clay and straw: This work showed only a weak interaction between clay and straw on compressive strength. Further testing to evaluate potential influence more carefully would provide valuable data for future material strength modeling.

- Model for tensile strength, bending strength, and modulus: This work failed to show significant differences in bending strength between different mix ratios. Also, this work did not evaluate tensile strength or modulus of elasticity for cobs of different mixes. Future work to identify appropriate testing procedures for tensile behavior of cob, if necessary, and if ingredient ratios can significantly influence bending strength and modulus of elasticity would meaningfully contribute to design standards for cob construction.

- Influence of clay species on mechanical behavior: Clay shrinkage was been proposed as a primary mechanism in the strengthening of clay soils as they dry. Because different species of clay have different swelling, stickiness, and plasticity behavior with respect to water content, the species of clay in local soil may have significant influence on cob strength.

- Determination of critical properties of clay soil: As Chapter 7 demonstrated, different local soils can produce different cob strengths. If clay species fails and particle size distribution of soils fail to show significant influences on cob strength, other mechanisms must be explored.

- Test method for field quantification of soil clay content: While various qualitative field tests exist to evaluate the relative clay content in a soil, or compare one soil to another, no standard method of quantitatively determining clay content of a soil is well suited to rapid field evaluation. Such a test method would provide straightforward comparison of various potential soils and ensure an appropriate sand-soil ratio was used to maintain optimum clay content in the produced cob.

- Moisture transport characterization: The behavior of liquid-phase water as moisture gradients and capillary action transport it through cob could be important to characterize for understanding of structural degradation when exposed to rain or standing water. Tests outlined by the New Mexico adobe code include characterization of vertical drip-down rate, vertical up-whick rate, and side intrusion rate. Such characterization would be necessary for performing finite element modeling on water-exposure worst-case scenarios.

- Creep testing of earthen materials: Because earthen materials are intended to be used for long duration under both static and dynamic loads, characterizing the behavior of cob and other earthen materials under load and potential humidity cycling may be important for long-term structural safety. Creep testing of concrete beams in three-point bending has been described in ASTM C512 [10]. While anecdotal evidence suggests that cob can survive long periods of regular use, regular refurbishment may obfuscate slow changes to material changes.

- Fatigue characterization: Because structures experience dynamic loading from wind, snow, rain, and seismic and thermal stresses, the behavior of cob under fatigue loading is important for understanding long-term safety of earthen buildings.

- Fastener and reinforcement pullout testing: Embedding non-earthen elements in earthen walls is the most common means of securing walls to foundations, roofs, and built-in non-earthen elements. The use of structural reinforcement inside earthen walls has also been explored. The pullout strength of various materials and geometries of potential wall attachment methods, including re-bar, bolts, nails, and embedded anchors, is necessary for adequate design of reinforcement and mounting points. Pullout testing in concrete has been standardized in ASTM C900 [9].

9.4 Conclusion

As construction with earthen materials becomes more well characterized, standards can be written which ensure safety while minimizing burdens on designers and builders. Thorough characterization and modeling allows a greater range of novel designs to be evaluated at lower cost and with greater accuracy. As building codes are written and designs become refined, construction with earthen materials may become more common and accessible for both owner-builders and traditional construction firms. The benefits of material cost, durability, embodied energy, energy efficiency, and safety will draw more people to use this abundant and viable construction medium.

BIBLIOGRAPHY

[1] Bhagwan D. Agarwal, Lawrence J. Broutman, and K. Chandrashekhara. *Analysis and Performance of Fiber Composites*. John Wiley & Sons, Hoboken, NJ, 2006.

[2] Umaima Al Aqtash and Paola Bandini. Prediction of unsaturated shear strength of an adobe soil from the soil-water characteristic curve. *Construction and Building Materials*, 98:592–599, 2015.

[3] Jean-Michel Albert-Thenet. *The Earthquake Resistance of Cob Structures*. Bachelor of engineering, University of Technology Sydney, 2008.

[4] Judith Alfrey. 'The habitations of wretchedness'? Clom buildings in Wales. *Vernacular Archaeology*, 39:71–77, 2008.

[5] ASTM. C1018 - Standard Test Method for Flexural Toughness and First-Crack Strength of Fiber-Reinforced Concrete (Using Beam With Third-Point Loading), 1997.

[6] ASTM. D1140 - Standard Test Methods for Amount of Material in Soils Finer Than the No. 200 (75-um) Sieve, 2000.

[7] ASTM. D2488 - Standard practice for description and identification of soils (visual manual procedure), 2000.

[8] ASTM. D4318 - Standard Test Methods for Liquid Limit, Plastic Limit, and Plasticity Index of Soils, 2000.

[9] ASTM. C900 - Standard Test Method for Pullout Strength of Hardened Concrete, 2001.

[10] ASTM. C512 - Standard Test Method for Creep of Concrete in Compression, 2002.

[11] ASTM. D2487 - Classification of Soils for Engineering Purposes (Unified Soil Classification System), 2002.

[12] ASTM. D422 - Standard Test Method for Particle-Size Analysis of Soils, 2002.

[13] ASTM. C78 - Standard Test Method for Flexural Strength of Concrete (Using Simple Beam With Center-Point Loading), 2007.

[14] ASTM. C1609 - Standard test method for flexural performance of fiber-reinforced concrete (using beam with third-point loading), 2010.

[15] ASTM. D2216 - Standard Test Methods for Laboratory Determination of Water (Moisture) Content of Soil and Rock by Mass, 2010.

[16] ASTM. E2392 - Standard Guide for Design of Earthen Wall Building Systems. 2010.

[17] ASTM. D2166 - Standard Test Method for Unconfined Compressive Strength of Cohesive Soil, 2013.

[18] ASTM. D5821 - Standard Test Method for determining the percentage of fractured particles in coarse aggregate, 2014.

[19] ASTM. C136 - Standard Test Method for Sieve Analysis of Fine and Coarse Aggregates, 2015.

[20] Givanildo Azeredo, Jean Claude Morel, and Normando Perazzo Barbosa. Compressive strength testing of earth mortars. *Journal of Urban and Environmental Engineering*, 1(1):26–35, 2007.

[21] Belkacem Belhadj, Madani Bederina, Khadra Benguettache, and Michele Queneudec. Effect of the type of sand on the fracture and mechanical properties of sand concrete. *Advances in concrete construction*, 2(1):13–27, 2014.

[22] Robert H Bradley and Diane L Putnick. Housing Quality and Access to Material and Learning Resources within the Home Environment in Developing Countries. 83(1):76–91, 2013.

[23] G. H. Brown and E. T. Montgomery. Dehydration of Clays. Technical report, 1913.

[24] Gabi Brunello, Jose Espinoza, and Alex Golitz. Cob Property Analysis. Technical report, Santa Clara University, 2018.

[25] State California. *2016 California Historical Building Code*. 2019.

[26] Canolfan TYWI. Understanding Traditional Buildings. Technical report, Sir Gar Carmarthenshire.

[27] Paul Chaikin. Random thoughts. *Physics Today*, 60(6, 8):207–208, 2007.

[28] Daniela Ciancio and Christopher Beckett. Rammed earth : an overview of a sustainable construction material. *Third international conference on sustainable construction materials and technologies*.

[29] Devon Earth Building Association. Cob Dwellings: Compliance with The Building Regulations. *Cob and Unbaked Earth Dwellings*, 2000:1–21, 2008.

[30] Devon Historic Buildings Trust. The cob buildings of Devon: History, Bulding Methods, and Conservation, 1992.

[31] P. Doat, A. Hays, H. Houben, S. Matuk, and F. Vitoux. Building With Earth, 1991.

[32] D Dowling and Bijan Samali. Low-Cost and Low-Tech Reinforcement Systems for Improved Earthquake Resistance of Mud Brick Buildings. *Proceedings of the Getty Seismic Adobe Project 2006 Colloquium*, pages 23–33, 2006.

[33] Christopher Dyer. Building in earth in late-medieval England. *Vernacular architecture*, 39(1):63–70, 2008.

[34] Earth Building Association of New Zealand. FAQ, 2019.

[35] EPA. Volatile Organic Compounds' Impact on Indoor Air Quality, 2017.

[36] Peter A Erkelens. Low-cost housing, a continuous struggle (overview, research, future). pages 2045–2054, 2007.

[37] Mariana Estrada. *A case study of cob earth based building technique in Matagalpa , Nicaragua – LCA perspective and rate of adoption.* PhD thesis, Mid Sweden University, 2013.

[38] Ianto Evans, Michael Smith, and Linda Smiley. *The Hand-Sculpted House: A Practical and Philosophical Guide to Building a Cob Cottage.* Chelsea Green Publishing Company, 2002.

[39] Neil Finn. Mud and Frame Construction in South Leicestershire. *Vernacular Architecture*, 40(1):63–74, 2009.

[40] Terry Gilliam and Terry Jones. Monty Python and the Holy Grail, 1975.

[41] Global Solar Atlas. Global Wind Atlas, 2019.

[42] Steven Michael Rhyder Goodhew. *The Thermal Properties of Cob Buildings of Devon.* PhD thesis, The University of Plymouth, 2000.

[43] Matthew James Addison Greer. *The Effect of Moisture Content and Composition on the Compressive Strength and Rigidity of Cob Made From Soil of the Breccia Measures Near Teignmouth, Devon.* Dissertation, University of Plymouth, 1996.

[44] Ralph E. Grim. *Applied Clay Mineralogy.* McGraw-Hill Book Company, Inc., Urbana, Illinois, 1962.

[45] Erwan Hamard, Bogdan Cazacliu, Andry Razakamanantsoa, and Jean Claude Morel. Cob, a vernacular earth construction process in the context of modern sustainable building. *Building and Environment*, 106:103–119, 2016.

[46] N Hanson. *The Dreadful Judgement.* Transworld, 2011.

[47] Indian Standard. Improving Earthquake Resistance of Earthen Buildings - Guidelines, 1993.

[48] International Organization for Standardization. ISO 14688-1:2017. In *Geotechnical investigation and testing — Identification and classification of soil —*, volume Part 1: Id. International Organization of Standardization, 2017.

[49] Paul Jaquin and Charles Augarde. *Earth Building: History, Science and Conservation.* IHS BRE Press, 2012.

[50] Larry Keefe and Devon Historic Buildings Trust. The Cob Buildings of Devon: Repair and Maintanence, 1993.

[51] Joseph F. Kennedy, Michael Smith, and Catherine Wanek. *The Art of Natural Building: Design, Construction, Resources.* New Society Publishers, 2001.

[52] Jong-jin Kim, Brenda Rigdon, Project Intern, Jonathan Graves, Urban Planning, and Ann Arbor. Qualities , Use , and Examples of Sustainable Building Materials. *Building*, (December 1998), 1998.

[53] L. W. King. EAWC Anthology: Hammurabi's Code of Laws, 2008.

[54] Sedona Leza, Karin Komshian, and Jordan Cho. Sustainable Construction Material Research Project - Cob Flexure. Technical report, 2017.

[55] Tamil Salvi Mari. Embodied energy of building materials A comparative analysis of terraced houses in Malaysia. In *41st Annual Conference of the Architectural Science Association at Deakin University*, number Raia 2004, pages 165–173, Selangor, 2007.

[56] Kevin McCabe. Kevin McCabe Cob Building Specialist, 2019.

[57] R. C. Mielenz and M. F. King. Physical-chemical properties and engineering performance of clays. *Clays and Clay Technology*, 169(V):196–254, 1952.

[58] Douglas A. Miller and Richard A. White. A Conterminous United States Multilayer Soil Characteristics Dataset for Regional Climate and Hydrology Modeling. *Earth Interactions*, 2(2):1–26, 2002.

[59] Gernot Minke. Construction manual for earthquake-resistant houses built of earth. *Building Advisory Service and Information Network*, pages 1–52, 2001.

[60] Jonathan Morris. West Country cob houses: The man building a house out of mud, feb 2014.

[61] Bruce R. Munson, Theodore H. Okiishi, Wade W. Huebsch, and Alric P. Rothmayer. *Fundementals of Fluid Mechanics*. John Wiley & Sons, Hoboken, NJ, 7th edition, 2013.

[62] New Mexico. New Mexico Earthen Building Materials Code, 2009.

[63] John Norton. Building With Earth: A Handbook. *Statewide Agricultural Land Use Baseline 2015*, 1, 1986.

[64] Oklahoma Historical Society. Sod House Museum, 2019.

[65] V. I. Osipov. Density of clay minerals. *Soil Mechanics and Foundation Engineering*, 48(6):231–240, 2012.

[66] Owens Corning. EcoTouch PINK Fiberglas Insulation. Technical Report 100113811-D, 2016.

[67] PBS NewsHour. Ecuador looks to pick up pieces and rebuild after devastating earthquake, may 2016.

[68] Quinn M Pullen and Todd V Scholz. Index and Engineering Properties of Oregon Cob. *Journal of Green Building*, 6(2):88–106, 2011.

[69] Enrico Quagliarini and Stefano Lenci. The influence of natural stabilizers and natural fibres on the mechanical properties of ancient Roman adobe bricks. *Journal of Cultural Heritage*, 11(3):309–314, 2010.

[70] John Raithby. Charles II, 1666: An Act for rebuilding the Citty of London, Volume 5, 1628-80, 1819.

[71] Michael Scoles Rizza and Hana Mori Böttger. Effect of Straw Length and Quantity on Mechanical Properties of Cob. Technical report, University of San Francisco, San Francisco, 2018.

[72] Curtis T. Rueden, Johannes Schindelin, Mark C. Hiner, Barry E. DeZonia, Alison E. Walter, Ellen T. Arena, and Kevin W. Eliceiri. ImageJ2: ImageJ for the next generation of scientific image data. *BMC Bioinformatics*, 18(529), 2017.

[73] Johannes Schindelin, Ignacio Arganda-Carreras, Erwin Frise, Verena Kaynig, Mark Longair, Tobias Pietzsch, Stephan Preibisch, Curtis Rueden, Stephan Saalfeld, Benjamin Schmid, Jean-Yves Tinevez, Daniel James White, Volker Hartenstein, Kevin Eliceiri, Pavel Tomancak, and Albert Cardona. Fiji: an open-source platform for biological-image analysis. *Nature Methods*, 9(7):676–682, 2012.

[74] Ashish Shukla, G. N. Tiwari, and M. S. Sodha. Embodied energy analysis of adobe house. *Renewable Energy*, 34(3):755–761, 2009.

[75] Michael Smith. *The Cobber's Companion: How to Build Your Own Earthen Home*. Cob Cottage Company, 2000.

[76] Clarke Snell and Tim Callahan. *Building Green, New Edition. ; A Complete How-to Guide to Alternative Building Methods Earth Plaster * Straw Bale * Cordwood * Cob * Living Roofs*. Lark Crafts, 2 edition, 2009.

[77] The Document Foundation. LibreOffice: The Document Foundation, 2019.

[78] The GIMP Team. GIMP - The GNU Image Manipulation Program, 2018.

[79] The Shelly Company. Sand and Gravel in Concrete, 2014.

[80] The Welsh House. Ty Unnos, 2019.

[81] Aurora Torres, Jodi Brandt, Kristen Lear, and Jianguo Liu. A looming tragedy of the sand commons. *Science*, 357(6355):970–971, 2017.

[82] UNESCO World Heritage Centre. Fujin Tulou, 2008.

[83] U.S. Climate Data. Climate Coquille - Oregon, 2019.

[84] Julio Vargas, Marcial Blondet, and Nicola Tarque. The Peruvian Building Code for Earthen Buildings. *Getty Seismic Adobe Project 2006 Colloquium*, (September 2016):45–51, 2006.

[85] Peter. Walker and Standards Association of Australia. *The Australian earth building handbook*. Standards Australia International, Sydney, 2002.

[86] L. Watson and Matthew James Addison Greer. The composition and properties of cob: a traditional West Country building material. *Transactions on the Built Environment*, 4, 1993.

[87] Herbert L. Whittemore, Ambrose H. Stang, Elbert Hubbell, and Richard S. Dill. Structural, Heat-Transfer, and Water-Permeabilty Properties of Five Earth-Wall Constructions. Technical report, U.S. Department of Commerce, National Bureau of Standards, Building Materials and Structures Report BMS78, 1941.

[88] Sir Clough Williams-Ellis, John Charles Eastwick-Field, and Elizabeth Eastwick-Field. *Building in cob, pise, and stabilized earth*. Routledge, 1947.

[89] World Monuments Fund. Basgo Gompa (Maitreya Temples).

[90] David J. Wright. CobModelGPR, 2019.

[91] YourHome. Embodied energy. Technical report, 2006.

[92] Philip Zak, Taha Ashour, Azra Korjenic, Sinan Korjenic, and Wei Wu. The influence of natural reinforcement fibers, gypsum and cement on compressive strength of earth bricks materials. *Construction and Building Materials*, 106:179–188, 2016.

[93] Mohammad Sharif Zami and Angela Lee. Economic benefits of contemporary earth construction in low-cost urban housing - State-of-the-art review. *Journal of Building Appraisal*, 5(3):259–271, 2010.

[94] Standards New Zealand. NZS 4297:1998 Engineering design of earth buildings, 1998.